Aus der Klinik und Poliklinik für Frauenheilkunde und Geburtshilfe
Klinik der Ludwig-Maximilians-Universität München
Direktor: Prof. Dr. Sven Mahner

# The role of Tumor-associated Macrophages (TAMs) and Transcription Factor KLF11 in breast cancer (BC) and KLF11-mediated Transcriptional Regulation of BC-associated TAMs


Dissertation
zum Erwerb des Doktorgrades der Medizin
an der Medizinischen Fakultät der
Ludwig-Maximilians-Universität zu München

vorgelegt von
**Lili Lin**
aus
Zhejiang, China

Jahr
2022

Mit Genehmigung der Medizinischen Fakultät
der Universität München

| | |
|---|---|
| Berichterstatter: | Prof. Dr. Udo Jeschke |
| Mitberichterstatter: | Prof. Dr. Heiko Adler |
| | Priv.Doz. Dr. Ulrich Andergassen |
| Mitbetreuung durch den promovierten Mitarbeiter: | Dr. Anna Hester |
| Dekan: | Prof. Dr. med. Thomas Gudermann |
| Tag der mündlichen Prüfung: | 29.09.2022 |

# Table of content

# Zusammenfassung (Deutsch):

**Hintergrund**

Brustkrebs (BC) ist eine heterogene Erkrankung, bei der immunologische Faktoren eine wesentliche Rolle spielen. Eine hohe Infiltration von tumorassoziierten Makrophagen (TAM) kann unabhängig von der Prognose des menschlichen BC auf eine schlechte Prognose hinweisen. TAM können jedoch in verschiedenen Phänotypen und an verschiedenen Stellen im Brusttumorgewebe auftreten, deren Bedeutung noch nicht vollständig geklärt ist. Das Fettgewebe der Brust trägt bei fettleibigen BC-Patientinnen und bei Personen mit normalem Body-Mass-Index (BMI) zur Progression des BC bei. Fettgewebsmakrophagen sind ein wichtiger Bestandteil des Fettgewebes. Es besteht eine Wechselwirkung zwischen BC-Tumorzellen und tumorassoziierten Adipozyten. Ob TAM im Brustfettgewebe ebenfalls beteiligt ist, bleibt eine interessante Frage, die es zu klären gilt.

Die Polarisierung von TAM kann durch Transkriptionsfaktoren (TFs) und nukleare Rezeptoren (NRs) transkriptionell reguliert werden. Die Familie der Krüppel like Faktors (KLF) ist nachweislich an der Tumorprogression durch die Regulierung von Tumorzellen und dem damit verbundenen Tumormikroenvironment (TME) beteiligt. Es hat sich gezeigt, dass mehrere KLF-Mitglieder an der Polarisierung von TAM beteiligt sind. Die Mitglieder der KLF-Familie in BC sind systematisch zusammengefasst worden. Über die Rolle der KLF als Onkogene oder Tumorsuppressoren ist noch kein Konsens erzielt worden. KLF11, als Mitglied dieser volatilen/Kontext-abhängigen Familie, deren Ausdrucksmuster und prognostische Relevanz bei BC-Patienten unklar bleibt, ganz zu schweigen von seiner genauen Transkription Ellen Regulierung von TAM in der BC-TME oder BC-Tumorzellen.

**Methoden**

Unser Ziel war es, die Wirkung von TAMs auf BC auf der Grundlage ihrer unterschiedlichen Infiltrationsorte zu untersuchen. Darüber hinaus wollten wir klären, ob TAMs im Brustfettgewebe bei BC-Patientinnen unabhängig vom Vorhandensein von Fettleibigkeit zum Pro-Tumoreffekt des Brustfettgewebes beitragen. Daher haben wir CD68-IHC-Färbung als pan-makrophagen Marker in unserer Kohorte von primären BC-Patienten ohne vordefinierten Übergewichts- oder Adipositasstatus durchgeführt. Anschließend zählten wir die Anzahl der TAMs (CD68-gefärbte Zellen) im Schnitt des Brustfettgewebes, der als Brustfettgewebsmakrophage (BATM) bezeichnet wird, und des Brusttumor-Stromagewebes, der als Brusttumor-Stroma-Makrophage (BTSM) bezeichnet wird. Außerdem korrelierten wir die Häufigkeit von BATM und BTSM mit klinisch-pathologischen Merkmalen. Darüber hinaus führten wir eine prädiktive Überlebensanalyse von BATM und BTSM bei diesen BC-Patientinnen durch.

Als nächstes wollten wir klären, ob KLF11 als Onkogen oder als Tumorsuppressor bei BC wirkt. Da KLF11 zu einer derart volatilen/kontextabhängigen Familie von prognostischen Funktionen gehört, haben wir die Rolle von KLF11 bei BC-Patienten in zweifacher Hinsicht untersucht. Einerseits untersuchten wir die Rolle von KLF11 mRNA bei BC-Patienten, die durch Massen-RNA-seq-Datensätze identifiziert wurden. Andererseits haben wir die prognostische Rolle von KLF11 in unserer BC-Kohorte durch immunhistochemische (IHC) Färbung von KLF11 in den 298 Patientenproben erforscht und validiert, gefolgt von einer statistischen Analyse, um die genaue Pro- oder Anti-Tumor-Rolle von KLF11 zu überprüfen.

Schließlich wollten wir die Mechanismen der KLF11-vermittelten Regulierung der BC-Progression aus der Perspektive von TAMs und Tumorzellen untersuchen. Tumorzellen. Um ein allgemeines

Verständnis der Signalwege und biologischen Prozesse (BPs) zu erhalten, an denen KLF11 beteiligt sein kann, haben wir zunächst den Mechanismus vorhergesagt, der der Regulierung von KLF11 bei der BC-Progression zugrunde liegt, indem wir eine Analyse der funktionellen Anreicherung von Genen durchgeführt haben. Zweitens, bezogen auf die Vorhersage-Analyse, um weiter zu erforschen die Transkription Elle regulatorische Rolle von KLF11 in Brust-Tumor-assoziierten Makrophagen (Br-TAMs) und Tumorzellen von BC, respektive. Drittens, um die Wirkung von KLF11 auf BC-Tumorzellen zu validieren, haben wir siRNA-vermittelte loss-of-function von KLF11 der Zellproliferation und Zell Apoptose in drei verschiedenen molekularen Subtyp-Zelllinien.

**Schlussfolgerungen**

Dies ist das erste Mal, dass TAMs nachweislich unterschiedliche Auswirkungen auf den BC haben, je nachdem, wo sie versickern, d. h. in BTSMs und BATMs. BTSM schien eng mit den klinischen und pathologischen Merkmalen von BC verbunden zu sein, während BATM eng mit den Prognoseergebnissen von BC verbunden zu sein schien. Es zeigte sich, dass BTSM hauptsächlich mit den molekularen Subtypen von BC in Verbindung steht. Außerdem beobachteten wir die größte Häufigkeit von BTSM bei TNBC. Dies deutet darauf hin, dass BTSM eine vielversprechende Option für eine künftige gezielte Therapie bei TNBC sein könnte. Darüber hinaus könnte es auch als vielversprechender therapeutischer Marker dienen, um an der Risikostratifizierung von Patienten teilzunehmen und dann eine präzisere Behandlungsstrategie für Patienten auszuwählen.

Es hat sich jedoch gezeigt, dass eine höhere BATM-Infiltration ein unabhängiger prognostischer Faktor für ein schlechteres Gesamtüberleben (OS) und Krankheitsfreies Überleben (DFS) bei BC-Patienten ist. Darüber hinaus stellten wir fest, dass die BATM-Infiltration negativ mit der Prostaglandin-E-Rezeptor-3 (EP3) -Expression bei BC assoziiert war, und die negativen Auswirkungen von BATM auf die Überlebensprognose wurden durch die EP3-Expression deutlich abgeschwächt. Eine Kombination aus "BATM-hoch" und "EP3-niedrig" führte zu einem schlechteren Ergebnis. Diese Ergebnisse deuten darauf hin, dass die gezielte Beeinflussung von BATM und die Beeinflussung von BATM in Verbindung mit der Beeinflussung des PGE2/EP3-Signalwegs vielversprechende therapeutische Konzepte für die BC-Immuntherapie sein könnten.

Außerdem konnten wir *in silico* nachweisen, dass *KLF11* mRNA in BC-Tumorgewebe weniger stark exprimiert wurde als in nicht/parakarzinomatösem Brustgewebe. Außerdem war die *KLF11*-mRNA-Expression positiv mit aggressiven BC-Merkmalen assoziiert. Die erhöhte Expression von *KLF11* mRNA ist ein unabhängiger Indikator für das schlechte OS von BC. Wir bestätigten auch, dass ein höherer KLF11-Proteingehalt in einem aggressiveren molekularen Subtyp von BC gefärbt war. Die erhöhte Expression von KLF11 blieb jedoch ein unabhängiger Indikator für das schlechte DFS und Fernmetastasenfreies Überleben (DMFS) von BC, das in unserer Patientenkohorte festgestellt wurde. Es ist das erste Mal, dass direkt und überzeugend gezeigt werden konnte, dass KLF11, obwohl es in BC-Geweben nur in geringem Maße exprimiert wurde, offenbar ein Pro-Tumor-KLF-Mitglied und ein prognostischer Risikofaktor bei BC ist.

Mechanistisch gesehen deuten die Ergebnisse der Gen-Ontologie (GO)- und Kyoto-Enzyklopädie der Gene und Genome (KEGG)-Anreicherungsanalyse deuten darauf hin, dass KLF11 die BC-Progression unter zwei Aspekten regulieren könnte. Einerseits durch die Regulierung des Zellwachstums von Tumorzellen, andererseits durch die Regulierung von Komponenten im BC-TME wie der Makrophagen-Differenzierung oder anderen verwandten Immunreaktionen durch Interaktion mit NRs oder Beteiligung an krebsbezogenen Signalwegen. Aus der KLF11-TAM-Perspek-

tive haben wir gezeigt, dass KLF11 als tumorabhängiger Transkriptionsregulator der TAM-Polarisierung über die Formatierung als Transkriptionsverstärker mit NRs wie KLF11/PPARG- oder KLF11/PPARG/THRA- fungieren könnte und an der Regulierung der Transkription des Genprogramms spezifischer TAM-Phänotypen beteiligt ist. Aus der Perspektive der KLF11-BC-Tumorzellen konnten wir zeigen, dass KLF11 als tumorabhängiger Transkriptionsregulator der Transkription von Genprogrammen verschiedener molekularer Subtypen und der Genprogramme im Zusammenhang mit Zellproliferation und Zell Apoptose fungieren könnte. Wichtig ist, dass wir experimentell bestätigt haben, dass KLF11 als Pro-Tumor-Faktor der BC-Progression über die Förderung der Zellproliferation und die Induktion der Zell Apoptose von BC-Tumorzellen wirkt.

Zusammengenommen ist es das erste Mal, dass die Rolle von KLF11 direkt in BC-Zelllinien erforscht wird. Wichtiger noch, es ist das erste Mal, dass KLF11 in die Regulierung der TAMs-Polarisierung eingeführt wird und das erste Mal, dass KLF11/PPARG- oder KLF11/PPARG/THRA-vermittelte Transkriptionsverstärker der Genprogramme von Br-TAMs vorgeschlagen werden. Die Spekulationen über die KLF11-TAMs-Regulierung sollten jedoch in zukünftigen Forschungen überprüft werden. Eine Kombination aus scRNA-seq und räumlicher Transkription (ST) kann optimal an formalinfixierten und in Paraffin eingebetteten (FFEP) Objektträgern von BC-Gewebeproben durchgeführt werden, um das Transkriptionsnetzwerk von KLF11 in den Tumorzellen, BATM bzw. BTSM, zu untersuchen.

Schließlich, basierend auf der Beobachtung seiner beeindruckenden Rolle bei der Regulierung sowohl im TAM als auch in den Tumorzellen von BC, untersuchten wir auch die Korrelation zwischen dem Ausdruck von KLF11 und PD-1, PD-L1 und PD-L2 in BC. Zwischen KLF11 und PD-1-Liganden (PD-L1 und PD-L2) wurde eine stärkere Korrelation beobachtet als bei PD-1. Daher schlagen wir vor, dass die Beachtung der Interaktion zwischen PD1/PD-L2 eine Lösung zur Behandlung von PD1/PD-L1-Resistenzen oder zur Verbesserung niedriger Ansprechraten sein könnte. Noch wichtiger ist, dass insbesondere bei Tumoren, die geringe Ansprechraten auf Immun-Checkpoint-Therapien zeigen, die gezielte Behandlung von Transkriptionsfaktoren wie KLF11 eine synergistische oder alternative Option für die Immun-Checkpoint-Therapie sein könnte.

# Abstract (English):

**Background**

High infiltration of tumor-associated macrophage (TAM) can independently indicate the unfavorable prognosis of human breast cancer (BC). However, TAMs can occur in different phenotypes, and at different locations in breast tumor tissue, the significance of which has not yet been fully understood. Breast adipose tissue contributes to BC progression both in obese BC patients and normal body-mass index (BMI) individuals. Adipose tissue macrophages are an important component of adipose tissue. There exist an interaction between BC tumor cells and tumor-associated adipocytes. Whether TAM in breast adipose tissue is also involved remains an interesting question to be addressed

The polarization of TAM can be transcriptionally regulated by transcription factors (TFs) and nuclear receptors (NRs). Increasing evidence has demonstrated that the krüppel like factor (KLF) family regulates tumor progression via regulating tumor cells and the related tumor microenvironment (TME). Several KLFs members have been revealed to be involved in the polarization of TAM. KLF family members in BC have been systematically summarized. KLF act as oncogenes or tumor-suppressors has not yet reached consensus. KLF11, as a member of this volatile/context-dependent family, the expression pattern and prognostic relevance of which in BC patients

remains unclear, not to mention its precise transcriptional regulation of TAM in the BC-TME or BC tumor cells.

**Methods**

We aimed to explore the effects of TAMs on BC based on their different infiltration locations. Furthermore, we aimed to clarify whether TAMs in breast adipose tissue contribute to the pro-tumor effect of breast adipose tissue in BC patients irrespective of the presence of obesity. Therefore, we performed CD68-IHC staining as a pan-macrophage marker in our cohort of primary BC patients with no prespecified overweight or obesity status. We then counted the number of TAMs (CD68-stained cells) in the section of breast adipose tissue termed “breast adipose tissue macrophage (BATM)” and of breast tumor-stroma tissue termed “breast tumor-stroma macrophage (BTSM)”. And further, we correlated the abundances of BATM and BTSM, respectively, to clinicopathological characteristics. In addition, we performed predictive survival analysis of BATM and BTSM, respectively, in these BC patients.

Next, we aimed to clarify whether KLF11 acts as an oncogene or a tumor-suppressor in BC. Given that KLF11 belongs to such a volatile/context-dependent family of prognostic roles, we conducted a dual exploration of the role of KLF11 in BC patients. On the one hand, we explored the role of *KLF11* mRNA in BC patients identified by bulk RNA-seq datasets. Then, on the other hand, we researched and validated the prognostic role of the KLF11 in our BC cohort by applying immunohistochemistry (IHC) staining of KLF11 in the 298 patients samples, followed by statistical analysis to make sure the precisely pro- or anti-tumor role of KLF11.

Finally, we aimed to explore the mechanisms of KLF11-mediated regulations of BC progression from the perspective of TAMs and tumor cells, respectively. Firstly, to have a general understanding of signaling pathways and biological processes (BPs) KLF11 may involve, we predicted the mechanism underlying the regulation of KLF11 in BC progression using gene functional enrichment analysis. Secondly, refereed to the prediction result, we aim to explore the transcriptional regulation of KLF11 in breast-tumor-associated macrophage (Br-TAMs) and tumor cells of BC, respectively. Thirdly, to validate the effect of KLF11 on BC tumor cells, we did siRNA-mediated loss-of-function of KLF11 of cell proliferation and cell apoptosis in three different molecular subtype cell lines.

**Conclusions**

This is the first time that TAMs are shown to have different effects on BC based on different infiltration locations, i.e., BTSMs and BATMs. BTSM preferred to be associated with the clinicopathological characteristics of BC, while BATM appeared to be associated closely with the prognosis outcomes of BC. BTSM was shown to be mainly related to the BC molecular subtypes. Furthermore, we observed the highest abundance of BTSM in TNBC. This suggests that BTSM may provide a promising selection option for future targeted therapy in TNBC. In addition, it may also serve as a promising therapeutic pointing marker to participate in the risk stratification of patients and then select a more precise treatment strategy for patients.

However, a higher BATM infiltration independently indicated a lower survival probability of BC. Furthermore, we also found that BATM infiltration was negatively presented with prostaglandin E receptor 3 (EP3) expression in BC patients. In addition, the negative impact of BATM on survival prognosis was significantly attenuated by EP3 expression. A combination of “BATM-high” and “EP3-low” led to an inferior outcome. These results indicate that targeting BATM and targeting BATM accompanied with targeting the PGE2/EP3 pathway could be promising therapeutic concepts of BC immunotherapy.

In addition, we demonstrated *in silico* that *KLF11* mRNA was lower expressed in BC tumor tissue than in the non/para-cancerous breast tissues. Furthermore, *KLF11* mRNA expression was positively associated with aggressive BC features. Its elevated expression remained to independently indicate the poor OS of BC. We also confirmed that a higher KLF11 protein level was stained in a more aggressive molecular subtype of BC. However, its elevated level remained to independently indicate the poor disease-free survival (DFS) and Distant-metastasis-free survival (DMFS) of BC identified by our patient's cohort. It is the first time to demonstrate directly and convincingly that although it was low expressed in BC tissues, KLF11 appeared to be a pro-tumor KLF member and a prognostic risk factor in BC.

Mechanistically, GO and KEGG enrichment analysis results indicate that KLF11 might regulate BC progression from two aspects. On the one hand, via regulating cells growth of tumor cells, on the other hand, through regulating components in the BC-TME such as macrophages differentiation or other related immune response via interacting with NRs or involving in the cancer-related signaling pathways. From the KLF11-TAMs perspective, we demonstrated that KLF11 might act as a tumor-dependent transcriptional regulator of TAM polarization via formatting as a transcriptional enhancer with NRs such as *KLF11/PPARG*- or *KLF11/PPARG/THRA*- and involved in the regulation of the transcription of gene program of specific TAM phenotypes. From the KLF11-BC tumor cells perspective, we showed that KLF11 might act as a tumor-dependent transcriptional regulator of the transcription of gene programs of different molecular subtypes and the gene programs related to cell proliferation and cell apoptosis. Importantly, we experimentally validated that KLF11 did act as a pro-tumor factor of BC progression via promoting cell proliferation and inducing cell apoptosis of BC tumor cells.

Taken the explored effects of KLF11 on BC by this study together, it is the first time to explore the role of KLF11 directly in BC cell lines. More meaningfully, it is the first time introducing KLF11 into the regulation of TAMs polarization and the first time proposing the *KLF11/PPARG*- or *KLF11/PPARG/THRA*-mediated transcriptional enhancers of the gene programs of Br-TAMs. However, the speculation of KLF11-TAMs regulation should be verified in future research. A combination of scRNA-seq and spatial transcriptome (ST) can be optimally performed on BC tissue samples' formalin-fixed and paraffin-embedded (FFEP) slides to explore the transcriptional network of KLF11 involved in the tumor cells, BATM and BTSM, respectively.

Finally, based on the observation of its impressive regulation role both in the TAM and tumor cells of BC, we also explored the correlation between the expression of *KLF11* and PD-1, PD-L1, and PD-L2 in BC. A stronger was observed between KLF11 and PD-1 ligands (PD-L1 and PD-L2) compared to that with PD-1. Therefore, we propose that paying attention to the interaction between PD1/PD-L2 might be a solution to treat PD1/PD-L1 resistance or improve low response rates. More importantly, particularly for tumors that show low response rates to immune checkpoints therapies, targeting transcription factors such as KLF11 might be a synergistic or an alternative option for immune checkpoints therapy.

# List of figures

# List of tables

# List of abbreviations

| | |
|---|---|
| AUC | Area under curve |
| BATM | Breast adipose tissue macrophage |
| BC | Breast cancer |
| BLCA | Bladder Urothelial Carcinoma |
| BMI | Body mass index |
| BP | Biological process |
| BRCA | Breast invasive carcinoma |
| BrdU | 5-bromo-2'-deoxy-uridine |
| Br-TAM | Breast-tumor-asociated macrohage |
| BTSM | Breast tumor-stroma macrophage |
| CAR | chimeric antigen receptor |
| CC | Cell component |
| CI | Confidence interval |
| C-index | Concordance-index |
| CLS | Crown-like structure |
| CSF | Colony-stimulating factor |
| DFS | Disease-free survival |
| DMFS | Distant-metastasis-free survival |
| DMSO | Dimethyl sulfoxide |
| EMT | Epithelial-mesenchymal transition |
| EP3 | Prostaglandin E receptor 3 |
| ER | Estrogen receptor |
| FDR | False discovery rate |
| FFEP | Formalin-fixed and paraffin-embedded |
| FPKM | Fregments Per Kilobase per Million |
| FPR | False positive rate |
| GEPIA 2 | Gene Expression Profiling Interactive Analysis 2 |
| GM | Gene modules |
| GO | Gene Ontology |
| GSE | Gene expression data series |
| GSEA | Gene set enrichment analysis |
| GTEx | The Genotype-Tissue Expression |
| H3K27ac | Acetylation of lysine 27 on histone H3 protein subunit |
| HDACs | Histone deacetylases |
| HER2 | Human epidermal growth factor receptor 2 |
| HER2 Lu-like | HER2 amplified luminal-like; |
| HER2 non-Lu-like | HER2 amplified non-luminal-like |
| HNSC | Head and Neck squamous cell carcinoma |
| HR | Hazard ratio |
| IDC | Infiltrating ductal carcinoma |
| IF | Immunofluorescence |
| IHC | Immunohistochemistry |
| IL-4 | Interleukin-4 |
| IL-6 | Interleukin-6 |
| IL-12 | Interleukin-12 |
| IRF | Interferon regulatory factors |

| | |
|---|---|
| IRS | Immunoreactive score |
| KEGG | Kyoto encyclopedia of genes and genomes |
| KICH | Kidney chromophobe |
| KIRC | Kidney renal clear cell carcinoma |
| KIRP | Kidney renal papillary cell carcinoma |
| KLF | Krüppel like Factor |
| KM | Kaplan-Meier |
| LAMs | Lipid-associated macrophages |
| LIHC | Liver hepatocellular carcinoma |
| LPS | Lipopolysaccharide |
| LRFS | Local recurrence-free survival |
| LSD1 | Lysine (K)-specific demethylase 1 |
| LuA | Luminal A |
| LUAD | Lung adenocarcinoma |
| LuB | Luminal B |
| LUSC | Lung squamous cell carcinoma |
| LXRα | Liver X receptor alpha |
| MCSF | Macrophage colony stimulating factor |
| MDSC | Myeloid-derived suppressor cells |
| MF | Molecular function |
| MTT | Dimethyl-thiazolyl-diphenyl-tetrazolium bromide |
| NES | Normalize enrichment score |
| NHR | Nuclear hormone receptor |
| NF-κB | Nuclear factor kappa B |
| NLS | Nuclear localization signal |
| OD | Optical density |
| OS | Overall survival |
| PAM50 | Prediction Analysis of Microarray 50 |
| PBS | Phosphate buffered saline |
| PGE2 | Prostaglandin E2 |
| pN | pathological N |
| PPARγ/PPARG | Peroxisome proliferator activated receptor gamma |
| PR | Progesterone receptor |
| PRAD | Prostate adenocarcinoma |
| pT | pathological T |
| RARα | Retinoic acid receptor |
| READ | Rectum Adenocarcinoma |
| ROC | Receiver operator characteristic |
| RT | Room temperature |
| RXRα/RXRA | Retinoic X receptor alpha |
| SCSubtype | Intrinsic subtyping for scRNA-seq data |
| scRNA-seq | single-cell sequencings |
| ST | Spatial transcriptome |
| STAT | Signal transducer and activator of transcription |
| TAM | Tumor-associated macrophage |
| TCGA | The Cancer Genome Atlas |
| TF | Transcription factor |

| | |
|---|---|
| TFPI-2 | Tissue factor pathway inhibitor-2 |
| TGF-β | Transforming growth factor-β |
| THCA | Thyroid carcinoma |
| THRα/THRA | Thyroid hormone receptor alpha |
| THRβ/THRB | Thyroid hormone receptor beta |
| TIIC | Tumor infiltrating immune cells |
| TLR | Toll-like receptor |
| TME | Tumor microenvironment |
| TNBC | Triple negative breast cancer |
| TNFα | Tumor necrosis factors alpha |
| TPM | Transcripts per million reads |
| TPR | True positive rate |
| UCEC | Uterine corpus endometrial carcinoma |
| VDR | Vitamin D receptor |
| YO | Years old |
| ZA | Zoledronic acid |
| ZNF | Zinc finger protein |

# 1. Introduction

## 1.1 Breast Cancer Briefing

Breast cancer (BC) is a type of malignancy with high mortality among women [1-4]. It is a complicated and heterogeneous disease characterized by diverse molecular subtypes. BC is mainly classified into three main subtypes according to the expression pattern of “estrogen receptor (ER)”, “progesterone receptor (PR)” and “human epidermal growth factor receptor 2 (HER2)”: luminal-BC (ER+, PR+/−, HER2 unamplified), HER2-BC (HER2 amplified, ER/PR +/−) and triple-negative-BC (TNBC) (ER−, PR−, HER2 unamplified) [5-7]. For clinical implementation purposes, the proliferation marker Ki-67 has also been taken into account [8]. These molecular biomarkers then stratify BC into five subtypes: liminal-A (ER+, PR+/-, HER2-unamplified, Ki-67 ≤ 14%), luminal-B (ER+, PR+/-, HER2-unamplified, Ki-67 > 14%), TNBC (ER−, PR−, HER2-unamplified), HER2-amplified-luminal (HER2-amplified, ER+, PR+/-) and HER2-amplified-non-luminal (HER2-amplified, ER-, PR-) [9]. The cut-offs of Ki-67 are various from 1% to 29% and remain debatable, thus limiting its clinical utility [10]. In recent decades, it has also become possible to imply specific therapies based on these molecular subtypes' associated parameters, like endocrine therapies for ER-positive or anti-HER2 therapies for HER2 amplification subtypes, which have dramatically improved the prognosis of specific patient groups [11-14]. However, in BC patients with ER-positive undergoing endocrine therapy, 20% of them are either ineffective or resistant to endocrine therapy [15]. The molecular subtype based on gene expression profile has also been widely used to support making treatment decisions for BC patients [16, 17]. Molecular subtype classification has achieved therapy implementation. However, the heterogeneity of tumor cell molecular subtypes and their interaction with tumor-associated cells in that TME enables different types of BC to have distinct therapy strategies and exhibit different therapeutic effects.

In search of constant improvement, current therapy concepts move one step further and include the tumor microenvironment (TME). One approach used to treat cancers is introducing chimeric antigen receptors (CARs) into bulk peripheral T cells, termed “CAR-T therapy” [18]. However, solid tumors respond poorly to “CAR-T therapy” [19]. In TME, the expression of immune checkpoints molecules and the presence of large numbers of immunosuppressive cells, including tumor-associated macrophage (TAM), may contribute to this low response rate [20-22]. The remarkable progress of therapeutic immune-checkpoint inhibition has revolutionized cancer therapy [23], which also displays a resistant and low response in cancers, including BC [24-26]. Despite improvements through the implementation of biologically individualized therapies, BC patients remain who experience recurrence and distant metastasis or therapy resistance.

To imply more effective and precise treatment of BC, we need to know about BC-TME and its genomic and transcriptomic alteration response to different TME, which consist of tumor cells and tumor-infiltrating immune cells (TIICs), tumor-associated adipocytes, and other kinds of tumor-associated cells [27].

## 1.2 Characteristics of Tumor-Associated Macrophage

Macrophages that infiltrate the TME are named TAMs. The generally accepted theory of TAM polarization is that the peripheral blood-derived monocytes undergo M1- or M2-like polarization

in response to various stimuli in the TME [28]. The M1-like phenotype is characterized as an anti-tumor state, whereas the M2-like phenotype is a pro-tumor state [29].

Research on the polarization of TAM is increasing and deepening. Indeed, its role in the TME is far more complicated and fine-scaled than we initially thought. TAM is not actually polarized into the M1 or M2 phenotype. Due to its heterogeneity, the theory mentioned above is not sufficient for understanding the complicated functions of TAM when the living condition turns *in vivo*. They are either from the resident macrophage, which differentiates in situ, or circulating monocytes and myeloid-derived suppressor cells (MDSC) recruited to TME and then differentiated into TAMs [30]. Different from existing in a non-tumor context, when turned to a tumor context, the population and transcriptomes of macrophages were reported to be altered [31]. The phenotype of macrophages in the TME is no longer limited to M1 or M2, and its phenotype may be between M1 and M2 or may be far beyond M1 and M2 [32]. M1 or M2 markers can be expressed on individual TAM [32]. They cannot be simply used to distinguish whether the TAM is M1-like or M2-like [32]. For example, CD163+TAM and CD206+TAM are commonly associated with M2-like phenotype, were found to function as M1-like TAMs in stimulating T cell activity in gastric, intestinal, and ovarian cancer [33]. Depending on the currently widely used biomarkers, it is unclear whether TAMs exert either pro-tumor or anti-tumor effects [34]. Understanding the activation statutes and functions of TAMs relies greatly on the M1-M2 paradigm, which can be a distortion of our perception. Our knowledge of macrophage markers is far from enough to uncover the identity and complexity of macrophages in the TME. The positive expression of multiple markers is now more recommended to classify the phenotype of TAM than to use the dichotomous classification between M1- and M2-like [35].

Even turned to the unique population termed TAM under cancer context, TAM also shows tissue-specific programming [31]. Tumors of different tissue types have tissue-specific infiltration of the TAM population [31]. For instance, TAM infiltration act as a poor prognostic indicator of pancreatic cancer [36] and bladder cancer [37], while a favorable prognostic indicator of ovarian cancer [38] and colorectal cancer [39]. In addition to the different tumor tissues, TAM's location in the TME can also be a reason. Distinct location of TAM within the tumor tissue can reflect intra-tumor heterogeneity of TAM and correlate with different tumor progression. For instance, in “non-small cell lung cancer (NSLSC)”, a higher abundance of TAM in tumor tissue relates to a better survival outcome, whereas a higher quantity of TAM in the tumor-stroma section of the tumor tissue turned out to relate a worse prognosis [40, 41]. Additionally, in gastric cancer, it was found that TAMs in tumor stroma and tumor margin have a stronger relationship with tumor progression than TAMs in tumor nest [42]. As well as for the progression of “esophageal squamous cell carcinoma” and melanoma, TAMs in tumor stroma is more prominent than the TAMs in tumor nest [43, 44].

These previous studies indicated that TAM's distinct phenotypes and functions in the TME depend on its inter-tumor and intra-tumor heterogeneity, related to cancer types, polarization status, and the localization of TAMs. To discriminate the different functions of TAM, the condition that TAM is involved in needs to be clarified. It seems to lack detailed knowledge about the functionally activated statues of TAMs within different TME.

## 1.3 The Role of TAM in BC

### 1.3.1 Communication between TAMs and Tumor cells in BC

In general, the role of TAM in BC can be described as either pro-tumor or anti-tumor. TAM is also a macrophage essentially with the ability to present tumor antigens to T cells and the capability of killing tumor cells directly [45]. Its anti-tumor effects are involved in the anti-HER2 therapy in BC [46]. However, increasing evidence suggests that breast-tumor-associated macrophages (Br-TAMs) exhibit dominantly a pro-tumor phenotype. TAM is recruited into the tumor or surrounding tissues derived factors. In turn, TAMs secrete cytokines, chemokines, growth factors, and inflammatory mediators and thereby play a role in regulating BC tumor cells both in primary tumor and in metastasis sites *in vitro* and *in vivo*, including benign tumor to malignant tumor transition, tumor cell intravasation and extravasation, tumor initiation, tumor cell proliferation, tumor cell migration and invasion, angiogenesis [45, 47-51]. The infiltration level of TAMs increases when the malignancy of BC progresses in the mouse model [52, 53]. Interestingly Br-TAMs can produce estrogen to promote tumor cell proliferation in vitro and confirmed in tissue samples of BC patients [54].

Tumors evade natural immune surveillance through immune ignorance or active immune suppression. In BC, tumor cells evade immune surveillance through decreasing MHC-I expression [45]. TAMs suppress the anti-tumor immune response via activating immunosuppressive cells and inactivating cytolytic effector T cells [45, 49-51]. In addition, how TAMs affect tumor progression is related to their location in tumor tissue. For example, in BC, TAMs in tumor nest promote angiogenesis more than TAMs in tumor stroma [55].

### 1.3.2 The Prognostic role of TAMs in BC

In BC, TAM is an aggressive feature. TAMs accumulate in poor vascularization, hypoxia, and necrosis [56, 57]. A high level of TAM infiltration leads to increased proliferation and poor differentiation of tumor cells [58]. Furthermore, TAM infiltration is positively correlated to lymphatic angiogenesis and blood angiogenesis in BC [59]. BC patients with more TAMs infiltrating tend to have higher grades, larger tumors, and more necrotic tissue [60]. Moreover, a high level of TAMs is inversely correlated to ER [61], PR [58], and HER2 expression [60]. Then it is understandable that TAM is more likely to infiltrate TNBC-type tumors [62, 63].

Multiple clinical studies demonstrated that the higher TAM infiltration independently indicates the poorer prognosis of BC [50, 64-67]. A high density of a combination of TAMs, tumor cells, and endothelial cells relates to distant metastasis of BC [68, 69]. Another clinical study demonstrated that higher TAM quantity leads to poor survival [70]. However, patients with lymphatic metastasis were reported to have a lower TAM infiltration, indicating that the phenotype of TAMs may be altered when the location of TAMs transfer to the lymph node [70].

### 1.3.3 The Specific of Br-TAM

Due to the inter-tumor and intra-tumor heterogeneity of TAMs, single-cell sequencing (scRNA-seq)-dependent studies can display a more precise and specific role of Br-TAMs. A recently identified Br-TAMs signature showed neither a preferential enrichment for M2-associated genes nor M1-associated genes detected by Cassetta et al. [31]. In addition, several well-known M2-like TAMs markers, such as *Arg1* (arginase-1), are not specifically or even lower expressed in Br-TAMs [31]. Interestingly, another study recently identified two new TAMs phenotypes using sin-

gle-cell sequencing (scRNA-seq) analysis in BC [71, 72]. Their signatures are outside the conventional M1/M2 classification, termed lipid-associated macrophages (LAMs) [71]: LAM1 and LAM2. In addition, an application of single-cell mass cytometry [73, 74] in BC samples demonstrated that Br-TAMs enriched for immunosuppressive TAMs phenotypes [75]. Br-TAMs and BC tumor cells can regulate each other via an auto-regulatory loop [31]. Furthermore, Br-TAMs signature is highly correlated to aggressive BC, and poor prognosis [31], which is consistent with the outcome of TMAs infiltration in BC mentioned above.

### 1.3.4 The Therapy of Targeting TAMs in BC

The pro-tumor TAMs are promising therapeutic targets as they can modulate the TME through immunosuppression or by promoting tumor cell growth and invasion [51, 76]. The therapy strategies for targeting TAM can be summarized into two groups: reducing the number of pro-tumor TAMs or reprogramming the TAM from pro-tumor phenotype to anti-tumor phenotype [77, 78]. Preclinical evidence has shown that several macrophage-targeted therapies can benefit in vivo of the BC model. Colony-stimulating factor (CSF)-1 can promote M2 macrophage polarization [79], and blocking CSF-1 or its receptor decreases the M2-like TAMs infiltration, suppress tumor growth, and reverses chemotherapy resistance in vivo [80, 81]. However, the clinical trials associated with this strategy in other solid tumors turned out to be not uniformly effective [82]. The same situation happens to anti-CCL2/CCR2 approach. Although shown effective in preclinical models of BC [83], it has been reported as failed in clinical trials of other solid tumors [84, 85]. Further preclinical experiments revealed even worse outcomes for this treatment strategy in BC [86].

Instead of killing, turning the “enemy” into a “friend” makes more sense. And the alteration of the cell phenotype is based on the alteration of the transcription of gene programs. Toll-like receptors (TLRs) agonist has been reported to be effective in preclinical models that can re-polarize TAMs from a “tumor-friend” phenotype to a “tumor-enemy” phenotype and are well-tolerated [87-90]. In addition, a clinical trial from a small group of BC patients (n=10) indicates that TLR agonists imiquimod has shown a beneficial effect on BC patients with skin or chest wall metastasis and are well-tolerated [91]. Blocking TGFβ has also been confirmed to have this “re-programming” ability in BC from preclinical models [92]. Additionally, for addressing the challenge of CAR-T therapy, CAR macrophage (CAR-M) is also introduced to BC immunotherapy [93], which has achieved gorgeous success in preclinical mode [94].

Overall, the functions of subpopulations of TAM showed markedly intra-tumoral heterogeneity. Knowing more about how TAM phenotypes are affected by intra-tumoral conditions, e.g., distribution and the underlying transcriptional regulatory mechanisms will facilitate advances in BC immunotherapy. Numerous clinical studies demonstrated that TAM infiltration leads to poor prognostic outcomes in BC. However, whether distinct phenotypes of TAM distinguished by different localizations show different characteristics and prognoses of BC has not been fully elucidated.

## 1.4 The Role of Macrophages in Breast Adipose Tissue

Either adipose tissue or adipocytes can promote the proliferation of BC cell lines *in vitro* [95]. Adipocyte in BC acts as an active facilitator and interacts with BC tumor cells during carcinogenesis [96]. Adipocyte is a crucial component of BC-TME. Adipocyte-tumor cell interaction is a vicious cycle that promotes BC progression: tumor cells modify the surrounding adipocytes. The

tumor-modified adipocytes modify the tumor cells, thus to a more aggressive phenotype [97]. Therapies targeting breast adipose tissue are thought to educate the tumor-modified phenotype to normal adipocyte, thus suppressing its vicious circle with tumor cells. For example, PPARγ agonists' implementation in anti-adipogenic and anti-tumor has succeeded in preclinical modals in BC [98].

Adipose tissue macrophages are an important component of adipose tissue. Crown-like structures (CLS) are identified as obesity-associated and adipocyte hypertrophy-induced (also can happen in lean subjects) alterations of white adipose tissue macrophage that aggregated surrounding individual dead or dying adipocytes, which is extremely rare in lean subjects while abundance in obese subjects [99]. CLS is considered to act as a pro-inflammatory role in obese subjects [99] and is observed in obese breasts irrespective of the presence of cancer [100-103] and also in normal-weight BC patients undergoing mastectomy [104]. However, this pro-inflammatory CLS in early-stage BC patients undergoing mastectomy indicates a poor prognosis [105]. In addition, BC in obese women is more aggressive and has a poorer survival outcome and lower therapy response to chemotherapy and radiotherapy than standard body mass index (BMI) individuals [106]. Higher infiltration of CLS infiltrating in the BC of obese women could be a reason [106, 107]. Indeed, CLS is highly present in obese-related breast adipose tissue of BC and leads to a poor survival outcome [105].

In obese individuals, adipocytes can recruit and activate adipose tissue macrophages by releasing TNF or fatty acids [108]. Macrophages of obese-adipose tissues are polarized to M1, while macrophages of normal-adipose tissues are polarized to M2 [109]. In breast adipose tissue of normal BMI individuals, the number of M2 phenotype macrophages is four times that of the M1 phenotype. In contrast, in obese-breast adipose tissue, the number of M2 phenotype macrophages is only close to half of the M1 phenotype [110-112]. Obesity leads to a phenotypic transition of adipose tissue macrophage from M2 phenotype to M1 phenotype [109]. In addition, a phenotype is present in obese but not "lean" subjects, described as $F4/80^{+}CD11c^{+}$macrophage, which expressed a mixed gene profile of M1/M2 gene programs [109, 113]. Taken together, the role of TAMs in obsess-related and in normal BMI breast adipose tissue can be phenotypically different might also lead to distinct functions. Furthermore, multivariate analysis has demonstrated that even taking BMI into account, fatty breast remains associated independently with poor prognosis in BC [114]. Tumors in these fatty breasts were infiltrated with more M2-like TAMs [114]. However, the exact location and the specific phenotype of these infiltrating TAMs remain unclear.

In conclusion, breast adipose tissue promotes the progression of BC independent of the BMI of patients. The interaction of BC tumor cells and tumor-associated adipocytes contributes to this pro-tumor role of breast adipose tissue. However, previous studies also indicate that TAMs in the adipose tissue might also be necessary. Further evidence is needed to confirm this speculation.

## 1.5 Transcriptional Regulation of Macrophage Polarization by Transcription Factors

Gene programs transcription determines the proper temporal and spatial expression of encoding genes to maintain the proper functionality of cells, tissues, and organs [115]. It is controlled by a complicated transcriptional regulatory system that includes genome regulatory elements, abundant non-coding RNAs, and protein transcriptional regulators like transcription factors, co-factors,

and chromatin modifiers [115-117]. Changes in these regulators can alter transcriptional programs [118]. Transcription factors (TFs) are the key transcriptional regulators binding to the enhancer of target genes via their DNA binding domain, then translating the gene expression programs to cellular phenotype [117, 118]. Generalized TFs include “nuclear receptors (NRs)” and “C2H2-type zinc finger proteins(ZNFs)” broadly[119]. NRs act as ligand-activated TFs that function as heterodimers with their co-factors[120]. Moreover, NRs are the environmentally responsive regulator of gene expression [121]. Different compounds of NRs-related regulator determines the distinct transcription of different gene programs [122-126]. C2H2-type ZNFs act as narrow-sense TFs and can interact with NRs via their triple-zinc fingers or other binding domains [119, 127].

Macrophages are important coordinators of immune responses and tissue development and function under homeostatic and pathological contexts [128-130]. Macrophages can be involved in diverse biological processes (BPs) because they are endowed with exceptional plasticity [131]. Initially, M1/M2 paradigm is used to describe distinct macrophage activation programs triggered by IFNγ and IL-4, respectively. The tremendous complexity behind functional macrophage polarization has been widely recognized and demonstrated [132]. The transcriptional regulation of the phenotype of macrophages is influenced by different factors like C2H2-type transcriptional factors (TF), nuclear factors (NRs), and epigenetic changes. Epigenetic regulation, such as Histone deacetylases (HDACs), etc., are involved crucially in macrophage polarization [133]. For example, HDCA3 acts as an M1 polarization propeller and an M2 polarization blocker [134, 135].

TFs are the main regulators involved in various signaling pathways that could impact macrophage polarization and function. Distinct members of the TF family such as “signal transducer and activator of transcription (STATs)”, “hypoxia-inducible factors (HIFs)”, “interferon regulatory factors (IRFs)”, “nuclear factor kappa B (NF-κB)”, as well as “krüppel-like factors (KLFs)” have been demonstrated to regulate the macrophage polarization [136]. STAT1 can be activated by IFNγ etc., regulating transcription of genes directing M1 phenotype polarization, while STAT3 and STAT6 pathways can be activated by IL-4, etc., regulating transcription of genes directing M2 phenotype polarization [137-141]. HIF1α directs M1 phenotype polarization, while HIF2α directs M2 phenotype polarization [142]. In addition, HIF1α can also involve STAT3 mediated M2 macrophages polarization [143]. IRF3 and IRF5 increase the gene expression of the transcriptional program towards the M1 phenotype, while IRF5 induces the expression of the gene program towards the M2 phenotype [144-146]. Activation of NF-κB drives transcription of M1-associated gene programs [147]. However, NF-κB can also inhibit M1 phenotype polarization and promote M2 phenotype polarization under inflammation [148, 149]. NRs, such as PPARγ [150] and PPARδ [151, 152], transcriptionally regulate distinct gene programs associated with M2 phenotype activation. In addition, PPARγ in adipose posed tissue macrophage-specific PPARγ promotes M2 macrophage polarization in obese subjects [153]. And SATA6 can act as a facilitator of PPARγ in regulating gene expression towards M2 macrophages [154]. PPARgamma-coactivator-1beta (PGC-1β) initiates alternative M2 activation and suppresses inflammation [155].

Furthermore, the antitumor M1-like and pro-tumor M2-like phenotypes of TAMs can be intertransformed during the response to the changes in the TME [136]. This plasticity also results in different TAM subpopulations [132]. The flexible states of TAMs highlight TAM-reprogramming as a promising therapeutic concept to tune their phenotypes and functions to meet the demands of antitumor defenses. TAM polarization has been successfully stimulated to enhance antitumor function. TFs such as STATs are involved in this regulation of TAMs polarization. For example, in malignant glioma, the inhibition of STAT3 or STAT6 substantially reduces M2-like polarization

[156]. Consequently, TAMs exhibit a more M1-like phenotype, enhancing antitumor immunity [156].

Contrary to its dual role in “normal” macrophage (named as a contrast to the macrophage under tumor context) aforementioned, HIF1α only directs TAMs towards an M2-like phenotype in TME [157, 158]. TAMs expressed M1-like transcriptional program via inhibiting NF-κB signal and activating IRF-3/STAT1 signal [159, 160]. However, NF-κB activation has also been required for TAMs polarized to an immunosuppressive M2-like phenotype[161]. The inactivation of NF-κB can transit M2-like TAMs to tumor cytotoxic M1-like TAMs [161]. Furthermore, studies have shown that blocking specific TFs could exert cytotoxicity with a preference for specific cell types of TAMs [162-164]. To better distinguish the anti-tumor and pro-tumor phenotypes of TAMs in the TME and apply them to tumor immunotherapy, further studies on the transcription of specific gene programs and the underlying transcriptional mechanisms are in high demand.

## 1.6 Transcription Factors KLFs and their roles in Macrophage Polarization

KLFs family TFs belong to the triple-fingered proteins of the C2H2-type zinc finger family. Structurally, the C-terminus of KLFs is conserved while their N-terminus is variable [165]. In addition, due to the C-terminus of KLFs exists three tandem $C_2H_2$-type zinc fingers [165]. They are characterized as triple-fingered C2H2-type ZNFs [165]. These homologous zinc finger motifs in the C-terminus of KLFs bind to CACCC-, GC-, or GT- box elements found in the promoter or enhancer DNA [166]. The N-terminus of KLFs bind to their cofactors[167]. And the different bindings of the C-terminus and N-terminus contribute to distinct cellular functions that KLFs involve in [167]. In addition to the C-terminal DNA binding and N-terminal transcription regulatory domains, within KLF4, KLF8, and KLF11, the nuclear localization signaling (NLS) domain is closely next to or among the three zinc finger motifs [167]. The NLS exerts the function of KLF nuclear localization[167].

Functionally, transcriptional regulators KLFs regulate various cellular phenotypes and functions by regulating the transcription of related gene programs of cell differentiation, proliferation, apoptosis, migration and invasion, and tumor cell stemness [167-170]. Importantly, KLFs are also required for immune cell differentiation, such as lymphocytes, monocytes, macrophages, and adipocytes [165, 169, 171-174]. Besides, they are also involved in the macrophage’s immune response [175]. KLFs target different gene programs and thus regulate various cellular functions depending on the environment where the cells are located [176-180]. Mechanistically, on the one hand, KLFs regulate gene transcription directly [120, 181]. On the other hand, KLFs act as cofactors or downstream mediators, directly or indirectly influencing the activity of NRs that regulate these cellular functions [120, 181]. NRs are responsive environmental factors. KLFs have been reported to interact with nuclear receptors, influencing the NRs mediated transcriptional activity [120, 182], such as ER, PR, and PPARγ [120]. KLFs and NRs can cooperate through direct or indirect interaction and then regulate the target genes [181]. In addition, KLFs can affect the transcription of NRs target gene programs by altering the expression of the NRs [181]. Besides, the expression of KLFs can also be altered by nuclear receptors and then lead to the KLFs responsive genes [181]. These models are the primary interaction mechanism between KLFs and NRs in gene transcription.

Several KLFs members have already been revealed to be involved in the polarization of macrophages. KLF4 also plays a dual role in macrophage polarization as its role in BC. KLF4 has been demonstrated to cooperate with NF-κB inducing the inducible nitric-oxide synthase (iNOS) expression, which directs pro-inflammatory M1 phenotype polarization [183]. However, KLF4 is also found to cooperate with STAT6 to direct transcription of the gene program of the M2 phenotype and inactive NF-κB signal to inhibit transcription of the gene program of the M1 phenotype [184]. Consistently, KLF4 can promote the transition from M1 to M2 phenotype through upregulation of the level of liver X receptor (LXR) [185]. KLF2 attenuates HIF1α-induced M1 phenotype polarization [186]. In contrast, KLF6 cooperates with NF-κB to promote macrophage motility and recruitment, polarize them into an M1 phenotype, and inhibits PPARγ to suppress PPAR γ induced M2 phenotype polarization [187-189]. Gene program regulation at the transcriptional level is vital for macrophage polarization and TAMs re-plasticity or re-programming. However, a paucity of phenotypic regulation of KLFs in macrophage polarization, especially in TAMs in specific tissues, suggested the necessity for additional studies focusing on the interaction between KLFs and TAMs.

## 1.7 The Role of KLFs in BC

Seventeen KLF members are extensively studied in human tissue [165]. They affect the formation and progression of cancers [165, 190]. Remarkably, the aberrant expression of several KLFs is observed in BC [191]. They regulate cell proliferation, apoptosis, differentiation, invasion, migration, and cell metabolism of BC [191]. In addition, KLFs are highly correlated to the survival outcomes of BC patients [191].

### 1.7.1 From a clinical perspective

The effect of KLF4 on BC remains ***controversial***. Previous research reported that a high level of KLF4 expression was observed in BC tissue samples, while low expression was detected in adjacent tissue [192, 193]. The higher expression of KLF4 in BC does not significantly influence MFS [194]. In contrast, a higher nuclear KLF4 protein level was shown to have a poor outcome and was associated with aggressive features of BC in early-stage [195]. Interestingly, however, contrary to previous studies, it was noted that KLF4 is lower expressed in BC samples than that in normal samples [196-199]. In addition, KLF4 negatively relates to tumor grades and lymph node states [196]. Furthermore, KLF4 indicates a favorable prognosis of BC [199, 200].

***Poor outcome indicator.*** The expression of KLF5 has shown no difference between BC and normal [201]. However, it was also noted that KLF5 is higher expressed in BC cases than in normal cases [202]. It was found that *KLF5* is positively correlated with aggressive features of BC, such as oncogene *HER2* and proliferation marker *MKI67* expression [201]. Furthermore, KLF5 acts as a poor prognostic factor of BC [194, 201, 202]. Interestingly, KLF4 and KLF5 (termed KLF4/5 afterward) have a prognostic synergy effect. High KLF4/5 expression leads to a poor MFS of HER2-amplified BC [194]. Moreover, KLF6-SV1 is highly expressed in lymphatic metastasis individuals of BC [203]. And the elevated expression of KLF6-SV1 independently relates to the poor prognosis of early-stage BC patients [203]. In addition, KLF8 is aberrantly high in BC tissues [204, 205]. And although the expression is decreased in BC, KLF17 is associated with poor survival outcomes [206].

***Favorable outcome indicator***. KLF2 is lower expressed in BC than in normal breast tissue and positively associated with the survival of BC patients [207]. BC tissues show significantly reduced expression of KLF9 compared to normal breast tissue [208]. Additionally, KLF10 is lower expressed in BC tissues than in adjacent breast tissue and negatively associated with lymphatic metastasis [209, 210]. KLF10 positively relates to BC prognosis [210].

However, the prognostic relevance and expression pattern of KLF11 in BC patients remains ***unknown***, not to mention the establishment of KLF11-related prognostic models. The incidental results of two studies reported that KLF11 DNA is hypermethylated in lower-grade BC [211], and the mRNA expression of *KLF11* is reduced in 50 BC samples [178].

### 1.7.2 From a functional perspective

#### *Dual roles*

KLF4 expression is lower in BC cell lines than in the non-transformed breast cell line [197]. The function of KLF4 is determined by cell types and cell microenvironments. KLF4 can be an oncogene in BC. Furthermore, KLF4 maintains the stemness of BC stem cells irrespective of the molecular type [212, 213]. Consistently to the oncogenic role of KLF4 in BC, the knockdown of KLF 4 inhibits cell migration and invasion *in vitro* and decreases tumor metastasis in mice models [213]. In addition, KLF4 can also promote estrogen-induced growth of BC cells [193]. KLF4 can also be a tumor-suppressor in BC. Overexpression of KLF4 inhibits the growth and proliferation of TNBC cell lines [196, 200]. Similar to the inhibitory role of the KLF4 in TNBC cell lines, Yori et al. revealed that KLF4 overexpression prevents the epithelial-mesenchymal transition (EMT) process act as a metastasis suppresser *in vitro* and *in vivo* [214, 215]. In addition, KLF4 inhibits proliferation and induces apoptosis of HER2-type cell lines [197]. And KLF4 inhibits the estrogen-dependent growth of luminal cells [198]. Overexpression of KLF4 in luminal ER-positive cell suppress cell viability, migration and invasion [199]. Moreover, KLF4 functions a suppressor of angiogenesis in BC cells [216].

The role of KLF5 in BC also appears to be context-dependent. KLF5 is highly expressed in TNBC [217, 218]. KLF5 can act as an oncogene in BC cell lines. It promotes proliferation, migration, and invasion of TNBC cells [219-222]. In addition, KLF5 can promote proliferation and de-differentiation of luminal cell lines [202, 218, 223]. Moreover, KLF5 inhibits cell apoptosis in HER2-amplified cell lines [224] and induces EMT [225]. However, it also can act as a tumor suppressor. KLF5 inhibits oestrogen-induced proliferation of ER-positive luminal BC cells [226]. KLF4 and KLF5 are correlated positively with each other *in vivo* of BC [194]. Intriguingly, when acting in an oncogene role, KLF4 and KLF5 have a cooperative relationship in BC [194].

#### *As an oncogene*

Interestingly, KLF4α, the splicing of KLF4, acts as a KLF4 antagonist to activate the transcription of target genes, thereby stimulating the proliferation of TNBC cell lines [227]. Moreover, as a splicing of KLF6, KLF6-SV increases EMT [203, 228, 229]. In addition, KLF8 is higher expressed in TNBC cell lines than in luminal type or HER2 type [204, 205, 230], and it promotes proliferation, EMT, and lung metastasis of TNBC cell lines [204, 231, 232]. KLF8 also can induce pro-tumorigenic BC stem cells [233].

#### *As a tumor suppressor*

KLF2 suppresses tumor growth of TNBC cell line *in vivo* [207]. Furthermore, KLF6 suppresses ER-mediated cell growth in ER-positive BC cells but does not affect cell growth in ER-negative

cells [234]. Moreover, KLF9 was significantly higher expressed in luminal and HER2 cell lines than in TNBC cell lines [208]. It suppresses TNBC cell line migration and invasion [208, 235]. In addition, KLF10 protein levels were higher in less invasive BC cells than in more invasive cell lines [209], and it induces apoptosis of luminal cells lines [236]. KLF10 was also found to inhibit BC cell invasion and suppress tumorigenesis and lung metastasis in mice models [209]. Furthermore, KLF17 has been reported to suppress ER-mediated progression of BC [206], and the inhibition of KLF17 expression promotes EMT and invasion of BC cell lines [237].

***Indirect studies of KLFs in BC***

MiR-30d decreases cell apoptosis and promotes the EMT process of BC cells via altering the expression of KLF11 [238], while miR-205 induces apoptosis directly targeting the 3'-UTR of KLF12 in TNBC cell lines [239]. However, the direct role of these KLFs in the specific function in BC remained largely unknown.

### 1.7.3 From a therapeutic perspective

Since KLFs regulate multiple BPs and are essential for the function of BC tumor cells. KLFs have been suggested as a potential therapeutic target, and therapy concepts that target several of this family have been achieved in BC.

Tamoxifen is widely used for endocrine therapy of BC. KLF4 has decreased in tamoxifen-resistant BC patients, and overexpression of KLF4 can enhance the sensitivity of BC cells to tamoxifen treatment, indicating that targeting KLF4 therapy can be a promising strategy for tamoxifen-resistant patients [199]. Moreover, KLF4 is associated negatively with a lower pathological complete remission (pCR) in locally advanced BC patients receiving neoadjuvant chemotherapy [240]. And KLF4 can independently indicate the pCR of patients who underwent neoadjuvant chemotherapy [240]. In addition, dexamethasone is used as a pre-chemotherapy drug to prevent the side effects of chemotherapy. However, it can also induce resistance to docetaxel and cisplatin in TNBC cells via the upregulation of KLF5 expression *in vitro* and *in vivo* [241]. Importantly, when targeted to KLF5, dexamethasone loses its function of promoting tumor growth [241], indicating that targeting KLF5 can be a promising solution to chemotherapy resistance in TNBC patients [241]. Moreover, Mifepristone is widely used for abortion, can decrease the TNBC cancer stem cell population through KLF5 downregulation [242]. Furthermore, Compound 17 (FZU- 00,004) has been designed to improve the pharmacokinetic property of mifepristone on TNBC by inhibiting KLF5 expression [243]. Additionally, Mithramycin A, an inhibitor of DNA and RNA polymerase, inhibits proliferation and induces apoptosis of TNBC cells via the downregulation of KLF5 [244].

Interestingly, HER2 inhibitor lapatinib and trastuzumab target HER2-amplified BC, and they can upregulate both KLF4 and KLF5 protein levels in BC [194]. Knockdown of KLF4 or KLF5 can sensitize the HER2 type cells to lapatinib [194]. Furthermore, combined inhibition of KLF4 and KLF5 inhibits anchorage-independent growth of BC cells, promotes anoikis, and inhibits tumorigenicity in mice models [194], indicating that KLF4 and KLF5 act as cooperative oncogenes and critical regulators in lapatinib resistance.

Zoledronic acid (ZA) is used to treat bone metastases in BC and can decrease cell viability and induce apoptosis of luminal-type cells via enhancing the expression of KLF2 and KLF6 [245]. And combined treatment with probenecid increases the expression of the ZA-induced target gene KLF2 [246]. Moreover, to some extent, KLF10 can indicate ER status and BC patients' response to endocrine therapy [210]. Furthermore, overexpression of KLF17 sensitizes ER-positive BC cells to endocrine therapy [206]. Moreover, paclitaxel is a widely used cytotoxic antitumor agent,

and its role in inhibiting BC cell invasion and migration is partly based on the downregulation of KLF17 [247]. Furthermore, since no-cytotoxic melatonin and cytotoxic paclitaxel both can increase KLF17 expression and then inhibit BC cell invasion, combining the paclitaxel with melatonin can be better than only using a single of them [248].

The roles of several KLFs in BC have been systematically summarized, but they act as oncogenes or tumor suppressors have not yet reached consensus and need to be further explored in BC. However, there is no comprehensive study on the role of KLF11 in BC. Therefore, it is worth exploring whether KLF11 actually acts as an oncogene or a tumor suppressor in BC, implying its potential ability in predicting the prognosis and targeting therapy of BC patients.

## 1.8 KLF11 and Its Role in Cancers

KLF11 as a member of the KLFs family has been initially characterized as a transforming growth factor-beta (TGFβ) inducible early gene [249]. However, several studies have demonstrated that it is also inducible by growth factors and hormones, and several cytokines [250-252]. After induction, KLF11 binds to CACCC-, GC-, or GT- box elements of promoters DNA of target genes and then leads to various chromatin remodelings and epigenetic factors recruitment, such as mSin3A [253], heterochromatin protein 1(HP1)-HMT [254], and p300 [255]. KLF11 can regulate several gene network transcriptions as both an activator and a repressor [255-257].

### 1.8.1 KLF11 is involved in the regulation of normal cells

KLF11 suppresses cell proliferation and induces cell apoptosis of untransformed cells such as pancreatic epithelial cells, normal ovary cells, etc., *in vitro* and *in vivo* [178, 249, 251, 258, 259]. And the knockdown of KLF11 can abolish TGFβ-induced inhibition of cell growth and c-myc expression [260]. KLF11 inhibits Ras-mediated neoplastic transformation and induces cell apoptosis of transformed fibroblasts [178, 261]. In addition, KLF11 is downregulated in the Ras-mediated transformed normal fibroblasts [261].

From a mechanism perspective, KLF11 can strengthen TGFβ-induced cell growth inhibition and TGFβ-induced cell apoptosis [179, 259, 260]. The mechanism of KLF11 enhancing the TGFβ signaling pathway is documented as follows: TGFβ-induced growth inhibition is via activating the intracellular Smad signaling pathway [262, 263]. This signaling is mediated by the heteromeric complexes of specific TGFβ-type II and -type I kinase receptors, which phosphorylate the Smad2/Smad3 [263]. Phosphorylated Smad2/Smad3 forms a complex with Smad4 [264]. Afterward, the complex locates in the nucleus and regulates gene transcription, including KLF11 [264]. KLF11 then represses the expression of Smad7 by binding its promotor, which is mediated through the recruitment of the histone deacetylase co-repressor mSin3a [179, 253, 265]. There is a negative feedback loop within the TGFβ/Smad signaling pathway, Smad7, which binds to activated TGFβ type I receptors and prevents entry and phosphorylation of the Smad2/Smad3 receptors [266, 267]. Due to the induction of upstream KLF11, inhibitory Smad7 expression is decreased, which leads to the disruption of the negative feedback loop of TGFβ/Smad signaling to further strengthen the TGFβ/Smad signaling [179]. Disruption of TGFβ/Smad signaling is common in human cancers and facilitates tumor cells to evade TGFβ-induced cell inhibition [268, 269].

In addition, underlying the TGFβ-induced cell inhibition of untransformed epithelial cell, KLF11 also interact with Smad3 forming a transcription complex binding to the TGFβ-inhibitory element in the c-myc promoter [260] to repress its expression then inhibit cell growth. The mechanism of

KLF11 induces cell apoptosis also can be the inhibition of anti-apoptotic Bcl-XL expression in untransformed cells [258].

### 1.8.2 KLF11 is involved in the cellular immune response to the microenvironment

KLF11 can be upregulated by pro-inflammatory chemokines such as tumor necrosis factors alpha (TNFα) and lipopolysaccharide (LPS), and overexpression of KLF11 inhibits the expression of pro-inflammatory adhesion molecules, which leads to inflammation inhibition [252]. Vice versa, knockdown of KLF11 can enhance the cellular inflammatory response [252, 270]. From the mechanism perspective, in part, KLF11 inhibits the transcriptional activity of NF-κB-mediated TNFα-induced pro-inflammatory adhesion molecules by interacting with NF-κB [252, 271]. Therefore, KLF11 inhibits the recruitment of leukocytes, which are dependent on the inter-cellular adhesion ability in vitro and in vivo [252].

### 1.8.3 KLF11 is involved in cancers

The role of KLF11 in carcinogenesis is context-dependent. The expression of *KLF11* mRNA has been detected in small sample groups demonstrating its downregulation in pancreatic, breast, renal, ovarian, colon, and gastric cancers [178].

***Indicate a Dual role in Pancreatic cancer.***

KLF11 reveres its role as a cell growth suppressor to a cell growth promoter in pancreatic cancer. This reversal primarily depends on that TGFβ-induced inhibition of proliferation is inhibited in pancreatic cancer cells due to the RAS mutation [260]. Consequently, KLF11 turns out to promote tumor growth [260]. From the mechanism perspective, due to the oncogene-RAS mutation, the KLF11-mSin3a interaction is disrupted by the phosphorylated KLF11, which diminishes the termination of the inhibitory Smad7 loop in the TGFβ-inhibitory effect [179]. In addition, due to the RAS mutation, the ERK disrupts the complex formation of KLF11-Smad3 or/. It inhibits the binding of KLF11-Smad3 to the TGFβ-inhibitory element of c-myc [260].

Inconsistently, it has also been reported that the overexpression of KLF11 in pancreatic cancers cells inhibits proliferation, decreases anchorage-independent growth, induces apoptosis, reduces colony formation in tumor cells, and also inhibits tumor formation and pancreatic tumorigenesis in mice models [261], which consistent to its role in untransformed pancreatic cells [178]. From the mechanism perspective, KLF11 regulates these functions partly through that the full length KLF11 protein (independent of its co-repressors) directly binding to the promotor of cyclin A (*CCNA2*) to suppress its expression and then arrest the cell cycle [261].

***Indicate a Dual role in Esophageal cancer.*** KLF11 inhibits the proliferation of esophageal adenocarcinoma cell lines *in vitro* via its suppression of the biosynthesis of PGE2. However, when in esophageal cell lines with upregulated EGFR/AKT signaling, the tumor-suppressor role of KLF11 appears to be reversed [272]. From a mechanism perspective, in esophageal adenocarcinoma cell lines, KLF11 binds to the promoter of cytosolic phospholipase A2α (cPLA2α), a rate-limiting enzyme of oncogenic PGE2 biosynthesis, which in turn recruits chromatin co-suppressor Sin3a/HDAC then suppress the cPLA2α expression as well as decrease the PGE2 level [272]. When turning to an EGFR/AKT signaling activated context, due to the phosphorylation of the KLF11-Sin3a interaction domain, the whole signal pathway trend turned to be reversed [272].

***Indicate as a Tumor promoter in Ovarian cancer.*** DNA-methylation levels of KLF11 were higher in ovarian cancer samples than in samples from the non-tumor group [273]. Consequently,

*KLF11* mRNA expression is lower in tumors compared to normal samples [273]. In addition, *KLF11* is highly methylated in RAS-mediated transformed ovarian cancer cells [273]. From the mechanism perspective, since the low expression of *KLF11* also accompanies the low expression of *Smad2*, *Smad3,* and *Smad7*, KLF11 might regulate TGFβ/Smad signaling pathway in ovarian cancer.

***Indicate as a Tumor promoter in Endometrial cancer.*** KLF11 is located in the nuclei and cytoplasm of the cells in endometrial cancer tissue samples [274]. It is negatively correlated to PR statutes and its upregulation independently indicates the poor prognosis of endometrial cancer [274].

***Indicate as a Tumor promoter in Gastric cancer.*** KLF11 is higher expressed in gastric cancer tissue than in adjacent gastric tissue and positively correlated to aggressive features [275]. In addition, downregulation of KLF11 inhibits tumor cell migration and invasion *in vitro* [275]. From the mechanism perspective, KLF11 binds to the GC-rich promoter sequence of Twist1 to activate its expression. In turn, Twist1 binds to the promoter of the gene of E-cadherin to suppress its expression, consequently promoting the EMT process [275, 276].

***Indicate as a Tumor promoter in Liver cancer.*** Knockdown of KLF11 can block the promotion role of miRNA10b to EMT of hepatocellular carcinoma cells, which means the upregulation of KLF11 is indispensable in this process [277]. From a mechanism perspective, KLF11 is upregulated directly by the down-regulation of KLF4, which is due to the binding of miRNA10b to the 3'UTR of KLF4. Then KLF11 transcriptionally represses Smad7 expression, promoting Smad3 activation, resulting in Smad3 mediated EMT promotion [277].

***Indicate as a Tumor suppressor in Osteosarcoma.*** KLF11 is expressed lower in osteosarcoma samples than in non-tumor samples due to the DNA hyper-methylation of KLF11, and lower KLF11 levels lead to shorter disease-free survival (DFS) and OS in osteosarcoma patients [278]. Patients with lower expression of KLF11 have a more inadequate response to chemotherapy [278]. Knockdown of KLF11 promotes osteosarcoma stem cells' stemness [278]. PPARγ agonist thiazolidinedione can activate KLF11 and then sensitize cancer stem cells to chemotherapy *in vitro* [278]. From the mechanism perspective, originally, downregulation of KLF11 can upregulate the expression Yes Associated Protein (YAP) via recruiting the co-suppressor SIN3A/HDAC. In turn, the YAP effect is a negative feedback regulator to promote the expression of KLF11 in osteosarcoma non-stem cells [278]. However, due to KLF11 epigenetic silence in osteosarcoma stem cells, this negative loop is disrupted and increases osteosarcoma stem cells stemness [278].

***Indicate as a Tumor Suppressor in NSCLC.*** The expression of KLF11 can be increased by radiotherapy combined with hyperthermia in human NSCLC cells. The downregulation of KLF11 can inhibit this therapy effect [279]. In addition, KLF11 inhibits proliferation and induces apoptosis of NSCLC cells [279]. Furthermore, KLF11 reduces lung tumor growth in mice models after the treatment of radiotherapy/hyperthermia combination [279]. From the mechanism perspective, KLF11 up-regulates the expression of reactive oxygen species (ROS) [279].

KLF11 suppresses growth in untransformed cells and even transforms normal fibroblasts. Still, it appears to be a positive regulator of cancer progression ([280], **published as the first author**), suggesting that KLF11 might also be a cell growth-promote factor in breast tumor cells. Although the roles of KLF11 in BC tumor cells have been discussed indirectly [178, 238, 281], it remains to be revealed how KLF11 is directly involved in BC progression and the underlying regulatory mechanisms. Furthermore, the regulation pattern underlying KLF11 of TAMs is completely lacking.

## 1.9 Aims of the Study

Firstly, this study aims to explore the effects of TAMs on BC based on their different infiltration locations. Furthermore, this study aims to clarify whether TAMs in breast adipose tissue contribute to the pro-tumor effect of breast adipose tissue in BC patients irrespective of the presence of obesity. Therefore, we performed CD68-IHC staining as a pan-macrophage marker in our cohort of primary BC patients with no prespecified overweight or obesity status. We then counted the number of TAMs (CD68-stained cells) in the section of breast adipose tissue termed “breast adipose tissue macrophage (BATM)” and of breast tumor-stroma tissue termed “breast tumor-stroma macrophage (BTSM)”. And further, we correlated the abundances of BATM and BTSM, respectively, to clinic-pathological characteristics. In addition, we performed survival analyses of BATM and BTSM, respectively, in these BC patients.

Secondly, this study aims to clarify whether KLF11 acts as an oncogene or a tumor-suppressor in BC. Although the role of KLF family members in BC has been systematically summarized, KLF act as oncogenes or tumor-suppressors has not yet reached consensus. Given that KLF11 belongs to such a volatile/context-dependent family of prognostic roles, we conducted a dual exploration of the role of KLF11 in BC patients. On the one hand, we explored the role of *KLF11* mRNA in BC patients identified by bulk RNA-seq datasets. Then, on the other hand, we researched and validated the prognostic role of the KLF11 in our BC cohort by applying immunohistochemistry (IHC) staining of KLF11 in the 298 patients samples, followed by statistical analysis to make sure the precisely pro- or anti-tumor role of KLF11.

Thirdly, this study aims to explore the mechanism underlying KLF11-mediated regulation from both TAMs and tumor cells' perspectives. Firstly, to have a general understanding of which signaling pathways and BPs KLF11 may involve, we predicted the mechanism that may underlie the regulation of KLF11 in BC progression using gene functional enrichment analysis. Secondly, refereed to the prediction analysis, we further explored the transcriptional regulatory role of KLF11 in Br-TAMs and tumor cells of BC, respectively. Thirdly, to validate the effect of KLF11 on BC tumor cells experimentally.

# 2. Materials and Methods

## 2.1 For Clinical patient samples

### 2.1.1 BC Patients Cohort

"In this study, 320 consecutive patients who underwent surgery for BC from 2000 to 2002 at the Department of Gynecology and Obstetrics, Ludwig-Maximillian's-University of Munich, Germany, and of whom tumor tissue was still available were primarily included. To diagnose BC, all patients had undergone tumor biopsy prior to surgery for BC but no patient has undergone any other prior treatment. In the further analyses, only cases with a diagnosis of sporadic BC and without family history for BC were included (n = 306). Patients with primary distant metastases (n = 6) and patients with only ductal carcinoma in Situ (DCIS) but without invasive BC (n = 2) were excluded from further analyses." [47] (Obtained from a published paper related to this study, **as the First Author**).

Then, in total, 298 patients were included. "The Institute of Pathology, Ludwig-Maximillian's-University of Munich, assigned the tumor grading (according to the Elston-Ellis system)" [47] (Obtained from this related published paper **as the First Author**). "Patient data regarding patient age, HR status, HER2-amplification, metastasis, local recurrence, progression, and survival were retrieved from the Munich Cancer Registry" [47] (Obtained from this related published paper **as the First Author**). The surrogate molecular subtypes of these patients were defined: LuA-like (ER/PR+, HER2 unamplified, Ki-67 ≤ 14 %), LuB-like (ER/PR positive, HER2 unamplified, Ki-67 > 14 %), TNBC (ER-, PR-, HER2 unamplified), HER2 amplified Luminal-like (HER2 amplified, ER/PR+) and HER2 amplified non-Luminal-like (HER2 amplified, ER-, PR-). Prostaglandin E receptor 3 (EP3), the IHC-mediated expression analysis performed by our team [282], was used for further prognostic analysis. Patients were followed up for 12 years.

### 2.1.2 Immunohistochemistry

Formalin-fixed and paraffin-embedded (FFEP) slides of BC patients were used for immunohistochemistry (IHC) analysis. The samples were dewaxed in xylene substitutes ROTICLEAR (Art.-Nr. A538.5, Carl Roth) followed by rinsing with 100% ethanol. Next, the samples were soaked with 0.3% or 0.6% $H_2O_2$ diluted in methanol for 20 minutes to inhibit the endogenous peroxidase reaction. Subsequent gradually rehydrated in 100%, 75%, and 50% ethanol, followed by rinsing with distilled water. Afterward, a pressure cooker performed antigen retrieval with sodium citrate buffer (pH 6.0). Then, after twice washing with phosphate-buffered saline (PBS) and blocking with Reagent 1 of ZytoChem Plus HRP Polymer Bulk kit (Nr.POLHRP-100, Zytomed system), the slides were incubated with the primary antibody for 16 hours at 4 °C. Primary anti-CD68 antibody (Rabbit IgG polyclonal, 1:1000, Nr.HPA048982, Sigma Aldrich) and primary anti-KLF11-antibody (Mouse IgG2a kappa, 1:200, Nr.H00008462-M03, Novus Biologicals) were used for this study. The next day, after washing twice with PBS and post blocking with Reagent 2 of ZytoChem Plus HRP Polymer Bulk kit (Nr.POLHRP-100, Zytomed system). Afterward, the samples were incubated with HRP-Polymer (Reagent 3 of ZytoChem Plus HRP Polymer Bulk kit, Nr.POLHRP-100, Zytomed system). The color was then developed by Liquid DAB+ Substrate Chromogen System kit (Nr. K3468, Dako). Finally, the samples were counterstained with Himalayan. Subsequent

gradually dehydrated in 50%, 75%, 80%, 97%, 100% ethanol to ROTICLEAR, followed by mounting with Roti-Mount medium (Art.-Nr. HP68.1, Carl Roth). Placenta tissue was used to control staining. The staining samples were finally assessed by Leitz microscope (Type 307-148.001 514686, Wetzlar).

### 2.1.3 Quantity of TAMs

Pan-macrophage marker CD68 [283-285] was expressed in the membrane of the TAMs and stained as brownish/yellow particles. CD68-immunolabelled cells were assessed as the quantity of TAMs. The number of TAMs in four views of the breast tumor stroma section and four views of the breast adipose tissue section per IHC slide were counted by three investigators, respectively. The necrotic and high mitotic areas were distinguished and excluded when counting the TAMs in the breast tumor-stroma section. The TAM in the breast tumor-stroma section was named BTSM, and the TAM in the breast adipose tissue section was termed BATM. The average value of the four views of these two sections was calculated and used to represent the number of BTSMs and BATMs. The abundance of BTSMs and BATMs were further classified as “BATM-high/-low” and “BTSM-high/-low”. “Receiver operating characteristic (ROC)” analysis is commonly used to define optimal cutoff points of biomarkers with a curve based on the measurement of the accuracy evaluated by the “area under curve (AUC)” [286]. This analysis was performed to determine the cut-offs of BATM and BTSM classification. Then, the quantity of BATMs ≤ 9.5 was categorized as “BATM-low”, and the quantity of BATM > 9.5 was classified as “BATM-high”. The quantity of BTSMs ≤ 4.5 was categorized as “BTSM-low” and the quantity BTSMs > 4.5 was categorized as “BTSM-high”. The continuous variables of the absolute number of BTSMs and BATMs, as well as the categorized variables of “BTSM-high/-low” and “BATM-high/-low”, were used to correlate with clinical and pathological characteristics. Survival analyses were performed using the “BTSM-high/-low” and “BATM-high/-low” classified variables.

### 2.1.4 IHC Staining of KLF11 Reactive Evaluation

KLF11 was positively stained in the nuclei of cells of BC tissues. Immunoreactive score (IRS) was calculated to evaluate the protein level of KLF11. *“*This semi-quantitative score is calculated as follows: the optical staining intensity (grades: 0 = none, 1 = weak, 2 = moderate, 3 = strong staining) is multiplied by the total percentage of positively stained cells (0 = none, 1 < 10%, 2 = 11-50%, 3 = 51-80% and 4 > 81% of the cells)*”* [287]. This range of IRS is 0-12 [287]. The IRS of KLF11 expression was assessed by two experienced investigators independently. The IRS of KLF11 was further categorized as “KLF11-high” and “KLF11-low”. Cutoffs for KLF11 categorization were also determined using ROC analysis. The optimized cut-off IRS of KLF11 was 2. The IRS of KLF11 ≤ 2 was categorized as “KLF11-low”, and IRS > 2 was categorized as “KLF11-high”. The ordinal variables of the IRS of KLF11 and the categorized variables of “KLF11-high” and “KLF11-low” correlated to clinical and pathological characteristics. The categorized variables of “KLF11-high” and “KLF11-low” were then correlated to the prognostic outcomes of BC.

### 2.1.5 Double Immunofluorescence Staining

Double immunofluorescence (IF) staining of CD68 and KLF11 was performed to detect the presence of KLF11 in TAM of BC tissue. The FFPE slides were double-stained with primary anti-CD68 antibody (Rabbit IgG polyclonal, 1:200, Nr.HPA048982, Sigma Aldrich) for TAM and anti-KLF11 antibody (Mouse IgG2a kappa, 1:30, Nr.H00008462-M03, Novus Biologicals). The same experimental procedure of dewaxing, gradual rehydration, and antigen retrieval of the samples was

carried out as the procedures for IHC staining. Subsequently, after washing twice in PBS and blocking with UltraVision Protein Block (Nr.TA-060-PBQ, Epredia), the samples were incubated with the mixture of anti-CD68 and anti-KLF11 antibodies diluted with antibody diluent (Nr.S3022, Dako). Afterward, the samples were incubated in darkness with the fluorescent secondary antibodies diluted in antibody diluent (Nr.S3022, Dako). Secondary Goat-anti-Rabbit lgG Cy3 (1:500, Nr.111-165-144, Jackson ImmunoResearch) marked CD68 red, and secondary Goat-anti-Mouse IgG Alexa Fluor 488 (1:100, Nr.115-545-062, Jackson ImmunoResearch) marked KLF11 green was used for this study. Then, after washing in PBS and drying in the dark, the samples were mounted using an antifade mounting medium with DAPI (Nr.H-1200, Vector Laboratories) that stained the cell nuclei blue. The double IF staining slides were then analyzed with the Axioskop fluorescent photomicroscope (Zeiss; Oberkochen, Germany). Staining graphs were captured using the Axiocam camera system (Zeiss CF20DXC).

### 2.1.6 Ethics Approval and Consent to Participate

"This study has been approved by the Ethics Committee of the Ludwig-Maximilian-University Munich (approval number 048–08). The BC specimens were obtained in clinically indicated surgeries. When the current study was performed, all diagnostic procedures were completed, and the patients' data were anonymized. The ethical principles adopted in the Declaration of Helsinki 1975 have been respected. As per declaration of our ethics committee, no written informed consent of the participants or permission to publish is needed given the circumstances described above. Researchers were blinded from patient data during experimental and statistical analysis." [47] (Obtained from a published paper related to this study, **as the First Author**)

## 2.2 Bioinformatics Databases

### 2.2.1 TIMER

TIMER (https://cistrome.shinyapps.io/timer/) can be used to assess the immune infiltration systematically of diverse cancers [288]. The TIMER-Diff Exp module was used in this study to obtain the differential expression of *KLF11* across the 33 cancer types and respective normal tissue. The TIMER-Gene module was used to explore the association of *KLF11* with macrophage infiltration in TCGA-BC. The TIMER algorithm was performed to calculate the infiltration level. The TIMER-Correlation module was used to explore the correlation analysis of *KLF11* and common macrophage markers and the relationship between *KLF11* and immune checkpoints related genes in TCGA-BC. Gene expression in tumor tissue after tumor purity correction can more accurately reflect the correlation between genes and tumor immune infiltration [289]. Spearman coefficient (Cor) or tumor purity-adjusted Spearman coefficient (partial.cor) was displayed when using this server portal.

### 2.2.2 TISIDB

TISIDB (http://cis.hku.hk/TISIDB/index.php ) contains genomics, transcriptomic and clinical data on TCGA cancers [290]. It was used to assess the influence of *KLF11* on patients' overall survival (OS) across various human cancers in the TCGA cohort.

### 2.2.3 Kaplan-Meier Plotter

Kaplan-Meier (KM) Plotter (http://www.kmplot.com/analysis/ ) contains genomics, transcriptomic and clinical data across 25,000+ samples from 21 tumor types, including BC[291]. It was performed to analyze the correlations between KLF11 and OS, DFS, and distance-metastases-free survival (DMFS) of BC across gene expression data series (GSE) datasets [292].

### 2.2.4 STRING

STRING database (https://string-preview.org/ ) contains 14049 organisms, 67.6 million+ proteins, and 20 billion+ interactions that can be used to explore known and predicted protein-protein or gene-gene interactions of protein or gene of interest [293]. It was used for creating and exploring the protein-protein interaction network of KLF11.

### 2.2.5 CellMarker

CellMarker (http://biocc.hrbmu.edu.cn/CellMarker/index.jsp) can be used to explore characteristic markers of the cell type of interest in tumors or normal tissues [294]. The markers are identified based on scRNA-seq data and experimentally validated data [294]. It was used to obtain the most common markers of TAM.

### 2.2.6 GEPIA 2

GEPIA 2 (http://gepia2.cancer-pku.cn/#index) can be used to compare different gene signatures of interest in the given cancer/normal sample of TCGA and GTEx databases [295]. It was used to assess the correlation between *KLF11/PPARG* and *KLF11/PPARG/THRA* signature and TAMs marker signatures and the association of *KLF11* with specific BC molecular subtype signatures and Gene modules (GM) signatures across breast tumor tissue and breast normal tissue, respectively. Spearman coefficient (Cor) was displayed when using this database.

## 2.3 R programmer and R packages

All R scripts were running in R programmer version 3.6.3.

### 2.3.1 Download, Process, and Analysis of TCGA data

The fragments per kilo base per million (FPKM)-format bulk-RNA-seq data and associated clinical data of TCGA-BC were obtained from the TCGA database (https://portal.gdc.cancer.gov/). Afterward, FPKM-format data were normalized and converted into transcripts per million reads (TPM)-format. Differential expression of *KLF11* was analyzed using the R package “limma” [296]. ROC analysis was performed and the AUC were calculated to determine the diagnostic accuracy of *KLF11* expression using the R package “pROC”. The diagnostic value of the target gene can be determined by the AUC area value (0.5-1) under the ROC curve. The r package “ggplot2” was then used for plotting. Further, clinical data of TCGA-BC patients was integrated with the prognostic data [297]. The duplicated cases and the cases with missing clinical outcomes were then excluded. The R package “survival” for analysis and the R package “survminer” for plotting in the R programmer was then performed for prognostic analysis.

### 2.3.2 GO and KEGG Functional Enrichment Analysis

Gene ontology (GO) and Kyoto Encyclopedia of Genes and Genome (KEGG) enrichment analyses were performed with the encoded genes of KLF11 and its interacted proteins explored by STRING. R package “org.Hs.eg.db” was used for ID converting, and R package “clusterProfiler” was used for functional enrichment [298]. Enrichment results were then plotted using the R package “ggplot2”. GO terms include BP, cell component (CC), and molecular function (MF). The significant enriched Entries were determined by the request of p.adj value < 0.05 and q value (false discovery rate, FDR) < 0.25.

### 2.3.3 Nomogram Construction and Calibration

Multivariate Cox regression-identified Independent prognostic variables were integrated to create nomograms for survival probability predictions. Nomograms were modeled and developed using R packages “survival” and “rms”. The nomogram capability of discrimination can be assessed by the “concordance-index (C-index)” [299]. The value of C-index can be 0.5-1.0 [299]. C-index with a value closer to 1.0 indicates a perfect discriminative performance [299]. The prediction accuracy of the established model was evaluated with a calibration curve. In the calibration curve, the predicted prediction that falls on the diagonal indicates a very accurate prediction model

### 2.3.4 Heat Map of Correlation

The heat map of the Spearman pairwise correlations between KLF11, BATMs, BTSMs, and the nuclear molecules that were either significantly correlated to BATMs or BTSMs quantities or both were generated using the R programmer, and R package “ggplot” was used for plotting.

## 2.4 Experimental Validation of the Role of KLF11 in BC Tumor Cells

### 2.4.1 BC Cell Lines Culture

MCF7 (Nr.86012803, ECACC) as Luminal type, MDAMB231 (Nr.92020424, ECACC) as TNBC type, and SKBR3 (Nr.ACC736 DSMZ) as HER2 type were used to validate the functional findings of KLF11 involved in BC cell lines. The cell lines were cultured in RPMI medium 1640 (1X) + GlutaMAX™-1 Nr. 61870-010, Gibco) containing 10% fetal bovine serum (FBS Qualified, Nr.10270-106, Gibco). The culture medium was without antibiotics or antimycotics. The culture condition of the cells was an incubator with a stable temperature (37°C), stable CO2 level (5%), and high relative humidity (95%). Only cells detected to be free of Mycoplasma infection were used in subsequent experiments. Neubauer cell chambers were used to count cells when performing cell experiments.

### 2.4.2 siRNA-Mediated Knockdown

For siRNA knockdown experiments, BC cell lines were transfected with AllStars Negative Control (NC) siRNA (Nr.1027280, Qiagen), and two independent siRNAs target KLF11: *KLF11*-S1: CACGTAGATAACCGAGAGAAT (Nr.SI04139751, Qiagen) and *KLF11*-S2: AGGAAGCGGCATGACAGCGAA (Nr.SI4291175, Qiagen). The entire transfection procedure was performed as

the manual of Lipofectamine RNAiMAX reagent (Nr.13778-075, Invitrogen) documented. BC cell lines were pre-seeded in six-well plates. siRNA-transfection was performed when the cell density reached approximately 60%. Opti-MEM Reduced Serum Medium (Nr.31985-047, Gibco) containing siRNAs (25pmol) and Lipofectamine RNAiMAX Reagent (7.5µl) was used for the transfection of the cells. After 48 hours, BC cell lines were harvested for protein or RNA extraction and detection or further cell functional experiments.

### 2.4.3 RNA Extraction and Real-Time PCR

RNA was extracted following the procedure documented in the manual of RNeasy Mini Kit (Nr.74104, Qiagen). Subsequent reverse transcription was carried out with Biozym cDNA Synthesis Kit (Nr.331470L, Biozym) and implemented as the manual document. Real-Time PCR (rtPCR) was carried out to validate the knockdown of *KLF11* expression from mRNA level in different BC cell lines with FastStart Essential DNA Probes Master kit (Nr.06402682001, Roche) gene-specific primers using the LightCycler Nano (Roche). *ACTB* (β-actin) was used as the reference gene. The 20 µL reaction system was used, consisting of cDNA (1 µl), $H_2O$ (8 µl), and Mastermix (10 µL) and the mixture of forwarding primer (0.5 µl) and reversing primer (0.5 µl). The process of rt-PCR cycling was set as 10 minutes for pre-incubation and two step-amplification: 40 cycles of 20 seconds at 95 ℃ and 40 seconds at 60 ℃. The primers were *KLF11* (Forward: 5'-CTTCCATTCTTTATCGACTCTGTG-3' and Reverse: 5'- GATGGCTCCACGAGATCAG-3', Nr.100154265, Roche) and *ACTB* ("Forward: 5'- TCCTCCCTGGAGAAGAGCTA-3' and Reverse: 5'- CGTGGATGCCACAGGACT-3'" [300], Nr.100143492, Roche)

### 2.4.4 Colorimetric Cell-Based KLF11 ELISA

The KLF11 protein level in BC cell lines was detected using the colorimetric cell-based KLF11 ELISA Kit (Dr.DEIA-XYA1113, CD Creative Diagnostic). The kit was used to validate the siRNA-mediated knockdown of KLF11 from protein levels in different cultured BC cell lines. The siRNA transfection for KLF11 knockdown of BC cell lines was conducted as described above. Afterward, the entire measurement procedure was performed as the colorimetric cell-based KLF11 ELISA Kit manual documented. Cells were then seeded (20000 cells/well) into 96-well plates with triplicates for each cell line and grown in the 10% FBS-contained RPMI 1640 medium for 24 hours. The absorbance of optical density $(OD)_{450}$ was then measured for the target protein. The absorbance of $OD_{595}$ was measured for crystal violet cell staining using Elx800 universal Microplate Reader and analyzed using Gene 5 software. For data normalization, the absorbance of $OD_{450}$ of the target protein and internal reference protein were normalized using the absorbance of $OD_{595}$ via the portion, then normalized the target protein values with the internal reference protein values. Three replicates were performed with each cell line. To guarantee the reliability, we have repeated the experiment at least three times.

### 2.4.5 Cell Viability Assay

Cell viability assay of BC cell lines was performed using the Methylthiazolyldiphenyl-tetrazolium bromide (MTT). The siRNA transfection for KLF11 knockdown of BC cell lines was conducted as described above. Cells were then seeded (3500 cells/well) into three sets of 96-well plates with five replicates for each cell line and cultured in 10% FBS-contained RPMI 1640 medium for 24 hours, 48hours, and 72hours, respectively. Then incubation ended at three different time points and then to each time point to each well. Afterward, the MTT solution (20 µl/well, 5 mg/ml,

Nr.M5655, Sigma-Aldrich) was pipetted, and the plates were put back in the cell incubator for another 1.5 hours. After removing the MTT-containing incubation medium, dimethyl sulfoxide (DMSO, 200 µl/well) was piped in. A shaker was used to mix DMSO and formazan crystal thoroughly for 5 min at RT. The dissolved formazan crystals were used to represent the number of viable cells. The absorbance of $OD_{595}$ was measured using an Elx800 universal Microplate Reader and analyzed using Gene 5 software. To guarantee the reliability, we have repeated the experiment at least three times.

### 2.4.6 Cell Proliferation Assay

Cell proliferation assay was performed with the Cell Proliferation ELISA kit (Nr.11647229001, Roche) based on 5-bromo-2'-deoxy-uridine (BrdU) labeling and detection. The entire procedure has been performed the manual of the kit is documented. The siRNA transfection for KLF11 knockdown of BC cell lines was conducted as described above. Cells were then seeded (5000 cells/well) into two sets of 96-well plates with five replicates for each cell line and cultured in10% FBS-contained RPMI 1640 medium for 24 hours and 48 hours, respectively. Then incubation ended at two different time points, and then each time point to each well was supplemented with BrdU (20 µl/well), and the plates were put back in the cell incubator for another 24 hours. After removing the BrdU-contained incubation medium, the fixing solution (200 µl/well) was pipetted in the wells to fix the cells. Afterward, cells were incubated with anti-BrdU-POD (100 µl/well) to label the BrdU that was incorporated into the cellular DNA. After thoroughly washing, a substrate solution (100 µl/well) was pipetted in and incubated until the development of blue color. Sulfuric acid (1M, 25 µl/well) was then pipetted in to stop the reaction. The absorbance of $OD_{450}$ was measured using Elx800 universal Microplate Reader and analyzed using Gene 5 software. To guarantee the reliability, we have repeated the experiment at least three times.

### 2.4.7 Cell Apoptosis Assay

Cell apoptosis assay was performed using the Cell Death Detection ELISA kit (Nr.11544675001, Roche). The apoptosis was determined by DNA fragment analysis. The whole detection procedure was followed the manual instructions of the kit. The siRNA transfection for KLF11 knockdown of BC cell lines was conducted as described above. BC cell lines were then harvested and prepared as sample lyses for further detection. After forming the "sandwich", which consists of anti-histone antibody, sample lyses containing nucleosomes, and anti-POD-DNA-peroxidase determined the amount of peroxidase retained in the immune complex with substrate solution. The absorbance of $OD_{405}$ was measured using Elx800 universal Microplate Reader and analyzed using Gene 5 software. To guarantee the reliability, we have repeated the experiment at least three times.

## 2.5 Statistical Analysis

IBM SPSS (version 26) was used for statistical analysis of the data. Adobe Illustrator (AI) and Graphpad Prism 8.1 were used for illustrations.

Data analyzed statistically was first subjected to the Shapiro-Wilk normality test and Levene's equal variances test. Proper statistical test methods were selected according to the results of normality and variances and the number of comparison groups. It was described as follows: 1) Student's t-test (for two groups) and One-way ANOVA test (for multiple groups) were performed for the comparison of groups that met the assumptions of normality and homogeneity of variance;

2) Welch's test (for two groups) and Welch one-way ANOVA test (for multiple groups) were performed for the comparison of groups that that only met the assumption normality but not the assumption of homogeneity of variance; 3) Mann-Whitney U test (for two groups) and Kruskal-Wallis test (for multiple groups) were performed for the comparison of groups that did not meet the assumption of normality. Subsequent Dunn's test was implemented for pairwise comparisons within the multiple groups. In addition, Chi-Square Test was performed for the comparison of categorical variables. Furthermore, Pearson analysis (for the data met the assumptions of normality) and Spearman analysis (for the data did not meet the assumptions of normality) were performed for the correlation analysis of numerical and ordinal variables. "Pearson's r" and "Spearman's ρ" represented the Pearson and Spearman correlation coefficients, respectively.

For survival analysis of BC patients, KM analysis was performed for the generations of survival curves with the Log-rank test. Cox regression was also performed for the survival analysis using different models with a Hazard ratio (HR) and a 95% Confidence interval (CI). The proportional hazards assumption test was performed for each variable in all cox models using the Schoenfeld statistical test.

All reported p values are two-sided. P-values $< 0.05$ were considered statistically significant.

# 3. Results

## 3.1 The Distinct Roles of BATM and BTSM in our BC Cohort

To elucidate the role of the TAMs in the breast adipose tissue (BATM) and breast tumor-stroma tissue (BTSM), respectively, we performed CD68 IHC staining as pan macrophage marker in our clinical BC cohort. And further related to the abundance of BATMs and BTSMs respectively to clinic-pathological characteristics and the survival outcomes of these BC patients to explore the clinical significance of BATM and BTSM, respectively.

Interestingly, we found that BATM and BTSM are involved differently in BC. BATM appeared to be an independent and unfavorable indicator of the prognosis of BC, while a higher infiltration of BTSM seemed to be an indicator of a more aggressive molecular subtype of BC.

(This part of the results has been published recently in *Breast Cancer Research* [47], **as the First Author**)

### 3.1.1 Clinic-pathological Characteristics of BC Patients

Of the overall 298 patients, 241 (80.9 %) cases showed ER-positive, 170 (57.0 %) showed PR positive, 263 patients (88.3 %) showed HER2 unamplified and 167 cases (56 %) showed Ki-67 expression ≤ 14 % (**Table 3.1.1**). Defined by these surrogate biomarkers, 166 cases of all 298 patients (55.7 %) were luminal A-like, 60 cases (20.1 %) were defined as luminal B-like, and 38 cases (12.8 %) belonged to the TNBC subtype. Twenty-three patients (7.7 %) had HER2 amplified with a luminal-like feature, and only 9 of them (3.0%) had HER2 amplified but without a luminal-like feature (**Table 3.1.1**). Moreover, 226 of 298 patients (75.8 %) were older than 50 years (**Table 3.1.1**). The tumor sizes of 194 patients (65.1 %) were smaller than 2cm (**Table 3.1.1**). 164/298 (55.0 %) did not have axillary lymphatic metastasis (**Table 3.1.1**). One hundred three cases (34.6 %) were with the “Grade 2” histology feature (**Table 3.1.1**).

However, tumor grading was only available in 162/298 (54.3 %) cases, so its reliability is limited (**Table 3.1.1**). Not all clinic-pathological characteristics were available from all patients, so the sum of patient numbers in some subgroups may not match the total number of cases.

**Table 3.1.1 Distributions of BATM and BTSM in our BC cohort**

*This table was adopted from a related published paper [47], **by the First Author**.*

| Parameters | | Total | BATM-low | BATM-high | BTSM-low | BTSM-high |
|---|---|---|---|---|---|---|
| | | Number of cases (%) | Number of cases (%) | Number of cases (%) | Number of cases (%) | Number of cases(%) |
| **N** | | 298 (100) | 220 (73.8) | | 242 (81.2) | |
| **Age** | ≥50 years | 226 (75.8) | 170 (77.3)<br>123(75.0) | 50 (22.7)<br>41(25.0) | 42 (17.4)<br>31(17.2) | 200 (82.6)<br>149(82.3) |
| | < 50 years | 72 (24.2) | 47(83.9) | 9(16.1) | 11(16.7) | 51(77.3) |
| | **P-value** | | 0.169 | | 0.926 | |
| **Molecular subtype** | Luminal A-like | 166 (55.7) | 99(78.0) | 28(22.0) | 37(26.8) | 101(73.2) |
| | Luminal B-like | 60 (20.1) | 39 (79.6) | 10(20.4) | 2(3.8) | 50(96.2) |
| | Triple negative | 38 (12.8) | 16(66.7) | 8(33.3) | 0(0.0) | 30(100.0) |
| | HER2 Amplified luminal-like | 23 (7.7) | 11(78.6) | 3(21.4) | 1(6.3) | 15(93.7) |

| | | | | | | |
|---|---|---|---|---|---|---|
| | HER2 Amplified non luminal-like | 9 (3.0) | 5 (83.3) | 1(16.7) | 2(33.3) | 4(66.7) |
| | **P-value** | | 0.779 | | **0.000011*** ** | |
| **Grading** | G1 | 15 (5) | 7(63.6) | 4(36.4) | 4(30.8) | 9(69.2) |
| | G2 | 103 (34.6) | 56(77.8) | 16(22.2) | 12(15.0) | 68(85.0) |
| | G3 | 44 (14.8) | 25(78.1) | 7(21.9) | 7(20.6) | 27(79.4) |
| | **P-value** | | 0.594 | | 0.337 | |
| **Tumor foci** | Unifocal | 161 (54.0) | 87(74.4) | 30(25.6) | 21(16.0) | 110(84.0) |
| | Multifocal /Multicentric | 137 (46.0) | 83(80.6) | 20(19.4) | 21 (18.9) | 90 (81.1) |
| | **P-value** | | 0.272 | | 0.554 | |
| **Tumor size** | pT1 | 194 (65.1) | 114(80.3) | 28(19.7) | 31(20.0) | 124(80.0) |
| | pT2 | 87 (29.2) | 49(75.4) | 16(24.6) | 8(11.1) | 64(88.9) |
| | pT3 | 4 (1.3) | 1(33.3) | 2(66.7) | 0(0.0) | 3(100.0) |
| | pT4 | 13 (4.4) | 6(60.0) | 4(40.0) | 3(25.0) | 9(75.0) |
| | **P-value** | | 0.094 | | 0.276 | |
| **Axillary lymph node status** | pN0 | 164 (55.0) | 91(77.8) | 26(22.2) | 23(17.6) | 108(82.4) |
| | pN1 | 124 (41.6) | 73(76.8) | 22(23.2) | 18(17.6) | 84(82.4) |
| | pN2 | 4 (1.3) | 1(33.3) | 2(66.7) | 0(0.0) | 4(100.0) |
| | **P-value** | | 0.224 | | 0.796 | |
| **ER status** | Negative | 57 (19.1) | 28(75.7) | 9(24.3) | 4(8.9) | 41(91.1) |
| | Positive | 241 (80.9) | 142(77.6) | 41(22.4) | 38(19.3) | 159(80.7) |
| | **P-value** | | 0.799 | | 0.096 | |
| **PR status** | Negative | 128 (43.0) | 67(75.3) | 22(24.7) | 20(25.0) | 80(75.0) |
| | Positive | 170 (57.0) | 103(78.6) | 28(21.4) | 22(15.5) | 120(84.5) |
| | **P-value** | | 0.561 | | 0.362 | |
| **HER2 status** | Unamplified | 263 (88.3) | 154(77.4) | 45(22.6) | 39(17.8) | 180(82.2) |
| | Amplefied | 33 (11.1) | 16(76.2) | 5(23.8) | 3(13.0) | 20(87.0) |
| | **P-value** | | 1.000 | | 0.774 | |
| **Expression of Ki-67** | ≤14% | 167 (56.0) | 100(78.1) | 28(21.9) | 37(26.6) | 102(73.4) |
| | > 14% | 60 (20.1) | 39(79.6) | 10(20.4) | 2(3.8) | 50(96.2) |
| | **P-value** | | 0.832 | | **0.001**** | |
| **Expression of EP3** | Low (IRS ≤ 1 ) | 87 (29.2) | 43 (68.3) | 20 (31.7) | 16 (22.2) | 56 (77.8) |
| | High (IRS > 1 ) | 201 (67.4) | 124 (80.5) | 30 (19.5) | 26 (15.5) | 142 (84.5) |
| | **P-value** | | 0.051 | | 0.208 | |

"BATMs, Breast adipose tissue macrophages", "BTSMs, Breast tumor-stroma macrophages", "ER, Estrogen receptor", "PR, Progesterone receptor", "HER2, Human epidermal growth factor receptor 2", "EP3, Prostaglandin E receptor 3", "IRS, Immunoreactive score" [47] (Obtained from this related published paper, **as the First Author**); "*, $p < 0.05$; **, $p < 0.01$; ***, $p < 0.001$" [301].

### 3.1.2 Description and Distribution of BATM and BTSM

BATM staining was successfully performed on 220 samples in 298 patients. Of these cases, there were 50 cases with "BATM-high" distribution and 170 cases with "BATM-low" distribution (**Table 3.1.1**). BTSM was successfully stained in 242/298 specimens, of which 200 cases were classified as "BTSM-high" and 42 cases were classified as "BTSM-low" (**Table 3.1.1**). A highly positive correlation between the infiltration number of BATMs and BTSMs was observed (Spearman's $\rho = 0.5$, $p = 2.98E\text{-}15$, **Figure 3.1.1 E**). BATM infiltration rates were lower in BC patients < 50 years old (yo) than in those ≥ 50 YO ($p = 0.0325$, **Figure 3.1.1 A, B, F**). No correlation was found between BATM and other clinic-pathological characteristics. However, "BTSM-high/-low" subgroups were distributed differently in the different molecular subtypes of BC ($p = 0.000011$, **Table 3.1.1**). All TNBC cases were observed with a "BTSM-high" distribution.

Furthermore, when comparing the number of infiltration, a differential infiltration of BTSM across five surrogate BC molecule subtypes (p = 0.0003, **Figure 3.1.1 G**), and the infiltrating BTSMs in LuA-like BC were less than those in TNBC (p = 0.0005, **Figure 3.1.1 G**). BTSM infiltrating number in ER-positive was also less than those in ER-negative cases (p = 0.002, **Figure 3.1.1 H**).

A “BTSM-high” distribution was observed less frequently in cases with ki-67 ≤ 14% than in cases with ki-67 > 14% expression (96.2 % vs. 73.4 %, p = 0.001, **Table 3.1.1**). No correlation was found between BTSM and other clinic-pathological characteristics (**Table 3.1.1**). These results indicate that BTSM had a more intimate relationship with clinical or pathological parameters of BC than BATM did.

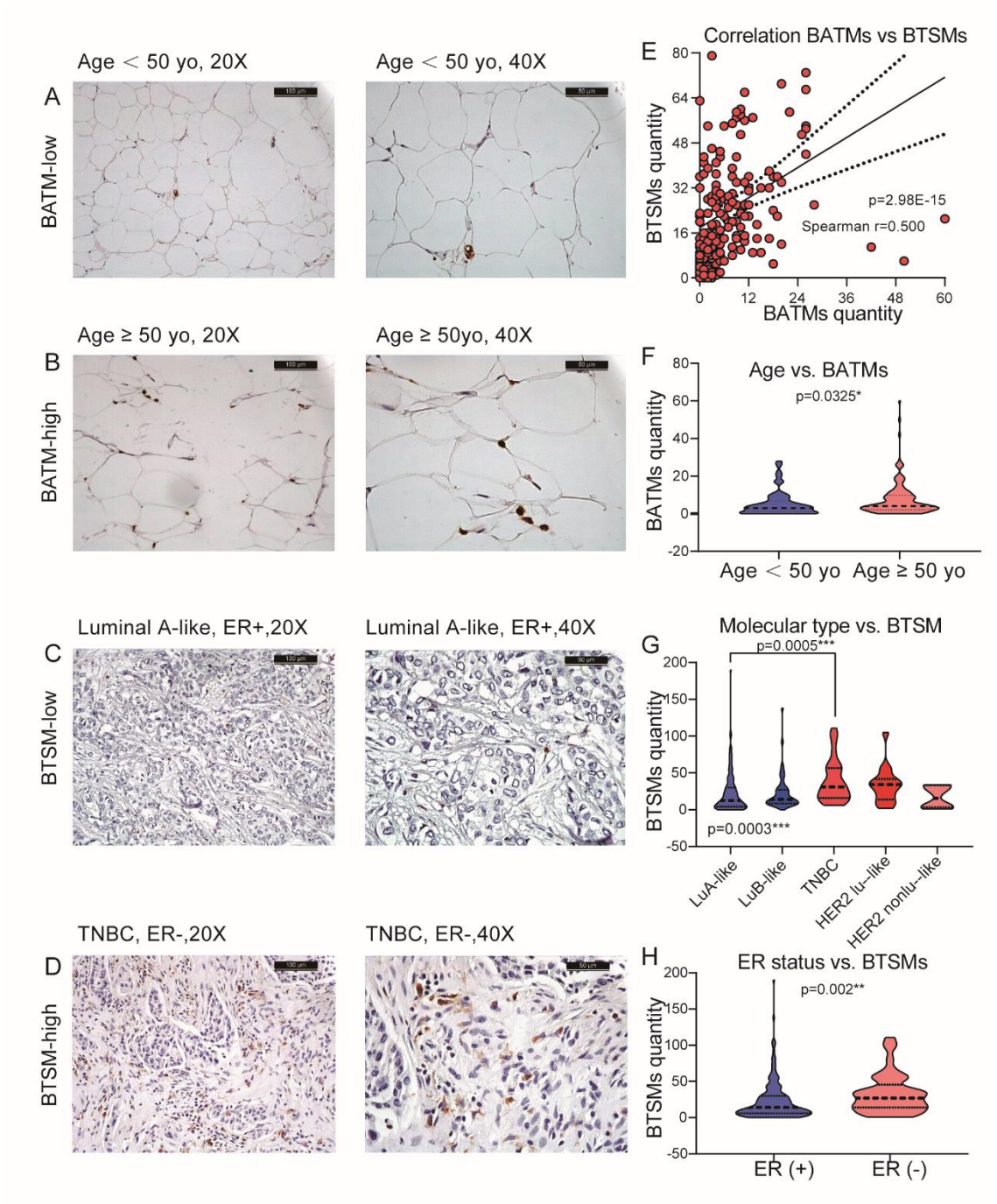


**Figure 3.1.1 The distribution of BATM and BTSM in BC.**

*This figure was adopted from a related published paper [47],* ***by the First Author****.*

**A**-B. Representative IHC images of CD68 staining of breast adipose tissue section show the infiltration of BATM was lower in patients < 50 YO (**A**) than in those ≥ 50 YO (**B**). Magnification: 20 X (left), 40X (right). **C-D.** Representative IHC images of CD68 staining of breast tumor-stroma tissue section show the infiltration of BTSM was lower in luminal A-like BC and ER-positive BC **(C**) compared to TNBC and ER-negative BC **(D**). Magnification: 20 X (left), 40X (right). **E.** Scatterplot showed a highly positive correlation between BATM infiltration and BTSM infiltration (Spearman's ρ = 0.5, p = 2.98E-15). **F.** Violin plots showed that BATM infiltration was significantly lower in BC patients < 50 YO than in those ≥ 50 YO (p = 0.0325). **G.** Violin plots showed a differential infiltration of BTSM across five surrogate BC molecule subtypes (p = 0.0003). Further pairwise comparisons showed that the infiltrating BTSMs in LuA-like BC were less than those in TNBC (p = 0.0005). **H.** Violin plots showed that BTSM infiltrating number in ER-positive was less than those in ER-negative cases (p = 0.002). "BTAMs, breast adipose tissue macrophages; BTSMs, breast tumor-stroma macrophages; ER, estrogen receptor; HER2, human epidermal growth factor receptor 2; LuA-like, luminal A-like; LuB-like, luminal B-like; TNBC, triple-negative breast cancer; HER2 Lu-like, HER2 amplified luminal-like; HER2 nonLu like, HER2 amplified non luminal-like" [47] (obtained from this related published paper, **as the First Author)**.

### 3.1.3 Both BATM and BTSM were associated with impaired OS

Patients with higher BATM infiltration (HR = 2.483, 95%CI = 1.474-4.182, p = 0.000401, **Figure 3.1.2 A**) and patients with higher BTSM infiltration (HR = 2.445, 95%CI = 1.117-5.354, p = 0.021, **Figure 3.1.2 B**) had shorter OS than the respective BATM or BTSM lower subgroups. The median OS in the "BATM-high" patients (n = 50) was 7.48 years, while more than half of the patients with "BATM-low" distribution (n = 170) were still alive during the follow-up period (**Figure 3.1.2 A**). More than half of the patients with high or low BTSM infiltrating were alive during the follow-up. However, when we compared 75% OS, the 75% OS of the "BTSM-high" subgroup (n = 200) was 6.49 years, while of the "BTSM-low" subgroup (n = 42) was as much as 11.64 years (**Figure 3.1.2 B**). These results indicate that the influence of BATM on OS of BC was greater than BTSM did.

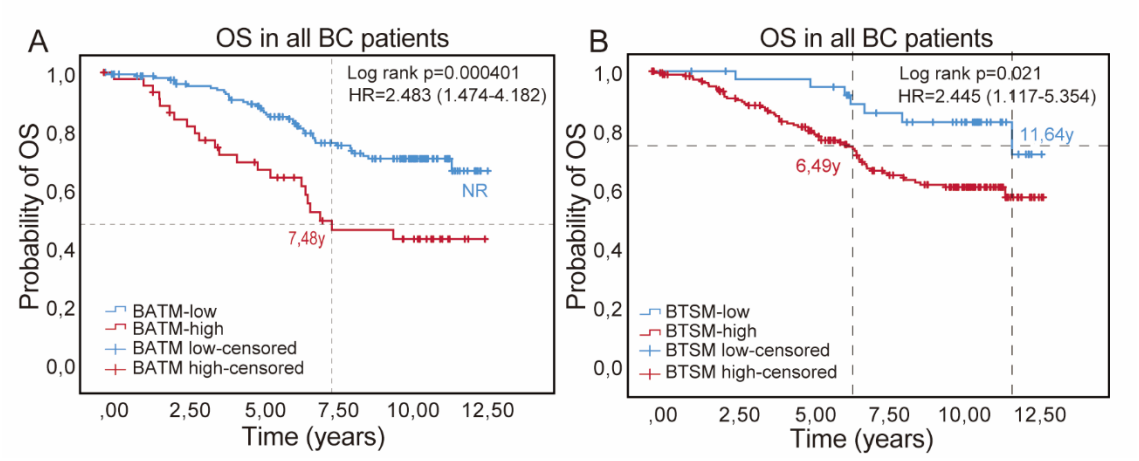


**Figure 3.1.2 BATM and BTSM were associated with impaired OS of all BC patients in our cohort.**

*This figure was adopted from a related published paper [47],* ***by the First Author****.*
**A.** Patients with higher BATM infiltration had shorter OS than the BATM lower subgroups (HR = 2.483, 95%CI = 1.474-4.182, p = 0.000401). **B.** Patients with higher BTSM infiltration had shorter OS than the BATM lower subgroups (HR = 2.445, 95%CI = 1.117-5.354, p = 0.021). "BTAMs, Breast adipose tissue macrophages; BTSMs, Breast tumor-stroma macrophages; OS, Overall survival", "HR, hazard ratio" [47] (Obtained from this related published paper, as **the First Author)**.

Furthermore, the prognostic role of BATM in OS across different subgroups that grouped by some clinicopathological parameters demonstrated that BATM was negatively correlated to OS both in

unifocal tumor (P = 0.006, n = 117, **Figure 3.1.3 A**) and in multifocal/multicentric tumors (P = 0.025, n = 103, **Figure 3.1.3 B**). In addition, higher BATM infiltration had a shorter OS both in PR-positive (P = 0.041, n = 131, **Figure 3.1.3 C)** and PR-negative cases (P = 0.005, n = 89, **Figure 3.1.3 D**). Moreover, high infiltration of BATM lead to a short OS of BC patients ≥ 50 YO (P = 0.001, n = 164, **Figure 3.1.3 E**), of Luminal A-like BC cases (P = 0.001, n = 127, **Figure 3.1.3 F**), of TNBC cases (P = 0.049, n = 24, **Figure 3.1.3 G**), of patients with tumor ≤ 2 cm ( P = 0.008, n = 142, **Figure 3.1.3 H**), of patients without lymphatic metastasis (P = 0.00021, n = 117, **Figure 3.1.3 I**), as well as of ER positive cases (P = 0.003, n = 183, **Figure 3.1.3 J**), of HER2 unamplified BC patients (P = 0.001, n = 199, **Figure 3.1.3 K**) and of cases assigned with Ki-67 expression ≤ 14% (P = 0.001, n = 128, **Figure 3.1.3 L**). No association between BATM infiltration and OS was found in corresponding other subgroups.

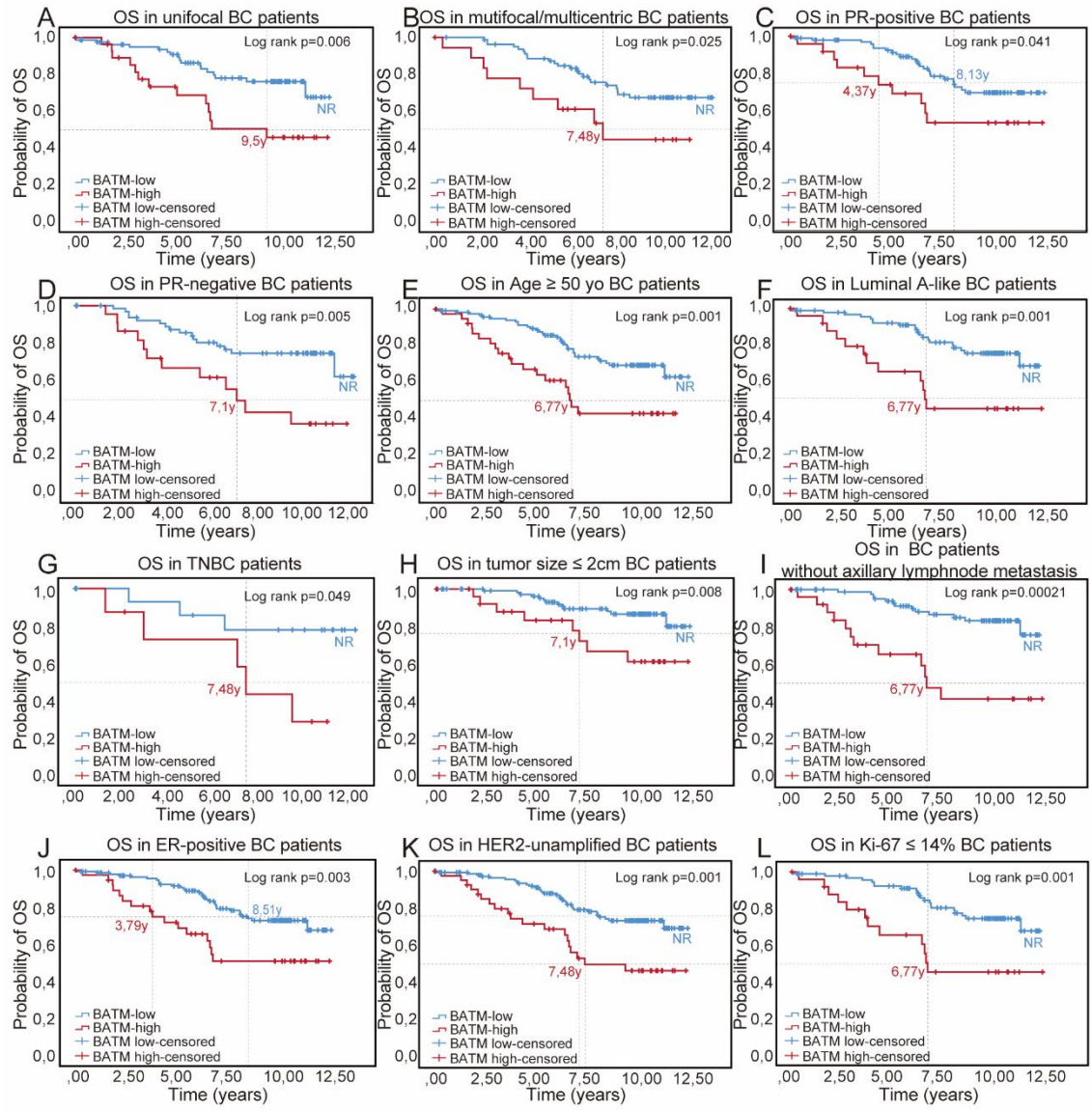


**Figure 3.1.3 Prognostic role of BATM in OS across subpopulations grouped by clinicopathological characteristic of BC patients.**

This figure was adopted from a related published paper [47], **by the First Author**.

**A-B.** BATM was negatively correlated to OS both in unifocal tumor (P = 0.006, n = 117, **A**) and multifocal/multicentric tumors (P = 0.025, n = 103, **B**). **C-D.** BATM was negatively correlated to OS both of PR-positive (P = 0.041, n = 131, **C**) and PR negative cases (P = 0.005, n = 89, **D**). **E-L.** BATM was negatively correlated to OS of patients ≥ 50 YO (P = 0.001, n = 164, **E**), of Luminal A-like BC patients (P = 0.001, n =

127, **F**), of TNBC patients (P = 0.049, n = 24, **G**), of patients with tumor ≤ 2 cm ( P = 0.008, n = 142, **H**), of patients without lymphatic metastasis (P = 0.00021, n = 117, **I**), as well as of ER positive cases (P = 0.003, n = 183, **J**), of HER2 unamplified cases (P = 0.001, n = 199, **K**) and of cases assigned with Ki-67 expression ≤ 14% (P = 0.001, n = 128, **L**). "BATMs, Breast adipose tissue macrophages", "OS, Overall survival", "ER, Estrogen receptor". "PR, Progesterone receptor", "HER2, Human epidermal growth factor receptor 2" [47] (Obtained from this related published paper, **as the First Author)**.

Additionally, the prognostic role of BTSM in OS across different subgroups that grouped by some clinical or pathological parameters demonstrated that a high BTSM infiltration lead to a short OS of patients ≥ 50 YO (P = 0.029, n = 180, **Figure 3.1.4 A**), of luminal A-like BC cases (P = 0.046, n = 138, **Figure 3.1.4 B**), of patients with multifocal/multicentric tumors (P = 0.026, n = 111, **Figure 3.1.4 C**), of patients with tumor ≤ 2 cm (P = 0.031, n = 155, **Figure 3.1.4 D**), of cases without lymphatic metastasis (P = 0.029, n = 131, **Figure 3.1.4 E**), of ER positive cases (P = 0.034, n = 197, **Figure 3.1.4 F**), of HER2 unamplified cases (P = 0.026, n = 219, **Figure 3.1.4 G**) and of patients with Ki-67 expression ≤ 14% (P = 0.039, n = 139, **Figure 3.1.4 H**). No significant correlation between BTSM infiltration and OS was found in the respective other subgroups.

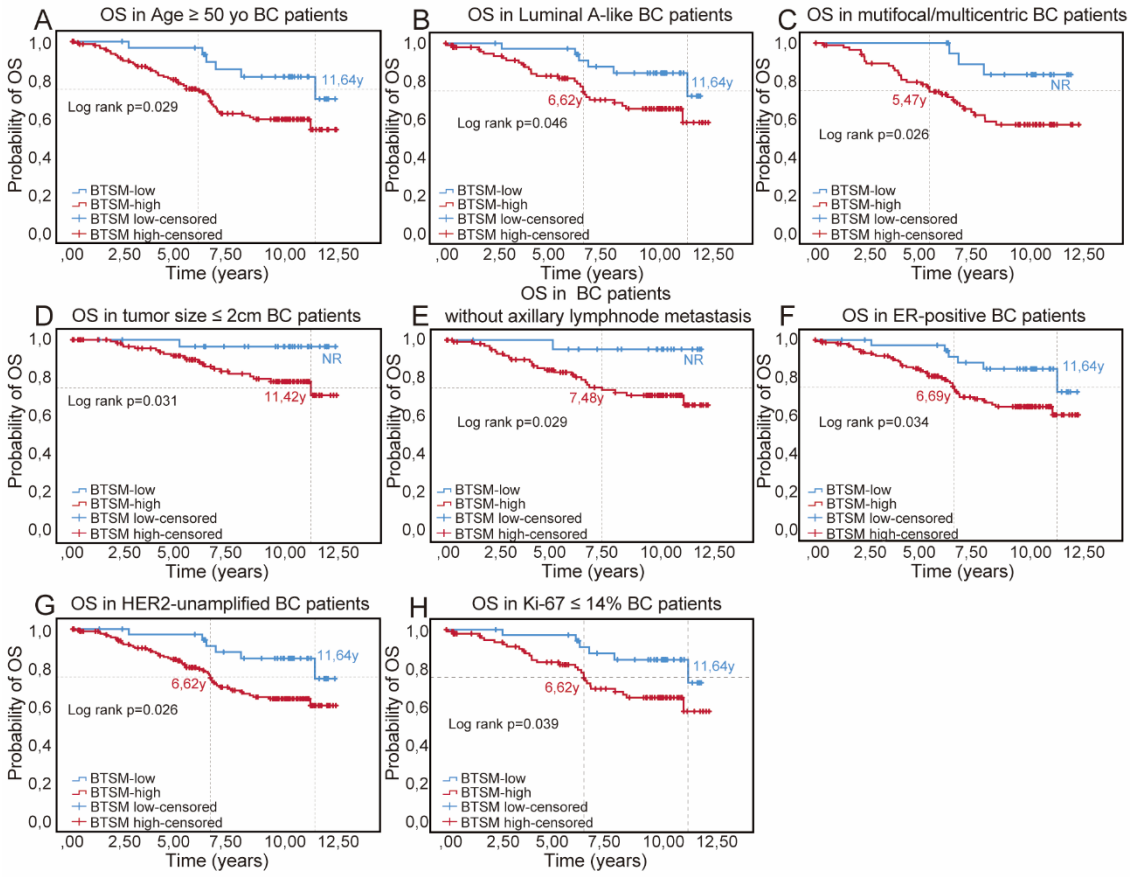


**Figure 3.1.4 Prognostic role of BTSM in OS across subpopulations grouped by clinicopathological characteristic of BC patients.**

This figure was adopted from a related published paper [47], **by the First Author**.
**A-H.** A high BTSM infiltration lead to a short OS of patients ≥ 50 YO (P = 0.029, n = 180, **A**), of luminal A-like BC patients (P = 0.046, n = 138, **B**), of patients with multifocal/multicentric tumors (P = 0.026, n = 111, **C**), of cases with tumor ≤ 2 cm (P = 0.031, n = 155, **D**), of cases with negative lymphatic metastasis (P = 0.029, n = 131, **E**), of ER positive cases (P = 0.034, n = 197, **F**), of HER2 unamplified cases (P = 0.026, n = 219, **G**) and of patients with Ki-67 expression ≤ 14% (P = 0.039, n = 139, **H**). "BTSMs, Breast tumor-stroma macrophages", "OS, Overall survival", "ER, Estrogen receptor", "PR, Progesterone receptor", "HER2, Human epidermal growth factor receptor 2" [47] (Obtained from this related published paper, **as the First Author)**.

### 3.1.4 Only BATM was associated with impaired DFS

Of all BC patients, the “BATM-high” infiltrated subgroup had lower DFS survival probability than the “BATM-low” infiltrated subgroup (HR = 1.800, 95%CI = 1.042-3.108), p = 0.032, **Figure 3.1.5 A**). The median DFS was only 5.35 years for “BATM-high” infiltrated patients (n=50) while 9.53 years for low BATM infiltration patients (n = 170) (**Figure 3.1.5 A**). BTSM infiltration had no association with DFS in the overall cohort (HR = 1.285, 95%CI = 0.687-2.403, p = 0.431, **Figure 3.1.5 B**).

Furthermore, the prognostic role of BATM in DFS across different subgroups grouped by some clinicopathological parameters revealed that a high BATM infiltration led to a short DFS of BC patients ≥ 50 YO (P = 0.015, n = 164, **Figure 3.1.5 C**) and of the patients with unifocal tumor (P = 0.016, n = 117, **Figure 3.1.5 D**). No significant correlation between BATM infiltration and DFS was found in the respective other subgroups.

These observations indicate that the influence of BATM on the prognosis of BC was more significant than BTSM did.

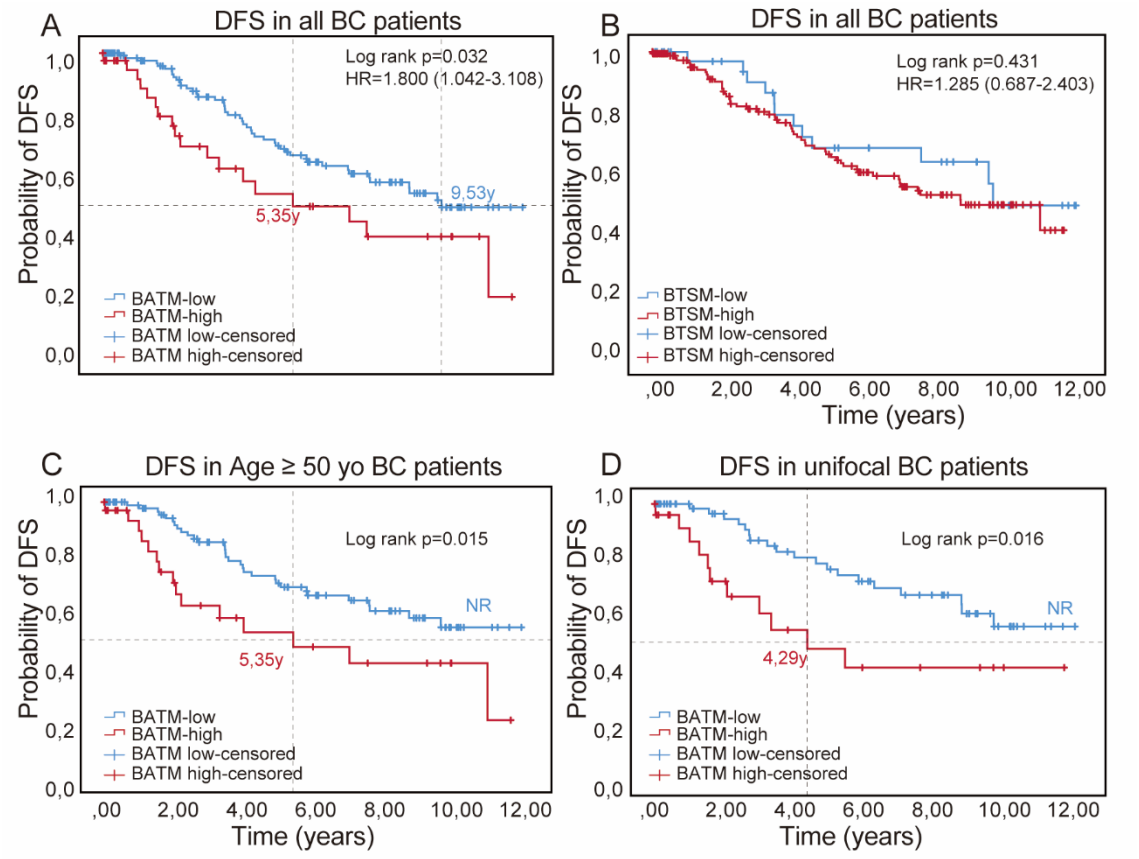


**Figure 3.1.5. Only BATM but not BTSM was associated with impaired DFS of the whole BC cohort and of some clinical characteristic-grouped subpopulations**

This figure was adopted from a related published paper [47], **by the First Author**.
**A.** A High BATM infiltration significantly correlated to an impaired DFS of the whole cohort of BC patients (HR = 1.800, 95%CI = 1.042-3.108, p = 0.032). **B.** No correlation was found between BTSM and DFS (HR = 1.285, 95%CI = 0.687-2.403, p = 0.431). **C-D**. A high BATM lead to a short DFS of the BC patients that ≥ 50 YO (P = 0.015, n = 164, **C**) and of the patients with unifocal tumor (P = 0.016, n = 117, **D**). “BTAMs, Breast adipose tissue macrophages; BTSMs, Breast tumor-stroma macrophages”, “DFS, Disease-free survival”, “HR, hazard ratio” [47] (Obtained from this related published paper, **as the First Author)**.

### 3.1.5 High BATM infiltration was an independent Indicator for impaired OS

The analysis result of univariate Cox regression demonstrated that "the BATMs subgroup (p = 0.001, HR = 2.483, 95% CI 1.474–4.182), the BTSMs subgroup (p = 0.025, HR = 2.445, 95%CI 1.117–5.354), the molecular subtype (p = 0.03, HR = 1.213, 95% CI 1.081–1.444), grading (p = 0.003, HR = 1.763, 95% CI 1.056–2.945), tumor size (p = 5.57E−13, HR = 2.064, 95% CI 1.695–2.513), axillary lymph node status (p = 0.002, HR = 1.859, 95% CI 1.256–2.749), and ER status (p = 0.026, HR = 0.589, 95% CI 0.369–0.940)" [47] (Obtained from this related published paper, **as the First Author**) were significant indicators for OS of BC patients (**Table 3.1.2**).

**Table 3.1.2 Univariate Cox regression analyses of BATM, BTSM and clinicopathological characteristics for OS in BC patients**

This table was adopted from a related published paper [47], **by the First Author**.

| Characteristics | Univariate analysis | | |
|---|---|---|---|
| | P | HR | 95%CI |
| **Age** ( < 50y vs. ≥50y) | 0.055 | 1.746 | 0.987-3.088 |
| **Molecular subtype** (LuA-like vs.LuB-like vs. TNBC vs. HER2 Lu-like vs. HER2 nonLu-like) | **0.03*** | **1.213** | **1.018-1.444** |
| **Grading** (G1 vs. G2 vs. G3) | **0.003**** | **1.763** | **1.056-2.945** |
| **Tumor foci** (unifocal vs. multifocal and muticentric) | 0.889 | 0.971 | 0.642-1.469 |
| **Tumor size** (pT1 vs. pT2 vs. pT3 vs. pT4) | **5.573E-13***** | **2.064** | **1.695-2.513** |
| **Axillary lymph node status** (pN0 vs. pN1 vs.pN2) | **0.002**** | **1.859** | **1.256-2.749** |
| **ER status** (ER- vs. ER+) | **0.026*** | **0.589** | **0.369-0.940** |
| **PR status** (PR- vs. PR+) | 0.088 | 0.697 | 0.461-1.054 |
| **HER2 status** (HER2- vs. HER2+) | 0.079 | 1.667 | 0.942-2.952 |
| **Expression of Ki-67** (Ki-67 ≤14% vs. Ki-67 > 14%) | 0.891 | 1.040 | 0.588-1.840 |
| **BATM** ( Low vs. High ) | **0.001**** | **2.483** | **1.474-4.182** |
| **BTSM** ( Low vs. High ) | **0.025*** | **2.445** | **1.117-5.354** |

"ER estrogen receptor, PR progesterone receptor, HER2 human epidermal growth factor receptor 2, LuA-like luminal A-like, LuB-like luminal B-like, TNBC triple-negative breast cancer, HER2 Lu-like HER2 amplified luminal-like, HER2 nonLu like HER2 amplified non luminal-like, BATMs breast adipose tissue macrophages, BTSMs breast tumor-stroma macrophages, HR hazard ratio, CI confidence interval" [47] (Obtained from this related published paper, **as the First Author**); "*, p < 0.05; **, p < 0.01; ***, p < 0.001" [301].

Multivariate Cox regression analysis of three models was performed. All three models included age, and the univariate regression-defined significant clinicopathological variables, such as molecular subtype, grading, tumor size, and axillary lymph node status. Model 1 included the variable BTSM to determine if high BTSM infiltration can independently predict poor OS of BC patients. Model 2 included BATM to determine if high BATM infiltration can independently indicate the poor OS in BC. Model 3 included both BATM and BTSM to determine if BATM, BTSM, or both can predict OS of BC patients independently when BTSM or BATM was also taken into account. The analysis results of model 1 demonstrated that high BTSM infiltration indicated the impaired OS dependently of BC patients (HR = 1.529, 95 %CI = 0.541-4.324, p = 0.424, **Table 3.1.3**). However, the analysis result of model 2 demonstrated that high BATM infiltration (HR = 4.259, 95 %CI = 1.666-10.887, p = 0.002, **Table 3.1.3**) independently indicated the poor OS of BC patients. Furthermore, the analysis result of model 3 demonstrated that even though BTSM was considered, BATM remained to independently indicate the OS of BC patients (HR = 4.464, 95 %CI = 1.624-12.269, p = 0.004, **Table 3.1.3**).

**Table 3.1.3 Multivariate Cox regression analyses of BATM, BTSM and clinicopathological characteristics for OS in BC patients**

This table was adopted from a related published paper [47], **as the First Author**).

| Characteristics | Multivariate analysis model 1 ( without BATM) | | | Multivariate analysis model 2 (without BTSM) | | | Multivariate analysis model 3 (with both BATM and BTSM) | | |
|---|---|---|---|---|---|---|---|---|---|
| | P | HR | 95% CI | P | HR | 95% CI | P | HR | 95% CI |
| **Age** ( < 50y vs. ≥50y) | 0.874 | 1.079 | 0.420-2.773 | 0.674 | 0.807 | 0.298-2.189 | 0.741 | 0.843 | 0.305-2.326 |
| **Molecular subtype** (LuA-like vs.LuB-like vs. TNBC vs. HER2 Lu-like vs. HER2 nonLu-like) | 0.332 | 1.224 | 0.814-1.841 | 0.186 | 1.351 | 0.865-2.109 | 0.185 | 1.351 | 0.866-2.107 |
| **Grading** (G1 vs. G2 vs. G3) | 0.580 | 1.219 | 0.604-2.459 | 0.376 | 1.434 | 0.646-2.911 | 0.405 | 1.403 | 0.633-3.110 |
| **Tumor size** (pT1 vs. pT2 vs. pT3 vs. pT4) | **0.001**** | **1.873** | **1.304-2.689** | **0.001**** | **1.847** | **1.283-2.658** | **0.001**** | **1.827** | **1.269-2.631** |
| **Axillary lymph node status** (pN0 vs. pN1 vs.pN2) | 0.476 | 1.368 | 0.578-3.238 | 0.295 | 1.620 | 0.656-4.002 | 0.285 | 1.650 | 0.659-4.131 |
| **ER status (**ER- vs. ER+) | 0.775 | 0.853 | 0.285-2.548 | 0.670 | 0.765 | 0.224-2.620 | 0.604 | 0.718 | 0.205-2.515 |
| **BATM** ( Low vs. High ) | | | | **0.002**** | **4.259** | **1.666-10.887** | **0.004**** | **4.464** | **1.624-12.269** |
| **BTSM** ( Low vs. High ) | 0.424 | 1.529 | 0.541-4.324 | | | | 0.737 | 0.813 | 0.243-2.721 |

"Multivariate analysis model 1 was performed without BATM, which was attempted to show whether BTSM is an independent prognostic factor of OS of the whole patient cohort; multivariate model 2 was performed without BTSM, which was attempted to show whether BATM is an independent prognostic factor of OS of the whole patient cohort" [47] (Obtained from the "**Additional file 3**" of this related published paper, **as the First Author**). "Multivariate analysis model 3 was performed with both BATMs and BTSMs, to determine if BATMs, BTSM, or both were an independent prognostic factor of OS when both subtypes of macrophages were considered. ER, Estrogen receptor; PR, Progesterone receptor; HER2, Human Epidermal growth factor receptor 2; LuA-like, Luminal A-like; LuB-like, Luminal B-like; TNBC, Triple-negative breast cancer, HER2 Lu-like, HER2 amplified Luminal -like; HER2 non-Lu like, HER2 amplified non-luminal-like; BATMs, Breast adipose tissue macrophages; BTSMs, Breast tumor-stroma macrophages; HR hazard ratio, CI, confidence interval" [47] (Obtained from this related published paper, **as the First Author**). "*, $p < 0.05$; **, $p < 0.01$; ***, $p < 0.001$" [301].

### 3.1.6 High BATM infiltration was an independent Indicator for impaired DFS

Univariate Cox regression analysis demonstrated that "the BATMs subgroup ($p = 0.035$, HR = 1.800, 95% CI 1.042–3.108), tumor grade ($p = 0.03$, HR = 1.669, 95% CI 1.050–2.654), tumor size ($p = 0.002$, HR = 1.493, 95% CI 1.159–1.922), and axillary lymph node status ($p = 0.01$, HR = 1.696, 95% CI 1.137–2.528)" [47] (Obtained from this related published paper **as the First Author**) were negatively correlated to DFS (**Table 3.1.4**). However, BTSM had no association with DFS of BC patients (HR = 1.285, 95 %CI = 0.687-2.403, $p = 0.432$, **Table 3.1.4**). Subsequent multivariate Cox analysis including variables of "age, grading, tumor size, axillary lymph node status and BATM" [47] (Obtained from this related published paper **as the First Author**) demonstrated that BATM remained to independently indicate the DFS of BC patients (HR = 3.240, 95 %CI = 1.423-7.378, $p = 0.005$, **Table 3.1.4**).

**Table 3.1.4 Univariate and multivariate Cox regression analyses of BATM, BTSM and clinicopathological characteristics for DFS in BC patients**

This table was adopted from a related published paper [47], **by the First Author**.

| Characteristics | Univariate analysis | | | Multivariate analysis | | |
|---|---|---|---|---|---|---|
| | **P** | **HR** | **95% CI** | **P** | **HR** | **95% CI** |
| **Age**( < 50y vs. ≥50y) | 0.19 | 0.732 | 0.459-1.167 | 0.134 | 0.537 | 0.238-1.210 |
| **Molecular subtype** (LuA-like vs.LuB-like vs. TNBC vs. HER2 Lu-like vs. HER2 nonLu-like) | 0.329 | 1.093 | 0.914-1.307 | n.i. | n.i. | n.i. |
| **Grading** (G1 vs. G2 vs. G3) | **0.03*** | **1.669** | **1.050-2.654** | **0.043*** | **1.825** | **1.018-3.271** |
| **Tumor foci** (unifocal vs. multifocal and muticentric) | 0.370 | 1.214 | 0.794-1.857 | n.i. | n.i. | n.i. |
| **Tumor size** (pT1 vs. pT2 vs. pT3 vs. pT4) | **0.002**** | **1.493** | **1.159-1.922** | **0.011*** | **1.646** | **1.120-2.418** |
| **Axillary lymph node status** (pN0 vs. pN1 vs.pN2) | **0.01*** | **1.696** | **1.137-2.528** | **0.856** | **1.078** | **0.482-2.411** |
| **ER status** (ER- vs. ER+) | 0.771 | 0.926 | 0.550-1.557 | n.i. | n.i. | n.i. |
| **PR status** (PR- vs. PR+) | 0.249 | 1.291 | 0.836-1.994 | n.i. | n.i. | n.i. |
| **HER2 status** (HER2- vs. HER2+) | 0.511 | 1.228 | 0.666-2.262 | n.i. | n.i. | n.i. |
| **Expression of Ki-67** (Ki-67 ≤14% vs. Ki-67 > 14%) | 0.093 | 1.569 | 0.928-2.653 | n.i. | n.i. | n.i. |
| **BATM** (Low vs. High) | **0.035*** | **1.800** | **1.042-3.108** | **0.005**** | **3.240** | **1.423-7.378** |
| **BTSM** (Low vs. High) | 0.432 | 1.285 | 0.687-2.403 | n.i. | n.i. | n.i. |

"ER estrogen receptor, PR progesterone receptor, HER2 human epidermal growth factor receptor 2, LuA-like luminal A-like, LuB-like luminal B-like, TNBC triple-negative breast cancer, HER2 Lu-like HER2 amplified luminal-like, HER2 nonLu like HER2 amplified non luminal-like, BTAMs breast adipose tissue macrophages, BTSMs breast tumor-stroma macrophages, HR hazard ratio, CI confidence interval, n.i not included in multivariate model, as p > 0.05 in univariate analysis" [47] (Obtained from this related published paper, **as the First Author**). "*, p < 0.05; **, p < 0.01; ***, p < 0.001" [301].

## 3.2 EP3 related to BATM Infiltration in our BC Cohort

(This part of the results has been published recently in *Breast Cancer Research* [47], **as the First Author**)

### 3.2.1 A Negative Correlation was found between EP3 and BATM Infiltration

A previous study of us has demonstrated that low EP3 expression independently indicates the favorable survival of BC patients [282]. However, tumor cell biology cannot explain the positive prognostic role of EP3, leading to the speculation that the EP3-regulated process in BC may be mediated by immune factors in the TME other than tumor cells of BC [302]. To explore whether EP3 is associated with TAMs infiltration in BC-TME, thus regulating BC progression, we did a correlation analysis of EP3 IRS with quantities of BATM and BTSM, respectively. Furthermore, the infiltrating number of BATMs (continuous variable) was negatively correlated to IRS of EP3 expression (ordinal variable) (Spearman's ρ = - 0.1977, p = 0.0034, **Figure 3.2.1 A**). Moreover, EP3 was higher expressed in the "BATM-low" subpopulation than that in the "BATM-high" subpopulation (p = 0.00392, **Figure 3.2.1 B**). Interestingly, when EP3-IRS was categorized as "EP3-high" (IRS > 1) and "EP3-low" (IRS ≤ 1), the number of infiltrating BATMs in the "EP3-high" subpopulation was less than those in the EP3-low subpopulation (P = 0.0322, **Figure 3.2.1 C**). These two categorical variables ("BATM-high/-low" and "EP3-high/-low") were also compared and

showed a borderline significant correlation (P = 0.051, **Table 3.1.1**). No association of EP3 expression with BTSM infiltration was observed in BC. These observations confirmed that EP3 expression was negatively correlated with BATM infiltration, indicating EP3 might regulate BC progression via influencing BATM phenotype infiltration.

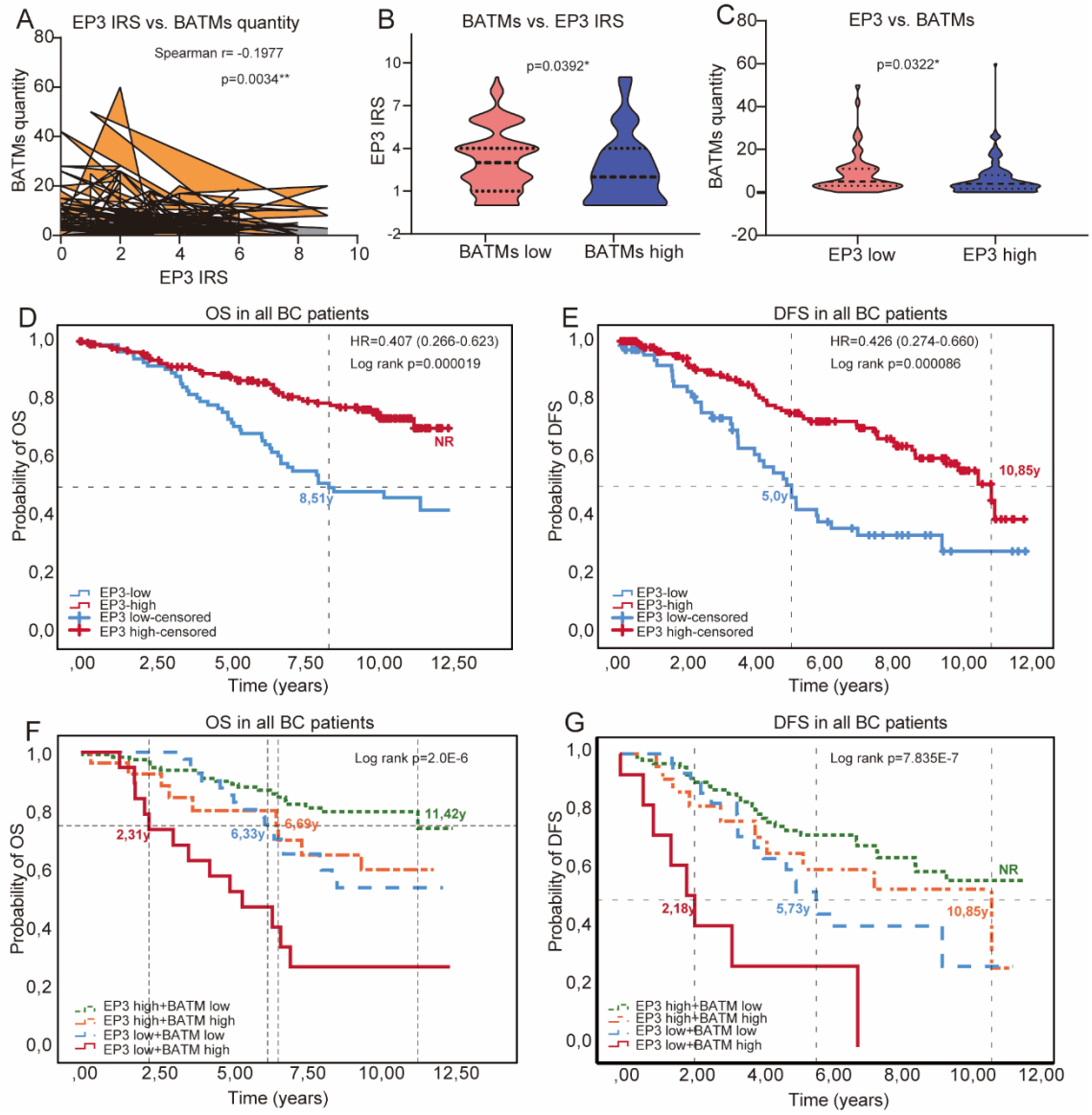


**Figure 3.2.1 The relationship between EP3 expression and BATM infiltration in our BC Cohort**

This figure was adopted from a related published paper [47], **by the First Author**.
**A.** The infiltrating number of BATMs (continuous variable) was negatively correlated to IRS of EP3 expression (ordinal variable) (Spearman's ρ = - 0.1977, p = 0.0034). **B.** Tumors with "BTAM-high" distribution showed lower EP3 than tumors with "BTAM-low" distribution (P = 0.00392). **C.** Infiltration number of BATMs in the "EP3-high" cases was less than that in the "EP3-low" cases (P = 0.0322). **D.** EP3 expression related to favorable OS outcomes of BC patients (HR = 0.407, 95%CI = 0.266-0.623, p = 0.000019). **E.** EP3 expression related to favorable DFS outcomes of BC patients (HR = 0.426, 95%CI = 0.274-0.660, p = 0.000086). **F.** Inferior OS prognosis was observed in the "EP3-low+BATMs-high" subgroup (P = 2.0E-6). **G.** Inferior DFS prognosis was observed in the "EP3-low+BATM-high" subpopulation (P = 7.835E-7). "BATMs, Breast adipose tissue macrophage; EP3, prostaglandin E receptor 3; OS, Overall survival; DFS, Disease-free survival", "IRS, Immunoreactive score" [47] (Obtained from a related published paper **as the First Author**).

### 3.2.2 Prognostic analysis that combined EP3 with BATM in BC patients

Then, to explore whether EP3 interacts with BATM involving in the BC progression, we did a prognostic survival analysis for EP3 expression and the combination parameter of EP3 expression with BATM abundance. Consistent with previous studies [282], EP3 expression related to favorable OS and DFS outcomes in BC patients (OS: HR = 0.407, 95%CI = 0.266-0.623, p = 0.000019, **Figure 3.2.1 D** and DFS: HR = 0.426, 95%CI = 0.274-0.660, p = 0.000086, **Figure 3.2.1 E**). We then compared the OS probability and DFS probability of four subgroups: "EP3-low+BATM-high", "EP3-low+BATM-low", "EP3-high+BATM-low" and "EP3-high+BATM-high". The subgroup characterized as "EP3-low+BATM-high" had an inferior OS (P = 2.0E-6, **Figure 3.2.1 F**) and DFS (P = 7.835E-7, **Figure 3.2.1 G**). Furthermore, via cox regression analysis, we observed that patients (n = 20) with "EP3-low+BATM-high" had the lowest survival probability, while patients with "EP3-high+BATM-low" (n = 124) showed the highest survival probability ( OS%: 35.0% vs.83.1%, HR = 1.756, 95%CI =1.391-2.217, p = 0.000002, **Table 3.2.1** part A; DFS%: 60.0% vs. 77.4%, HR = 1.922. 95%CI = 1.453-2.544, p = 0.000005, **Table 3.2.1** part A ).

Additionally, compared to the "EP3-high+BATM-low" subpopulation, the "EP3-low+BATM-high" distributed BC had a 1.756 times higher risk of death and a 1.922 higher risk of recurrence (**Table 3.2.1** part A). Of the BC patients with high BATMs infiltration, compared to the "EP3-high" subpopulation, "EP3-low" distributed BC had a 1.647 times higher risk of death (P = 0.023) and 2.107 times higher risk of recurrence (P = 0.004) (**Table 3.2.1** part B). Similarly, of the BC patients with low BATM infiltrating, compared to the "EP3-high" subpopulation, the EP3-low distributed BC had a 1.511 times higher risk of death (P = 0.01) and 1.405 times higher risk of recurrence (P = 0.028) (**Table 3.2.1** part C). However, in the BC patients with high EP3 expression, the infiltration of BATM did not influence the survival outcomes (**Table 3.2.1** part D). Interestingly, of the BC patients with "EP3-low" distribution, compared to the "BATM-low" subpopulation, the "BATM-high" distributed BC had a 2.722 times higher risk of death (P = 0.007) and 4.049 times higher risk of recurrence (P = 0.002) (**Table 3.2.1** part E).

These results indicate that EP3 might reduce the pro-tumor effect of BATM on BC. Vice versa, when EP3 is lower expressed, BATM appears to be riskier than in an EP3 high expressed context.

**Table 3.2.1 Survival analyses of different combined variables of EP3 and BATM in BC**

This table was adopted from a related published paper [47], **by the First Author**.

| | OS% | P value | HR | 95% CI | DFS% | P value | HR | 95% CI |
|---|---|---|---|---|---|---|---|---|
| **A.** | | | | | | | | |
| EP3-high+BATM-low | 83.1 | | | | 77.4 | | | |
| EP3-high+BATM-high | 70.0 | 0.059 | 2.128 | 0.973-4.658 | 66.7 | 0.326 | 1.437 | 0.697-2.962 |
| EP3-low+BATM-low | 58.1 | **0.01*** | **1.511** | **1.102-2.070** | 60.5 | **0.028*** | **1.405** | **1.037-1.902** |
| EP3-low+BATM-high | 35.0 | **0.000002***** | **1.756** | **1.391-2.217** | 60.0 | **0.000005***** | **1.922** | **1.453-2.544** |
| **B.** | | | | | | | | |
| BATM-high+EP3-high | 70.0 | | | | 66.7 | | | |
| BATM-high+EP3-low | 35.0 | **0.023*** | **1.647** | **1.070-2.536** | 60.0 | **0.004**** | **2.107** | **1.264-3.513** |
| **C.** | | | | | | | | |
| BATM-low+EP3-high | 83.1 | | | | 77.4 | | | |
| BATM-low+EP3-low | 58.1 | **0.01*** | **1.511** | **1.102-2.070** | 60.5 | **0.028*** | **1.405** | **1.037-1.902** |
| **D.** | | | | | | | | |

| | | | | | | | | |
|---|---|---|---|---|---|---|---|---|
| EP3-high+BATM-low | 83.1 | | | | 77.4 | | | |
| EP3-high+BATM-high | 70.0 | 0.059 | 2.128 | 0.973-4.658 | 66.7 | 0.326 | 1.437 | 0.697-2.962 |
| **E.** | | | | | | | | |
| EP3-low+BATM-low | 58.1 | | | | 60.5 | | | |
| EP3-low+BATM-high | 35.0 | **0.007**** | **2.722** | **1.321-5.609** | 60.0 | **0.002**** | **4.049** | **1.665-9.847** |

"BATMs breast adipose tissue macrophage, EP3 prostaglandin E receptor 3, OS overall survival, DFS disease-free survival, p value, HR hazard ratio, CI confidence interval" [47] (Obtained from this related published paper, **as the First Author**). "*, $p < 0.05$; **, $p < 0.01$; ***, $p < 0.001$" [301].

## 3.3 The Role of Transcriptional Factor *KLF11* in BC Tissue Samples

The role KLFs members in BC have been systematically summarized. However, whether KLFs act as oncogenes or tumor suppressors has not yet reached a consensus. Given that KLF11 belongs to such a volatile/context-dependent family, to clarify whether KLF11 acts as an oncogene or a tumor-suppressor in BC, we conducted a dual exploration of the role of KLF11 in BC patients. Firstly, we explored the role of *KLF11* mRNA expression in BC patients identified by bulk RNA-seq datasets. Secondly, we explored and validated the prognostic role of the KLF11 in our BC cohort by applying immunohistochemistry (IHC) staining of KLF11 in the 298 patients' samples, followed by correlating to clinic-pathological characteristics and survival outcomes to make sure the exactly pro- or anti-tumor role of KLF11.

We demonstrated *in silico* that *KLF11* mRNA was lower expressed in BC tumor tissue than in the non/para-cancerous breast tissues. Furthermore, *KLF11* mRNA expression was positively associated with aggressive BC features. Its elevated expression remained an independent indicator for poor OS of BC. In addition, *in vivo*, a higher KLF11 protein level was confirmed stained in the more aggressive molecular subtype of BC. It was negatively correlated with prognosis. In addition, high KLF11 protein levels remained to independently indicate the poor DFS and DMFS of BC identified by our patient's cohort. Interestingly, our results indicate that although it was low expressed in BC tissues, KLF11 appeared to be a pro-tumor factor in BC.

### 3.3.1 The Differential Expression and Diagnostic Value of *KLF11* in BC identified by Bulk RNA-seq Datasets

The differential expression of *KLF11* between the tumor tissues and their corresponding non-tumor tissues of diverse cancers was investigated using TIMER.

We observed that *KLF11* expression was lower in breast invasive carcinoma (BRCA, hereafter termed TCGA-BC), "bladder urothelial carcinoma (BLCA)", "kidney renal clear cell carcinoma (KIRC)", "kidney chromophobe (KICH)", "kidney renal papillary cell carcinoma (KIRP)", and "liver hepatocellular carcinoma (LIHC)", "lung adenocarcinoma (LUAD)", "lung squamous cell carcinoma (LUSC), prostate adenocarcinoma (PRAD)", "rectum adenocarcinoma (READ)", "thyroid carcinoma (THCA)" and "uterine corpus endometrial carcinoma (UCEC)" [303] than that in their corresponding non-tumor tissues (**Figure 3.3.1 A**). *KLF11* expression was only observed to be significantly higher in "head and neck squamous cell carcinoma (HNSC)" [303] compared to its corresponding non-tumor tissues (**Figure 3.3.1 A**). To further explore the *KLF11* expression of human BC in more detail, we downloaded and analyzed the expression of *KLF11* based on the TCGA-BC cohort using the R programmer. We observed that *KLF11* expression was lower in BC

than that in non-tumor breast tissues (P < 0.001, **Figure 3.3.1 B**) and the para-tumor breast tissues (P < 0.001, **Figure 3.3.1 C**). Moreover, we then evaluated the diagnostic value of *KLF11* mRNA expression between normal and tumor tissue by ROC analysis determined by the R package "pROC". The results showed the high accuracy of KLF11 mRNA expression in predicting breast normal or breast tumor (AUC = 0.910, CI = 0.884-0.936, **Figure 3.3.1 D**).

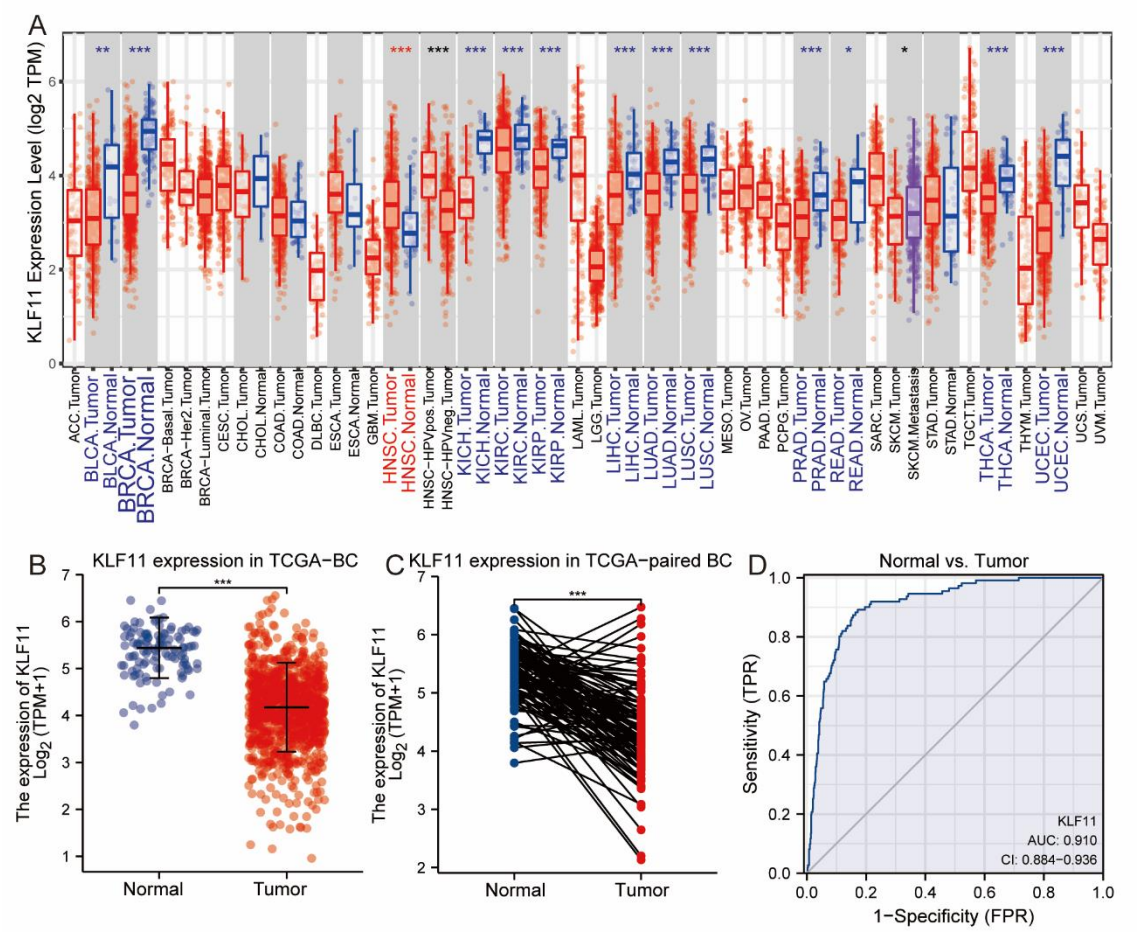


**Figure 3.3.1 The differential expression and diagnostic significance of *KLF11* in BC.**
**A.** The expression pattern of *KLF11* across different TCGA cancer types was explored using TIMER. **B-C.** *KLF11* expression was lower in BC than that in non-tumor breast tissues (P < 0.001, **B**) and that in the para-tumor breast tissues (P < 0.001, **C**). **D.** ROC curve showed the high accuracy of *KLF11* mRNA expression in predicting breast normal or breast tumor (AUC = 0.910, CI = 0.884-0.936). "*, p < 0.05; **, p < 0.01; ***, p < 0.001" [301].

## 3.3.2 Higher *KLF11* related to more Aggressive Features of BC identified by Bulk RNA-seq Datasets

*KLF11* mRNA differential expression was then analyzed in subgroups categorized by ER status, PR status, and molecular subtypes. The results demonstrated that higher *KLF11* related ER-negative statues (p < 0.001, **Figure 3.3.2 A**) and PR-negative status (p < 0.00 1, **Figure 3.3.2 B**). Furthermore, *KLF11* was higher expressed in TNBC compared to LuA-BC (p < 0.001), LuB-BC (p < 0.001), and HER2-BC (p < 0.01), respectively (**Figure 3.3.2 C**).

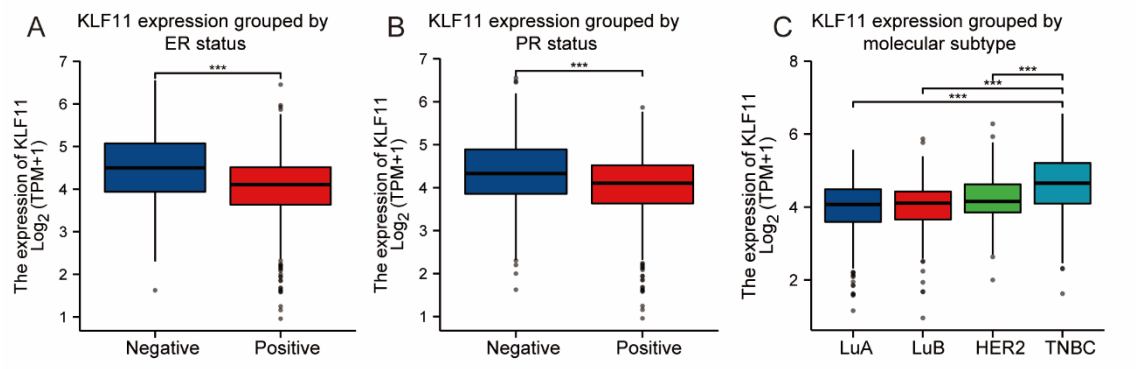


**Figure 3.3.2 KLF11 was associated with aggressive features of BC.**

**A-B.** Higher *KLF11* related ER-negative ($p < 0.001$, **A**) and PR-negative status ($p < 0.00$ 1, **B**). **C.** *KLF11* was higher expressed in TNBC compared to LuA-BC ($p < 0.001$), LuB-BC ($p < 0.001$), and HER2-BC ($p < 0$ .01). LuA, Luminal A; LuB, Luminal B; "*, $p < 0.05$; **, $p < 0.01$; ***, $p < 0.001$" [301].

### 3.3.3 Prognostic Potential of *KLF11* in BC identified by Bulk RNA-seq Datasets

Next, we explored the significance of *KLF11* for BC prognosis identified by bulk RNA-seq datasets using TISIDB, R programmer, and KM plotter server port. The TISIDB database demonstrated that a higher *KLF11* expression related to a shorter OS of BC and UCEC patients while a longer OS of KIRC patients among the *KLF11* lower expressed cancer types in TCGA cohorts ( **Figure 3.3.1 A, Figure 3.3.3 A**). Furthermore, a more detailed exploration of the TCGA-BC cohort revealed that a higher expression of *KLF11* did lead to a lower OS percentage using the TISIDB server (P = 0.0164, **Figure 3.3.3 B**) and R programmer (HR = 1.71, 95%CI = 1.19-2.44, n = 1064, p = 0.01, **Figure 3.3.3 C**). However, there was no correlation between *KLF11* and DFS of BC (HR = 1.20, 95%CI = 0.86-1.67, n = 1064, p = 0.274, **Figure 3.3.3 D**). Interestingly, when focusing on young BC patients (≤ 60 YO), *KLF11* was associated with impaired DFS (HR = 1.73, 95%CI = 1.11-2.70, n = 588, p = 0.013, **Figure 3.3.3 E**). In addition, the results from KM plotter showed that *KLF11* negatively related to OS in BC, data of which are obtained from GSE datasets (HR = 1.3, 95%CI = 1.08-1.58, n = 1879, p = 0.0064, **Figure 3.3.3 F**). Furthermore, the results from GSE database explored using KM plotter showed that higher *KLF11* led to a lower DFS probability (HR = 1.27, 95%CI = 1.15-1.41, n = 4929, p = 2.7e-06, **Figure 3.3.3 G**) and DMFS probability (HR = 1.56, 95%CI = 1.33-1.82, n = 2765, p = 2.5e-08, **Figure 3.3.3 H**) in BC. In conclusion, high *KLF11* expression might indicate the impaired BC prognosis.

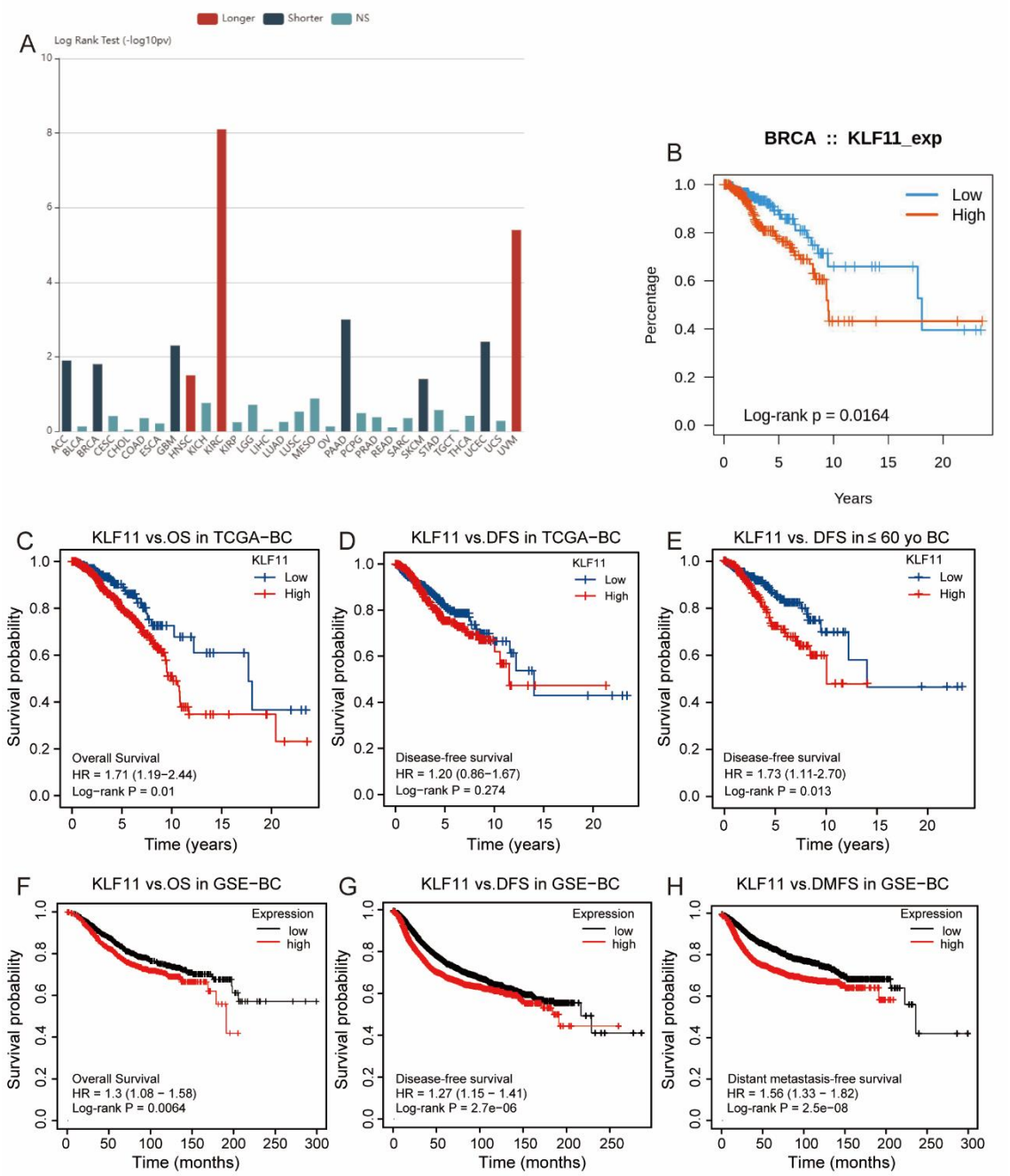


**Figure 3.3.3 The prognostic value of *KLF11* in BC identified by Bulk RNA-seq Datasets.**
**A.** Association between *KLF11* expression and OS across human cancers contained in TCGA database. **B-C.** A higher expression of KLF11 lead to a lower OS percentage using TISIDB server (P = 0.0164, **B**) and R programmer (HR = 1.71, 95%CI = 1.19-2.44, n = 1064, p = 0.01, **C**). **D-E.** No correlation between *KLF11* and DFS across the whole TCGA-BC cohort was found (HR = 1.20, 95%CI = 0.86-1.67, n = 1064, p = 0.274, **D**), but negative correlation between *KLF11* and DFS among the younger BC patients (≤ 60 YO) was found (HR = 1.73, 95%CI = 1.11-2.70, n = 588, p = 0.013, **E**). **F-H.** Higher KLF11 led to a lower OS probability (HR = 1.3, 95%CI = 1.08-1.58, n = 1879, p = 0.0064, **F**), DFS probability (HR = 1.27, 95%CI = 1.15-1.41, n = 4929, p = 2.7e-06, **G**) and DMFS probability (HR = 1.56, 95%CI = 1.33-1.82, n = 2765, p = 2.5e-08, **H**) in BC patients from GSE datasets.

To have a better knowledge of the prognostic role of *KLF11* in BC, the prognostic significance of *KLF11* across the subgroups defined by different clinic-pathological characteristics was then explored. TCGA-BC cohort was analyzed using an R programmer. The GSE-BC was analyzed using the KM plotter server.

We demonstrated that *KLF11* negatively related to OS probability of patients under 60 YO (HR = 2.00, 95%CI = 1.19-3.36, n = 588, p = 0.025, **Figure 3.3.4 A**), of patients with infiltrating ductal carcinoma (IDC) histology type (HR = 1.80, 95%CI = 1.22-2.65, n = 757, p = 0.004, **Figure 3.3.4 B**), of LuA BC (HR = 1.81, 95%CI = 1.04-3.16, n = 550, p = 0.017, **Figure 3.3.4 C**), of patients with T1/T2 stage (HR = 1.82, 95%CI = 1.22-2.71, n = 889, p = 0.008, **Figure 3.3.4 D**), of patients without lymphatic metastasis (HR = 2.37, 95%CI = 1.31-4.28, n = 507, p = 0.008, **Figure 3.3.4 E**) and of patients without distant metastasis (HR = 1.84, 95%CI = 1.25-2.70, n = 889, p = 0.006, **Figure 3.3.4 F**).

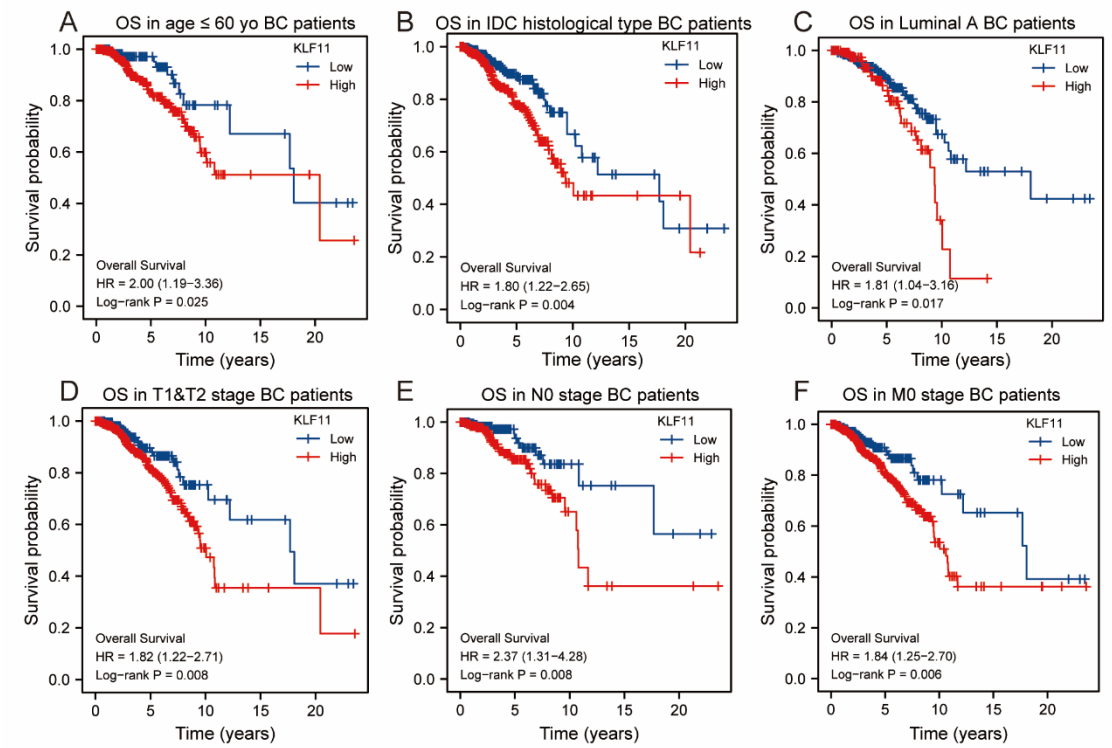


**Figure 3.3.4 *KLF11* expression was negatively associated with an impaired OS across some clinical-defined subpopulations of BC patients.**

**A-F.** The expression of *KLF11* negatively related to OS probability of patients of patients under 60 YO (HR = 2.00, 95%CI = 1.19-3.36, n = 588, p = 0.025, **A**), of patients with IDC histology type (HR = 1.80, 95%CI = 1.22-2.65, n = 757, p = 0.004, **B**), of luminal-A BC (HR = 1.81, 95%CI = 1.04-3.16, n = 550, p = 0.017, **C**), of patients with T1/T2 stage (HR = 1.82, 95%CI = 1.22-2.71, n = 889, p = 0.008, **D**), of patients without lymphatic metastasis (HR = 2.37, 95%CI = 1.31-4.28, n = 507, p = 0.008, **E**) and of patients without distant metastasis (HR = 1.84, 95%CI = 1.25-2.70, n = 889, p = 0.006, **F**).

Furthermore, results from the GSE-BC analyzed by KM plotter server showed that a higher *KLF11* expression indicated a shorter DFS of TNBC (HR = 1.14, 95%CI = 1.1-1.81, n = 953, p = 0.0061, **Table 3.3.1 part A**) and Luminal-A BC( HR = 1.27, 95%CI = 1.02-1.58, n = 1809, p = 0.029, **Table 3.3.1 part A**), of patients with Grade 2 feature (HR = 1.3, 95%CI = 1.04-1.64, n = 1177, p = 0.023, **Table 3.3.1 part A**) and Grade3 feature (HR = 1.27, 95%CI = 1.05-1.53, n = 1300, p = 0.012, **Table 3.3.1 part A**). And a high *KLF11* lead to an impaired DMFS of HER2 BC (HR = 1.69, 95%CI = 1.66-2.38, n = 401, p = 0.0049, **Table 3.3.1 part A**) and Luminal-A BC (HR = 1.57, n = 998, 95%CI = 1.05-1.53, p = 0.0078, **Table 3.3.1 part A**), of patients with Grade 2 feature (HR = 1.61, 95%CI = 1.19-2.16, n = 798, p = 0.017, **Table 3.3.1 part A**) and Grade3 feature (HR = 1.6, 95%CI = 1.23-2.07, n = 836, p = 4e-04, **Table 3.3.1 part A**). Regarding treatment strategies, accurately predicting prognosis of BC patients can guide precise clinical treatment and avoid medical waste. Thence, the prognostic value of *KLF11* was also investigated in

BC patients that grouped by with/without endocrine therapy or chemotherapy. Patients with higher *KLF11* expression had an inferior DFS of BC patients that without endocrine therapy (HR = 1.35, 95%CI = 1.15-1.58, n = 1935, p = 0.00021, **Table 3.3.1 part B**) and of BC patients after chemotherapy (HR = 1.64, 95%CI = 1.33-2.02, n = 1372, p = 3.9e-06, **Table 3.3.1 part B**), especially of the BC patients who took neoadjuvant chemotherapy (HR = 2.15, 95%CI = 1.58-2.93, n = 730, p = 6.e-07, **Table 3.3.1 part B**). Patients with higher mRNA expression of *KLF11* had worse DMFS of BC patients without endocrine therapy (HR = 1.72, 95%CI = 1.36-2.17, n = 1076, p = 4.4e-06, **Table 3.3.1 part B**) and of BC patients after chemotherapy (HR = 2.0, 95%CI = 1.53-2.60, n = 968, p = 2.1e-07, **Table 3.3.1 part B**), especially of the BC patients who took neoadjuvant chemotherapy (HR = 2.39, 95%CI = 1.73-3.3, n = 647, p = 5.8e-08, **Table 3.3.1 part B**).

**Table 3.3.1 Association of *KLF11* mRNA expression with DFS and DMFS across BC categorized by different clinic pathological factors or treatment strategies**

| | DFS (n = 4929) | | | DMFS (n = 2765) | | |
|---|---|---|---|---|---|---|
| **Part A.** Clinic pathological characteristics | | | | | | |
| | **N** | **HR (95%CI)** | **P** | **N** | **HR (95%CI)** | **P** |
| **Subtype - PAM50** | | | | | | |
| TNBC | **953** | **1.14 (1.1-1.81)** | **0.0061**** | 630 | 1.43 (1-2.06) | 0.051 |
| Luminal A | **1809** | **1.27 (1.02-1.58)** | **0.029*** | **998** | **1.57 (1.12-2.21)** | **0.0078**** |
| Luminal B | 1353 | 0.86 (0.7-1.05) | 0.14 | 673 | 1.29 (0.94-1.76) | 0.11 |
| HER2 | 695 | 1.23 (0.97-1.56) | 0.09 | **401** | **1.69 (1.66-2.38)** | **0.0049**** |
| **Grade** | | | | | | |
| Grade 1 | 397 | 0.72 (0.44-1.19) | 0.2 | 239 | 0.67 (0.29-1.55) | 0.34 |
| Grade 2 | **1177** | **1.3 (1.04-1.64)** | **0.023*** | **798** | **1.61 (1.19-2.16)** | **0.0017**** |
| Grade 3 | **1300** | **1.27 (1.05-1.53)** | **0.012*** | **836** | **1.6 (1.23-2.07)** | **4e-04***** |
| **Part B.** Patients with following systemic treatment | | | | | | |
| **Endocrine therapy** | | | | | | |
| Yes | 1496 | 1.09 (0.86-1.38) | 0.49 | 1065 | 1.18 (0.88-1.58) | 0.26 |
| No | **1935** | **1.35 (1.15-1.58)** | **0.00021***** | **1076** | **1.72 (1.36-2.17)** | **4.4e-06***** |
| Tamoxifen only | 829 | 0.77 (0.56-1.05) | 0.096 | 649 | 0.79 (0.53-1.18) | 0.26 |
| **Chemotherapie** | | | | | | |
| Yes | **1372** | **1.64 (1.33-2.02)** | **3.9e-06***** | **968** | **2 (1.53-2.6)** | **2.1e-07***** |
| No | 1873 | 1.13 (0.95-1.35) | 0.17 | 1100 | 1.22 (0.96-1.57) | 0.11 |
| Neoadjuvant only | **730** | **2.15 (1.58-2.93)** | **6e-07***** | **647** | **2.39 (1.73-3.3)** | **5.8e-08***** |

"*, p < 0.05; **, p < 0.01; ***, p < 0.001" [301].

At last, whether *KLF11* can independently indicate the OS of BC was explored by performing Cox regression analyses. The result of univariate and multivariate Cox regression demonstrated that "*KLF11*-high" expression independently related to the impaired OS of BC patients (HR = 1.476, 95%CI = 1.024-2.127, n = 1064, p = 0.037) (**Table 3.3.2**).

**Table 3.3.2 Univariate and multivariate Cox regression analyses of *KLF11* and clinicopathological characteristics for OS in BC patients**

| **Characteristics** | | **Univariate analysis** | | **Multivariate analysis** | |
|---|---|---|---|---|---|
| | **N** | **HR (95% CI)** | **P** | **HR (95% CI)** | **P** |
| **Pathologic stage** | 1041 | | | | |

| Characteristics | | Univariate analysis | | Multivariate analysis | |
|---|---|---|---|---|---|
| | **N** | **HR (95% CI)** | **P** | **HR (95% CI)** | **P** |
| Stage I | 179 | Reference | | | |
| Stage II | 606 | 1.595 (0.923-2.758) | 0.095 | 1.657 (0.921-2.979) | 0.092 |
| Stage III | 238 | **2.966 (1.666-5.280)** | **<0.001*** ** | **3.738 (2.020-6.916)** | **<0.001*** ** |
| Stage IV | 18 | **11.568 (5.550-24.113)** | **<0.001*** ** | **8.923 (4.021-19.799)** | **<0.001*** ** |
| **Age** | 1064 | | | | |
| <=60 | 588 | Reference | | | |
| >60 | 476 | **2.036 (1.468-2.822)** | **<0.001*** ** | **2.549 (1.761-3.689)** | **<0.001*** ** |
| **Histological type** | 959 | | | | |
| Infiltrating Ductal Carcinoma | 757 | Reference | | | |
| Infiltrating Lobular Carcinoma | 202 | 0.860 (0.546-1.355) | 0.516 | | |
| **PAM50** | 1024 | | | | |
| LuA | 550 | Reference | | | |
| LuB | 202 | **1.689 (1.103-2.587)** | **0.016*** | 1.460 (0.930-2.292) | 0.100 |
| HER2 | 82 | **2.292 (1.341-3.919)** | **0.002**** | **2.849 (1.633-4.969)** | **<0.001*** ** |
| TNBC | 190 | 1.187 (0.756-1.864) | 0.457 | 1.611 (0.987-2.630) | 0.057 |
| ***KLF11*** | 1064 | | | | |
| Low | 532 | Reference | | | |
| High | 532 | **1.72 (1.14-2.60)** | **0.01*** | **1.476 (1.024-2.127)** | **0.037*** |

LuA, Luminal A; LuB, Luminal B; "*, p < 0.05; **, p < 0.01; ***, p < 0.001" [301].

Taken together, it is conceivable that KLF11 was lower expressed in breast tumor tissues. However, high *KLF11* expression might still independently indicate the impaired OS and lead to impaired DFS and DMFS in BC patients.

### 3.3.4 The Description and Distribution of KLF11 Protein Expression in our BC Cohort

To further confirm and verify the above-discovered clinical and prognostic role of KLF11 in BC, IHC staining of KLF11 in 298 specimens of BC patients was performed and evaluated by the IRS and then correlated to clinicopathological characteristics and survival outcomes. KLF11 was successfully stained in 292/298 samples due to technical issues. We demonstrated that KLF11 protein levels were positively associated with Ki-67 expression (P = 2.4e-03, **Figure 3.3.5 A, B, C**). KLF11 was also correlated with the BC molecular subtypes (P = 0.027, **Figure 3.3.5 D, E, F**) defined by surrogate biomarkers in our BC cohort. The lowest expression was obtained in luminal A-like BC (**Figure 3.3.5 F**). The further pairwise comparison demonstrated that KLF11 expression was higher in LuB-like BC than in LuA-like BC (P = 0.016, **Figure 3.3.5 F**).

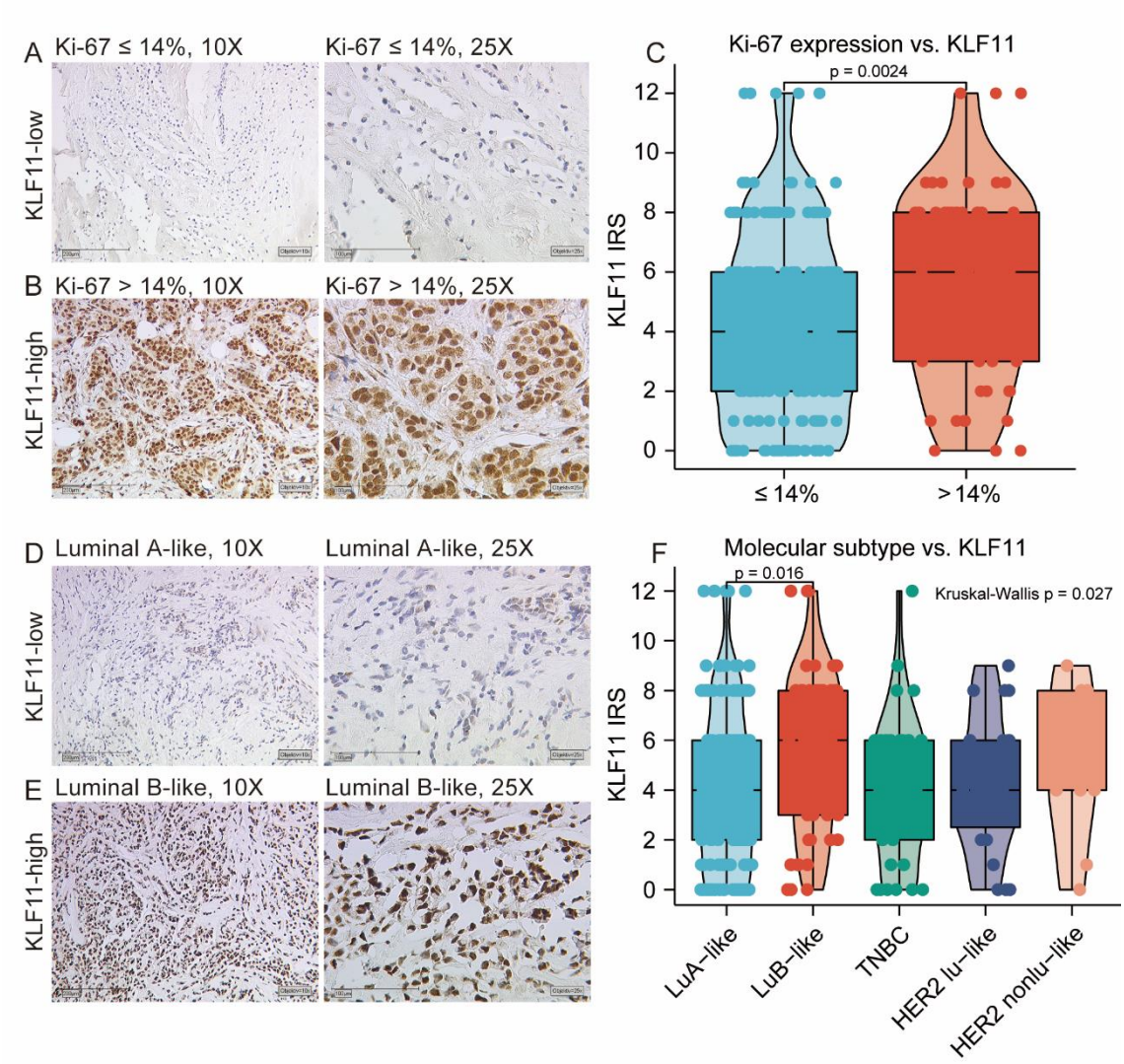


**Figure 3.3.5 Protein level of KLF11 and its association with clinicopathological characteristics in our BC cohort.**

**A-B.** Representative IHC images of KLF11 staining in BC tissues with Ki-67≤14% (**A**) and Ki-67 > 14% (**B**). Magnification: 10 X (left), 25X (right). **C.** Boxplot showed that KLF11 protein level in tumors with Ki-67 ≤ 14% is significantly lower than in tissue with Ki-67 > 14% (p = 0.0024). **D-E.** Representative IHC images of KLF11 staining in Luminal A-like BC tissues (**D**) and Luminal B-like BC tissues (**E**). Magnification: 10 X (left), 25X (right). **F.** The boxplot graph shows that the KLF11 protein level in Luminal A-like was significantly lowest among the five BC subtypes (P = 0.027). The further pairwise comparison demonstrated that KLF11 expression was higher in LuB-like BC than in LuA-like BC (P = 0.016). LuA, Luminal A; LuB, Luminal B; IRS, Immunoreactive score.

We then classified KLF11 into “KLF11-high/-low” protein levels and compared it to clinic pathological parameters. Of all 292 stained samples, 202 (69.2%) cases showed high, while 90 cases (30.8%) showed low KLF11 protein levels. We found that the distribution of “KLF11-high” protein levels in the luminal-A subtype was significantly lower in non-luminal A subtype BC patients (64.4% vs. 76.4%, p = 0.028, **Table 3.3.3**). Similarly, the distribution of “KLF11-low” protein level in Luminal A subtype was significantly higher in non-luminal A subtype BC patients (35.6% vs. 23.6%, p = 0.028, **Table 3.3.3**). Additionally, the distribution of “KLF11-high” protein level in Ki-67 ≤ 14% was significantly less than in Ki-67 > 14% BC patients (64.6% vs. 79.7%, p = 0.033, **Table 3.3.3**). Similarly, the distribution of the “KLF11-low” in cases with Ki-67 ≤ 14% was significantly more than in cases with Ki-67 > 14% BC patients (35.4% vs. 20.3%, p = 0.028, **Table 3.3.3**). No

association of KLF11 protein level with other clinic pathological parameters in BC patients was found.

Taken together, these results both of absolute KLF11-IRS and categorized “KLF11-high/-low” subgroups confirmed that high KLF11 expression was associated with aggressive features of BC, which is consistent with the results from bulk RNA-seq data analysis.

**Table 3.3.3 Distribution of KLF11 expression patterns**

| Characteristics | Total<br>Number of cases (%) | KLF11-low protein level<br>Number of cases (%) | KLF11-high protein level<br>Number of cases (%) | P value |
|---|---|---|---|---|
| **N** | **292 (98.3%)** | **90 (30.8%)** | **202 (69.2%)** | |
| **Age(y)** | | | | 0.127 |
| < 50y | 72 (24.7%) | 17 (23.6%) | 55 (76.4%) | |
| ≥ 50y | 220 (75.3%) | 73 (33.2%) | 147 (66.8%) | |
| **Tumor histology** | | | | 0.995 |
| Invasive Ductal | 118 (40.5%) | 36 (30.5%) | 82 (69.5%) | |
| Invasive lobular | 83 (28.5%) | 26 (31.3%) | 57 (68.7%) | |
| Mixed type | 37 (12.7%) | 11 (29.7%) | 26 (70.3%) | |
| other types | 53 (18.2%) | 17 (32.1%) | 36 (67.9%) | |
| **Molecular subtype** | | | | 0.254 |
| Luminal A-like | 163 (56.2%) | 58 (35.6%) | 105 (64.4%) | |
| Luminal B-like | 58 (20%) | 12 (20.7%) | 46 (79.3%) | |
| Triple negative | 37 (12.8%) | 10 (27.0%) | 27 (73.0%) | |
| Her2 amplified luminal-like | 23 (7.9%) | 6 (26.1%) | 17 (73.9%) | |
| Her2 amplified non luminal-like | 9 (3.1%) | 2 (22.2%) | 7 (77.8%) | |
| **Luminal A like subtype** | | | | **0.028*** |
| No | 127 (43.8%) | 30 (23.6%) | 97 (76.4%) | |
| Yes | 163 (56.2%) | 58 (35.6%) | 105 (64.4%) | |
| **Tumor grade** | | | | 0.328 |
| G1 | 15 (9.3%) | 6 (40.0%) | 9 (60.0%) | |
| G2 | 102 (63.4%) | 27 (26.5%) | 75 (73.5%) | |
| G3 | 44 (27.3%) | 16 (36.4%) | 28 (63.6%) | |
| **Tumor focus** | | | | 0.429 |
| Unifocal | 157 (53.8%) | 52 (33.1%) | 105 (66.9%) | |
| Multifocal&Multicentric | 135 (46.2%) | 38 (28.1%) | 97 (71.9%) | |
| **Axillary lymph node metastasis** | | | | 0.706 |
| No | 161 (56.3%) | 51 (31.7%) | 110 (68.3%) | |
| Yes | 125 (43.7%) | 37 (29.6%) | 88 (70.4%) | |
| **pT classification** | | | | 0.907 |
| pT1 | 190 (65.1%) | 59 (31.1%) | 131 (68.9%) | |
| pT2-4 | 102 (34.9%) | 26 (30.4%) | 60 (69.6%) | |
| **ER status** | | | | 0.467 |
| Negative | 56 (19.2%) | 15 (26.8%) | 41 (73.2%) | |
| Positive | 236 (80.8%) | 75 (31.8%) | 161 (68.2%) | |
| **PR status** | | | | 0.294 |
| Negative | 123 (42.1%) | 42 (34.1%) | 81 (65.9%) | |
| Positive | 169 (57.9%) | 48 (28.4%) | 121 (71.6%) | |
| **HER2 status** | | | | 0.467 |
| Negative | 259 (89%) | 81 (31.3%) | 178 (68.7%) | |
| Positive | 32 (11%) | 8 (30.6%) | 24 (69.4%) | |
| **Expression of Ki-67** | | | | **0.033*** |
| ≤14% | 164 (73.5%) | 58 (35.4%) | 106 (64.6%) | |
| > 14% | 59 (26.5%) | 12 (20.3%) | 47 (79.7%) | |

“ER, Estrogen receptor”, “PR, Progesterone receptor”, “HER2, Human epidermal growth factor receptor 2”[47] (Obtained from this related published paper, as the First Author). “*, $p < 0.05$; **, $p < 0.01$; ***, $p < 0.001$” [301].

### 3.3.5 Prognostic Relevance of KLF11 in BC identified by our cohort

Of the overall patient cohort, patients with a high KLF11 level led to an impaired DFS (HR = 2.41, 95%CI = 1.54-3.77, p = 0.001, **Figure 3.3.6 B**), an impaired DMFS (HR = 2.11, 95%CI = 1.23-3.63, p = 0.018, **Figure 3.3.6 C**) and an impaired LRFS (HR = 2.62, 95%CI = 1.42-4.81, p = 0.01, **Figure 3.3.6 D**). However, no association of KLF11 with OS of BC patients was found (HR = 1.13, 95%CI = 0.72-1.78, p = 0.601, **Figure 3.3.6 A**).

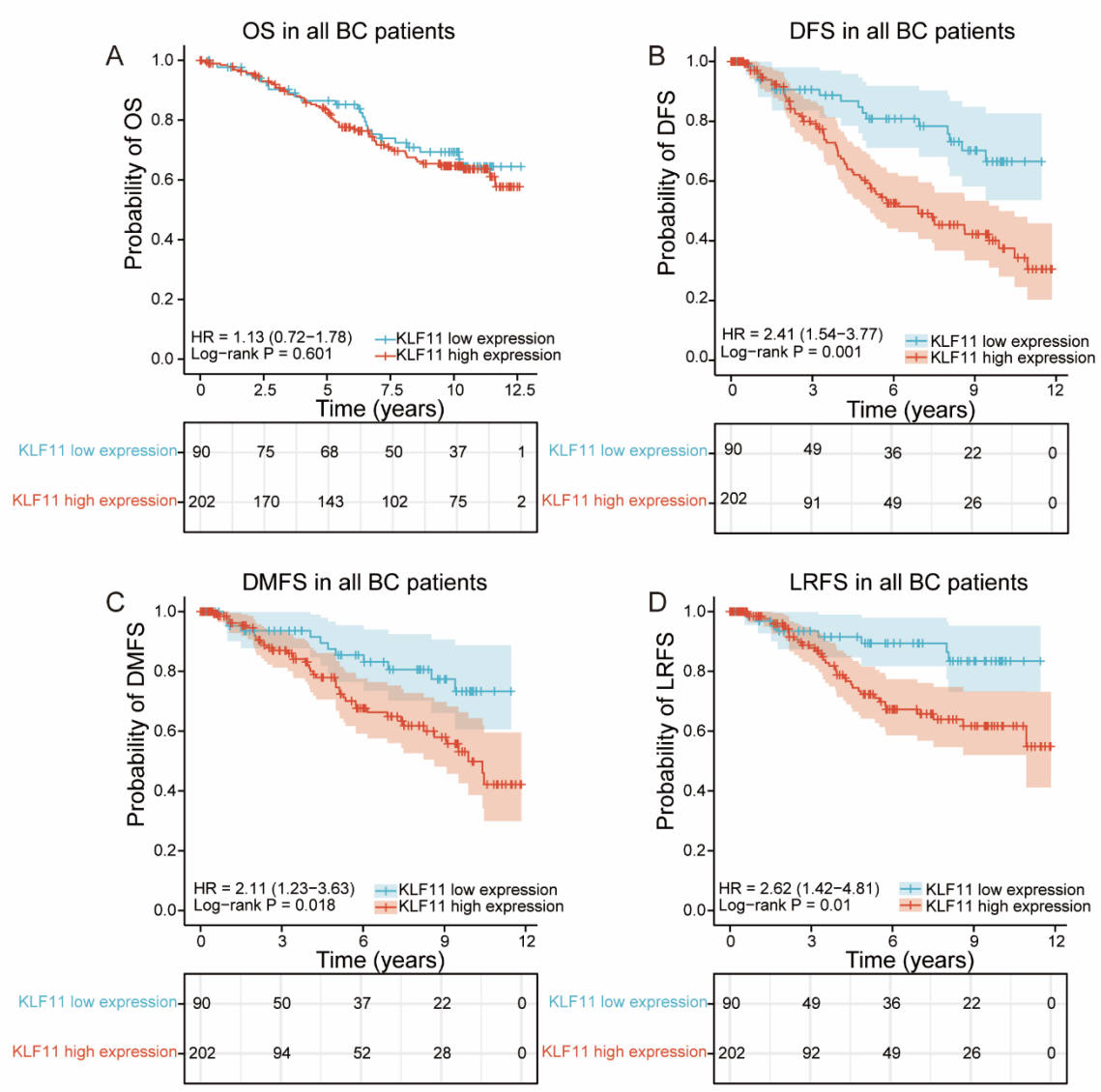


**Figure 3.3.6 Prognostic relevance of KLF11 protein level in our BC cohort.**
**A.** No association of KLF11 with OS of BC patients was found (HR = 1.13, 95%CI = 0.72-1.78, p = 0.601, A). **B-C.** Patients with a high KLF11 level led to an impaired DFS (HR = 2.41, 95%CI = 1.54-3.77, p=0.001, **B**), an impaired DMFS (HR = 2.11, 95%CI = 1.23-3.63, p = 0.018, **C**) and an impaired LRFS (HR = 2.62, 95%CI = 1.42-4.81, p = 0.01, **D**).

The subgroup analysis of DFS in our BC cohort showed that higher KLF11 lead to an inferior DFS both of age < 50 YO patients (HR = 5.021, 95%CI = 1.174-21.477, n = 72, p = 0.03, **Figure 3.3.7**) and of age ≥ 50 YO patients (HR = 2.016, 95%CI = 1.103-3.686, n = 220, p = 0.023, **Figure 3.3.7**). KLF11 was also negatively associated with DFS both of patients with unifocal tumor (HR = 2.487, 95%CI = 1.090-5.672, n = 157, p = 0.03, **Figure 3.3.7**) and with multifocal/multicentric tumor (HR = 2.505, 95%CI = 1.201-5.221, n = 135, p = 0.014, **Figure 3.3.7**). In addition, a higher KLF11

level lead to an inferior DFS of the patients with histological type of invasive ductal/invasive lobular/mixed type (HR = 2.173, 95%CI = 1.247-3.787, n = 238, p = 0.006, **Figure 3.3.7**), of Luminal A-like BC (HR = 2.831, 95%CI = 1.341-5.978, n = 163, p = 0.006, **Figure 3.3.7**), of patients with G1 or G2 feature ( HR = 3.108, 95%CI = 1.075-8.976, n = 117, p = 0.036, **Figure 3.3.7**), of patients without lymphatic metastasis (HR = 4.255, 95%CI = 1.650-10.976, n = 161, p = 0.003, **Figure 3.3.7**), of patients with tumor size smaller than 2cm (HR = 3.268, 95%CI = 1.517-7.028, n = 190 p = 0.002, **Figure 3.3.7**), of patients with ER positive (HR = 2.740, 95%CI = 1.488-5.045, n = 236 p = 0.001, **Figure 3.3.7**), of patients with PR positive ( HR = 2.591, 95%CI = 1.259-5.334, n = 169 p = 0.01, **Figure 3.3.7**) and of patients with HER2 unamplified (HR = 2.414, 95%CI = 1.343-4.339, n = 259, p = 0.003, **Figure 3.3.7**) and in BC subgroup with low proliferation rate (Ki-67 ≤ 14%) (HR = 2.831, 95%CI = 1.341-5.978, n = 164, p = 0.006, **Figure 3.3.7**).

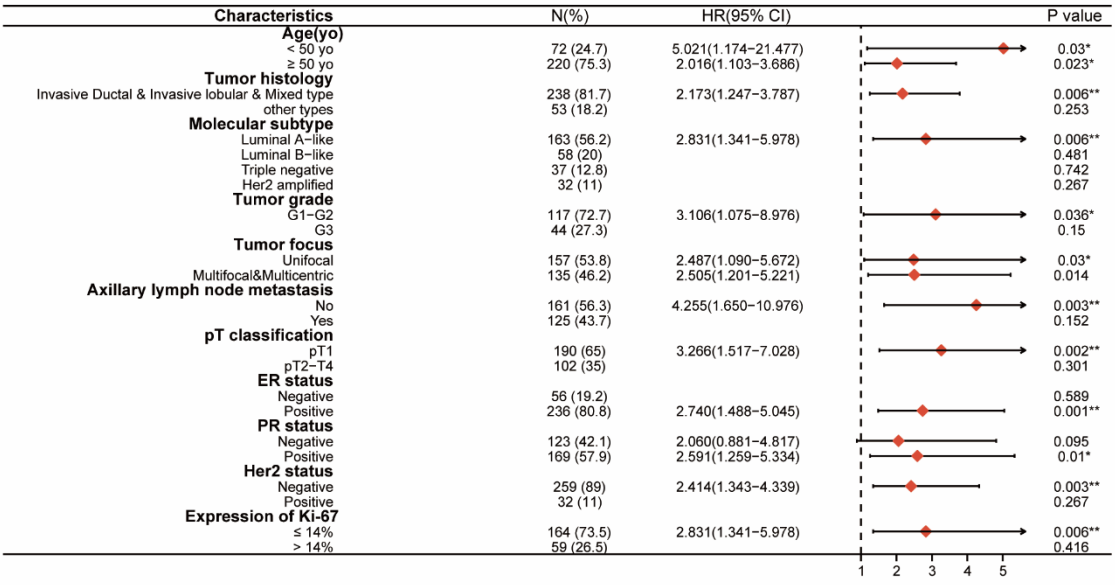


**Figure 3.3.7 Forest plot showed the subgroup analysis of DFS across clinic pathological parameters in our BC cohort.**

Then the DMFS analysis across various patient subgroups in our BC cohort showed that high KLF11 protein level significantly correlated to worse DMFS of the BC patients with histological type with invasive ductal/Invasive lobular/mixed type (HR = 1.926, 95%CI = 1.008-3.683, n = 238, p = 0.047, **Figure 3.3.8**), of patients without lymphatic metastasis ( HR = 6.256, 95%CI = 1.451-26.962, n = 161, p = 0.014, **Figure 3.3.8**), of patients with tumor size ≤ 2cm ( HR = 2.690, 95%CI = 1.004-7.205, n = 190, p = 0.049, **Figure 3.3.8**), of patients with ER positive (HR = 2.308, 95%CI = 1.097-4.853, n = 236, p = 0.028, **Figure 3.3.8**), of patients with PR positive (HR = 2.751, 95%CI = 1.047-7.228, n = 169, p = 0.04, **Figure 3.3.8**) and of patients with HER2 unamplified (HR = 2.169, 95%CI = 1.076-4.374, n = 259, p = 0.03, **Figure 3.3.8**).

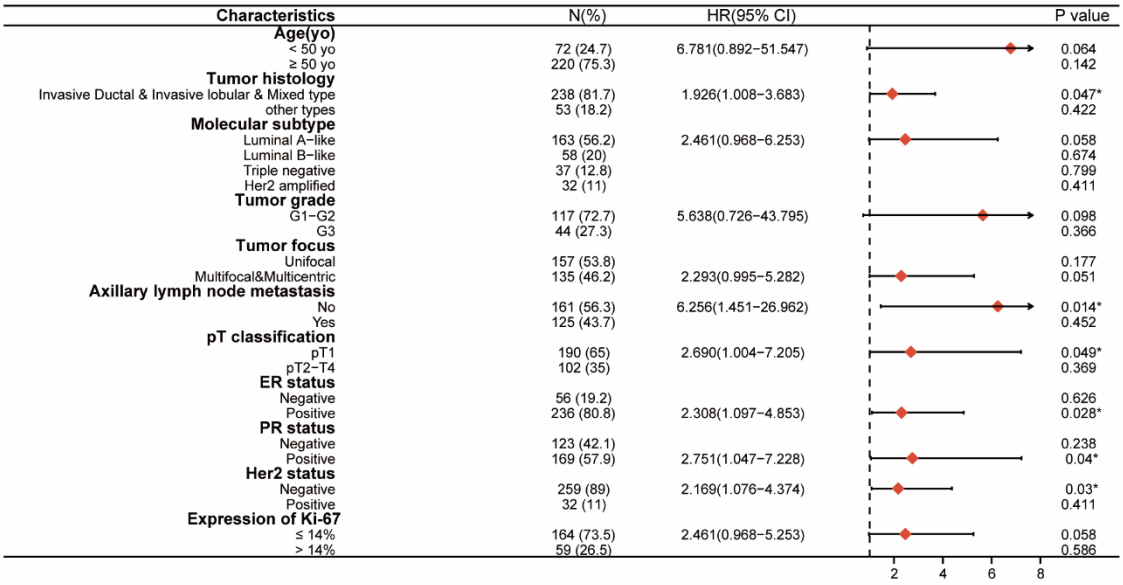


**Figure 3.3.8 Forest plot showed the subgroup analysis of DMFS across clinic pathological parameters in our BC cohort.**

Additionally, the subgroup analyses of LRFS showed that a high KLF11 level correlated with an impaired LRFS of patients aged older than 50y (HR = 2.382, 95%CI = 1.032-5.493, n = 220, p = 0.042, **Figure 3.3.9**), of patients with histological type of invasive ductal/Invasive lobular/mixed type (HR = 2.297, 95%CI = 1.054-5.005, n = 238, p = 0.036, **Figure 3.3.9**), of Luminal A-like BC (HR = 3.261, 95%CI = 1.220-8.722, n = 163, p = 0.019, **Figure 3.3.9**), of patients with unifocal tumor (HR = 3.001, 95%CI = 1.028-8.761, n = 157, p = 0.044, **Figure 3.3.9**), of patients without lymphatic metastasis (HR = 3.946, 95%CI = 1.157-13.463, n = 161, p = 0.028, **Figure 3.3.9**), of patients with tumor size smaller than 2cm (HR = 4.329, 95%CI = 1.504-12.461, n = 190, p = 0.007, **Figure 3.3.9**), of patients with ER positive (HR = 3.651, 95%CI = 1.522-8.756, n = 236, p = 0.004, **Figure 3.3.9**), of patients with PR positive (HR = 2.662, 95%CI = 1.017-6.968, n = 169, p = 0.046, **Figure 3.3.9**) and of patients with HER2 unamplified ( HR = 2.627, 95%CI = 1.156-5.970, n = 259, p = 0.021, **Figure 3.3.9**) and also of BC subgroup with low proliferation rate (Ki-67 ≤ 14%) (HR = 3.261, 95%CI = 1.220-8.722, n = 164, p = 0.019, **Figure 3.3.9**).

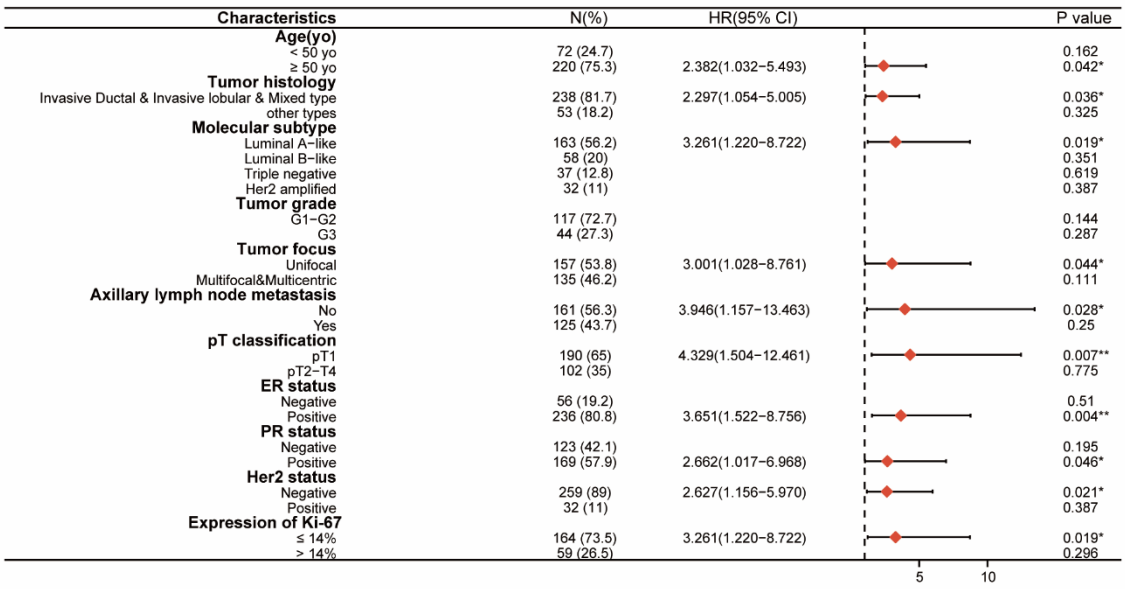


**Figure 3.3.9 Forest plot showed the subgroup analysis of LRFS across clinic pathological parameters in our BC cohort.**

Concerning OS, no correlation with KLF11 was found in the subgroup survival analysis, which is consistent with the result of the overall BC patients.

### 3.3.6 KLF11 was an independent Indicator for DFS and DMFS of BC identified by our cohort

Univariate regression showed that KLF11 (HR = 2.433, 95%CI = 1.407-4.208 p = 0.001), grading (HR = 1.940, 95%CI = 1.106-3.403, p = 0.021), tumor size (HR = 1.991, 95%CI = 1.301-3.047, p = 0.002) and lymph node status (HR = 1.832, 95%CI = 1.187-2.829, p = 0.006) were significantly associated with DFS in our BC cohort (**Table 3.3.4**). Multivariate regression was further performed with the univariate significant factors: grading, tumor size, lymph node status and KLF11. The multivariate Cox regression revealed that KLF11 (HR = 2.610, 95%CI = 1.241-5.488, p = 0.011), grading (HR = 2.260, 95%CI = 1.262 - 4.047, p = 0.006) and tumor size (HR = 2.624, 95%CI = 1.384 -4.975, p = 0.003) independently related to DFS of BC patients (**Table 3.3.4**).

**Table 3.3.4 Univariate and multivariate Cox regression analyses of KLF11 and clinicopathological characteristics for DFS in BC patients**

| Characteristics | Univariate analysis | | | Multivariate analysis | | |
|---|---|---|---|---|---|---|
| | p | HR | 95% CI | p | HR | 95% CI |
| **Age**( < 50 YO vs. ≥50 YO) | 0.223 | 1.337 | 0.893-2.130 | n.i. | n.i. | n.i. |
| **Molecular subtype** (non-LuA like vs.LuA-like) | 0.137 | 1.379 | 0.903-2.106 | n.i. | n.i. | n.i. |
| **Tumor histology** (Invasive Ductal & Invasive lobular & Mixed type vs. other types) | 0.075 | 1.938 | 0.935-4.015 | n.i. | n.i. | n.i. |
| **Grading** (G3 vs. G1-G2) | **0.021*** | **1.940** | **1.106-3.403** | **0.006**** | **2.260** | **1.262-4.047** |
| **Tumor focis** (multifocal & muticentric vs.unifocal ) | 0.238 | 1.292 | 0.844-1.976 | n.i. | n.i. | n.i. |
| **Tumer size** (pT2-pT4 vs. pT1) | **0.002**** | **1.991** | **1.301-3.047** | **0.003**** | **2.624** | **1.384-4.975** |
| **Axillary lymph node status** (yes vs. no) | **0.006**** | **1.832** | **1.187-2.829** | 0.901 | 1.042 | 0.547-1.985 |
| **ER status** (ER+ vs. ER-) | 0.608 | 0.875 | 0.525-1.457 | n.i. | n.i. | n.i. |
| **PR status** (PR+ vs. PR-) | 0.404 | 1.202 | 0.780-1.852 | n.i. | n.i. | n.i. |
| **HER2 status (**HER2+ vs. HER2-) | 0.544 | 1.208 | 0.565-2.226 | n.i. | n.i. | n.i. |
| **Expression of Ki-67**(Ki-67 > 14% vs. Ki-67 ≤14%) | 0.091 | 1.576 | 0.931-2.671 | n.i. | n.i. | n.i. |
| **KLF11** (High vs. Low) | **0.001**** | **2.433** | **1.407-4.208** | **0.011*** | **2.610** | **1.241-5.488** |

KLF11, Krüppel like Factor 11; non-LuA like, not luminal A-like; "DFS, Disease-free survival", "ER estrogen receptor, PR progesterone receptor, HER2 human epidermal growth factor receptor 2", "LuA-like luminal A-like", "HR hazard ratio, CI confidence interval, n.i not included in multivariate model, as p > 0.05 in univariate analysis" [47] (Obtained from this related published paper, **as the First Author**). "*, p < 0.05; **, p < 0.01; ***, p < 0.001" [301].

Furthermore, univariate regression revealed that KLF11 (HR = 2 .132, 95%CI = 1.125-4.043, p = 0.02), molecular subtype (HR = 1.772, 95%CI = 1.054-2.981, p = 0.031), grading (HR = 2.689, 95%CI = 1.281-5.644, p = 0.009), tumor size (HR = 3.044, 95%CI = 1.818-5.099, p = 0.000023) and lymph node status (HR = 2.328, 95%CI = 1.355-3.998, p = 0.002) were significantly associated with DMFS in BC (**Table 3.3.5**). Multivariate analysis was then performed with the univariate significant factors: molecular subtype, grading, tumor size, lymph node status and KLF11. The result of multivariate regression showed that KLF11 (HR = 2.744, 95%CI = 1.017-7.403, p = 0.046) and grading (HR = 3.276, 95%CI = 1.424 – 7.536, p = 0.005), tumor size (HR = 5.729,

95%CI = 2.266 -14.484, p = 0.000225) independently related to DMFS of BC patients (**Table 3.3.5**).

**Table 3.3.5 Univariate and multivariate Cox regression analyses of KLF11 and clinicopathological characteristics for DMFS in BC patients**

| Characteristics | Univariate analysis | | | Multivariate analysis | | |
|---|---|---|---|---|---|---|
| | p | HR | 95% CI | p | HR | 95% CI |
| **Age**( < 50y vs. ≥50y) | 0.514 | 1.211 | 0.682-2.150 | n.i. | n.i. | n.i. |
| **Molecular subtype** (non-LuA like vs.LuA-like) | **0.031*** | **1.772** | **1.054-2.981** | 0.367 | 1.488 | 0.628-3.529 |
| **Tumor histology** (Invasive Ductal & Invasive lobular & Mixed type vs. other types) | 0.100 | 2.158 | 0.862-5.400 | n.i. | n.i. | n.i. |
| **Grading** (G3 vs. G1-G2) | **0.009**** | **2.689** | **1.281-5.644** | **0.005**** | **3.276** | **1.424-7.536** |
| **Tumor focis** (multifocal & muticentric vs.unifocal ) | 0.074 | 1.607 | 0.955-2.704 | n.i. | n.i. | n.i. |
| **Tumer size** (pT2-pT4 vs. pT1) | **0.000023***** | **3.044** | **1.818-5.099** | **0.000225***** | **5.729** | **2.266-14.484** |
| **Axillary lymph node status** (yes vs. no) | **0.002**** | **2.328** | **1.355-3.998** | 0.942 | 1 .035 | 0.415-2.579 |
| **ER status** (ER+ vs. ER-) | 0.101 | 0.624 | 0.355-1.096 | n.i. | n.i. | n.i. |
| **PR status** (PR+ vs. PR-) | 0.479 | 0.831 | 0.497-1.388 | n.i. | n.i. | n.i. |
| **HER2 status** (HER2+ vs. HER2-) | 0.182 | 1.565 | 0.811-3.108 | n.i. | n.i. | n.i. |
| **Expression of Ki-67**(Ki-67 > 14% vs. Ki-67 ≤14%) | 0.083 | 1.796 | 0.927-3.480 | n.i. | n.i. | n.i. |
| **KLF11** (High vs. Low) | **0.02*** | **2.132** | **1.125-4.043** | **0.046*** | **2.744** | **1.017-7.403** |

KLF11, Krüppel like Factor 11; DMFS, Distant metastasis-free survival; non-LuA-like, not luminal A-like; "ER estrogen receptor, PR progesterone receptor, HER2 human epidermal growth factor receptor 2", "LuA-like luminal A-like", "HR hazard ratio, CI confidence interval, n.i not included in multivariate model, as p > 0.05 in univariate analysis" [47] (Obtained from this related published paper, **as the First Author**). "*, p < 0.05; **, p < 0.01; ***, p < 0.001" [301].

Concerning OS and LRFS, no independent prognostic value of KLF11 was found in the multivariate cox regression.

### 3.3.7 Nomograms Construction and Calibration for the Established KLF11 Related DFS and DMFS Cox Model identified by our BC Cohort

Based on the independent predictors found in the Cox regression analyses, we developed two nomograms for predicting BC patients' DFS (Figure 3.3.10 A) and DMFS (Figure 3.3.10 C). Nomograms estimate the survival probability for a patient after3, 5, and 10 years based on a total score calculated by the addition of zero to 100 points for every individual prognostic factor. Then the 3-, 5- and 10-year survival probabilities can be estimated by adding up all points. In the nomogram for predicting DFS (**Figure 3.3.10 A**), the KLF11 protein level showed a high impact due to the high level of KLF11 almost added up to 100 points to the final score. However, regarding DMFS, KLF11 protein level only showed a minor impact on outcome prediction (**Figure 3.3.10 C**).

The developed nomograms were internally validated using bootstrapping. The internal validation of the underlying regression models showed optimism adjusted C-index values of 0.694 for DFS and 0.8 for DMFS, respectively calculated by using the R programmer. The calibration of the

model was assessed with calibration curves, which analyze the fit between the model established by the Cox regression method and the actual situation. The calibration curve of the nomogram-predicted probability of DFS (**Figure 3.3.10 B**) indicated that the model's predicted survival probabilities for 3-, 5- 10- years were close to observed probabilities. Calibration for the 10-year probability of DFS prediction for the nomogram showed perfect model calibration with a high correlation of nomogram predicted probability of DFS and observed probability of DFS estimated by the KM method. The calibration plots for the probabilities of 3-, 5- and 10-year DMFS (**Figure 3.3.10 D**) also showed that the predicted-DMFS by nomogram fit well with the actual DMFS of BC patients. However, this prediction accuracy was not as good as the nomogram of the DFS prediction.

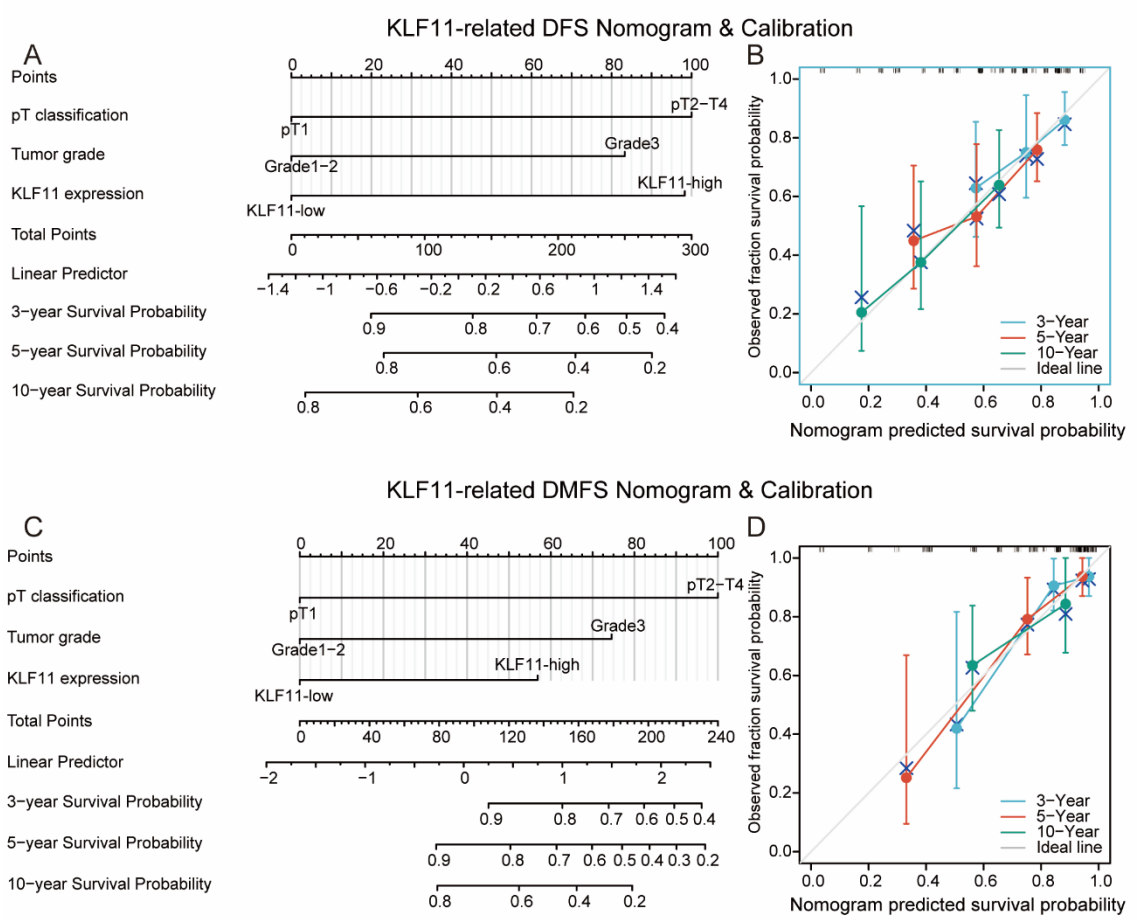


**Figure 3.3.10 Nomograms Construction and Calibration for the established KLF11-related DFS and DMFS Cox model.**

**A, C.** Nomograms of DFS (**A**) and DMFS (**C**) prediction of BC patients were displayed. For every parameter, a score on the upper points scale was given. For each patient, the sum of all separate parameter points can be used for the estimation of survival probabilities. **B, D.** Calibration analysis of the nomograms for 3-year, 5-year, and 10-year DFS (**B**) and DMFS (**D**). "Nomogram-predicted survival is plotted on the x-axis, and actual survival is plotted on the y-axis. Vertical bars represent 95% CI measured by KM analysis. Dashed lines along the 45° line through the origin point represent a perfect calibration model." [304].

Taken all together, the results part from the analysis of our BC cohort confirmed that a high KLF11 level leads to a poor prognosis of BC, which was consistent with the bulk RNA-seq data analysis of *KLF11*. "KLF11-high" protein level remained independently related to impaired DFS and DMFS identified by our BC cohort. However, "*KLF11*-high" mRNA expression independently related to impaired OS, which was identified by the bulk RNA-seq analysis of the TCGA-BC cohort. In addition, the poor prognosis predictive value of KLF11 appeared to be more markedly in the patients

with a “low risk” tumor context. These observations suggest that the prognostic role of KLF11 in BC might differ depending on intertumoral heterogeneity.

## 3.4 Mechanistic Prediction of Transcriptional Factor KLF11 in BC

### 3.4.1 The Protein regulatory Network of KLF11 in Human being

To explore underlying mechanisms that might contribute to the poor clinical outcome of BC regulated by KLF11, we firstly investigated the proteins that interact with KLF11 in human beings to have a general understanding of the regulation network of KLF11. The interaction network of proteins was created using STRING showed that 30 potential target proteins interacted with KLF11 (**Figure 3.4.1**).

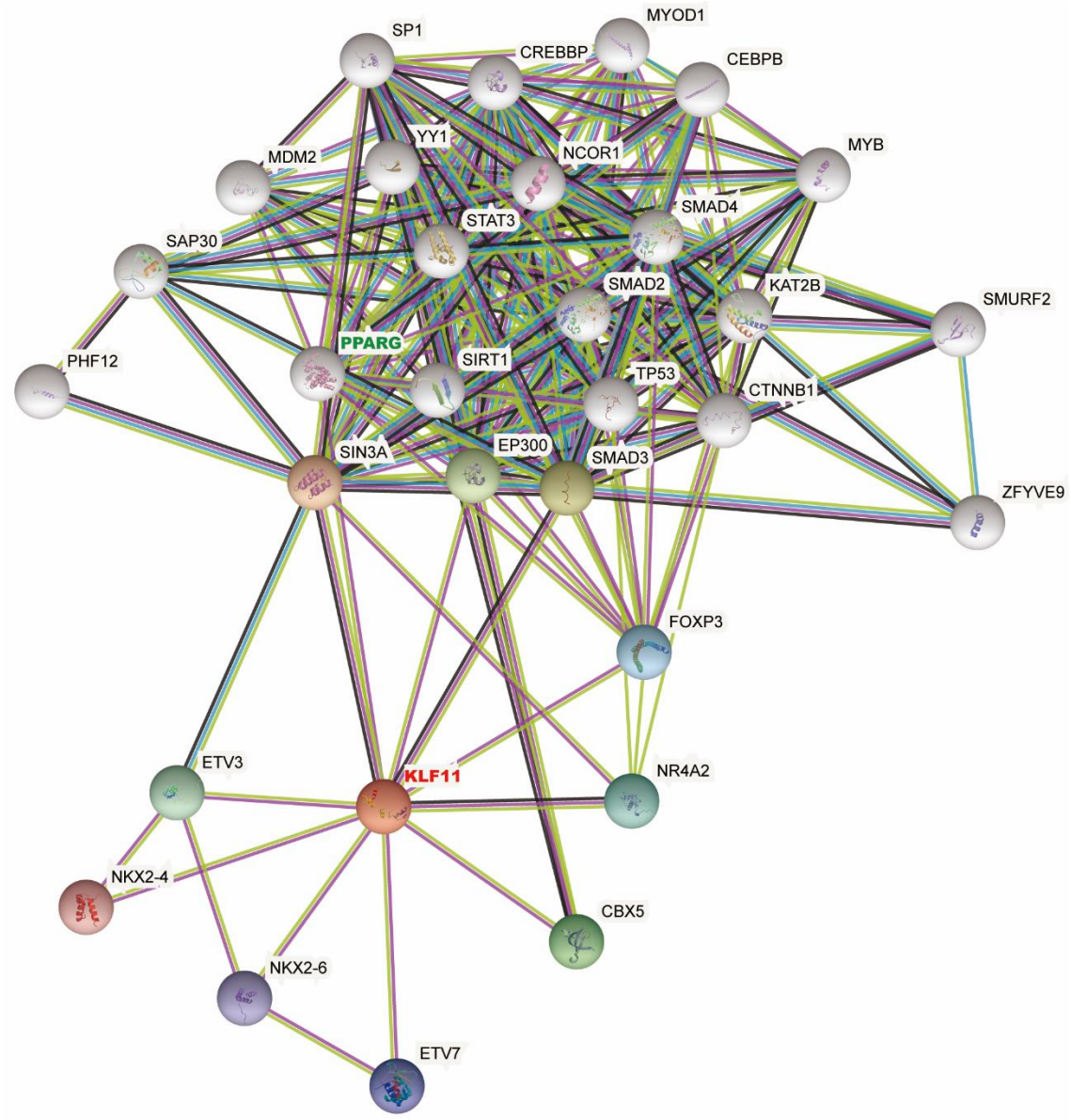


**Figure 3.4.1 The network diagram of KLF11 interacted proteins explored by STRING.**

### 3.4.2 Functional Enrichment of the Genes that encode KLF11 and its interacted Proteins

To have an overview of KLF11-related signaling pathways and cellular functions, the GO and KEGG functional enrichment analyses input the genes that encode the proteins interacting with KLF11 were performed using the R programmer. The BP, CC, and MF that KLF11 might involve were identified by GO analysis. The results of GO enrichment suggested that KLF11 might contribute to BPs such as epithelial cell migration and proliferation, and cell growth **Figure 3.4.2 A**). Moreover, KLF11 might be involved in cell differentiation, such as myeloid cell differentiation, macrophage-derived foam cell differentiation, and fat cell differentiation **Figure 3.4.2 A**). Furthermore, it might regulate the cellular response to retinoic acid, prostaglandin, estrogen, and the hormone-mediated signaling pathway (**Figure 3.4.2 A**). Interestingly, KLF11 might also be involved in regulating inflammatory and innate immune responses (**Figure 3.4.2 A**).

In addition, KLF11 consisted of the CCs such as transcription factor complex and nuclear chromatin (**Figure 3.4.2 B**). KLF11 was also involved in MFs such as prostaglandin receptor activity and DNA-binding transcription activity, nuclear hormone receptor binding, androgen receptor binding, ER binding, retinoic acid receptor (RAR) binding, and retinoic X receptor (RXR) binding, as well as p53 binding (**Figure 3.4.2 B**).

The signaling pathways enrichment analysis of KLF11 was explored by KEGG. It was revealed that KLF11 was involved in the cell cycle process, and in the signaling pathways that relate to thyroid hormone, TGFβ, FoxO, Wnt, Notch, and p53 (**Figure 3.4.2 C**). In addition, KLF11 was closely related to endocrine resistance and platinum drug resistance pathways (**Figure 3.4.2 C**). Furthermore, KLF11 was also involved in the transcriptional miss regulation in many cancers, including BC (**Figure 3.4.2 D**).

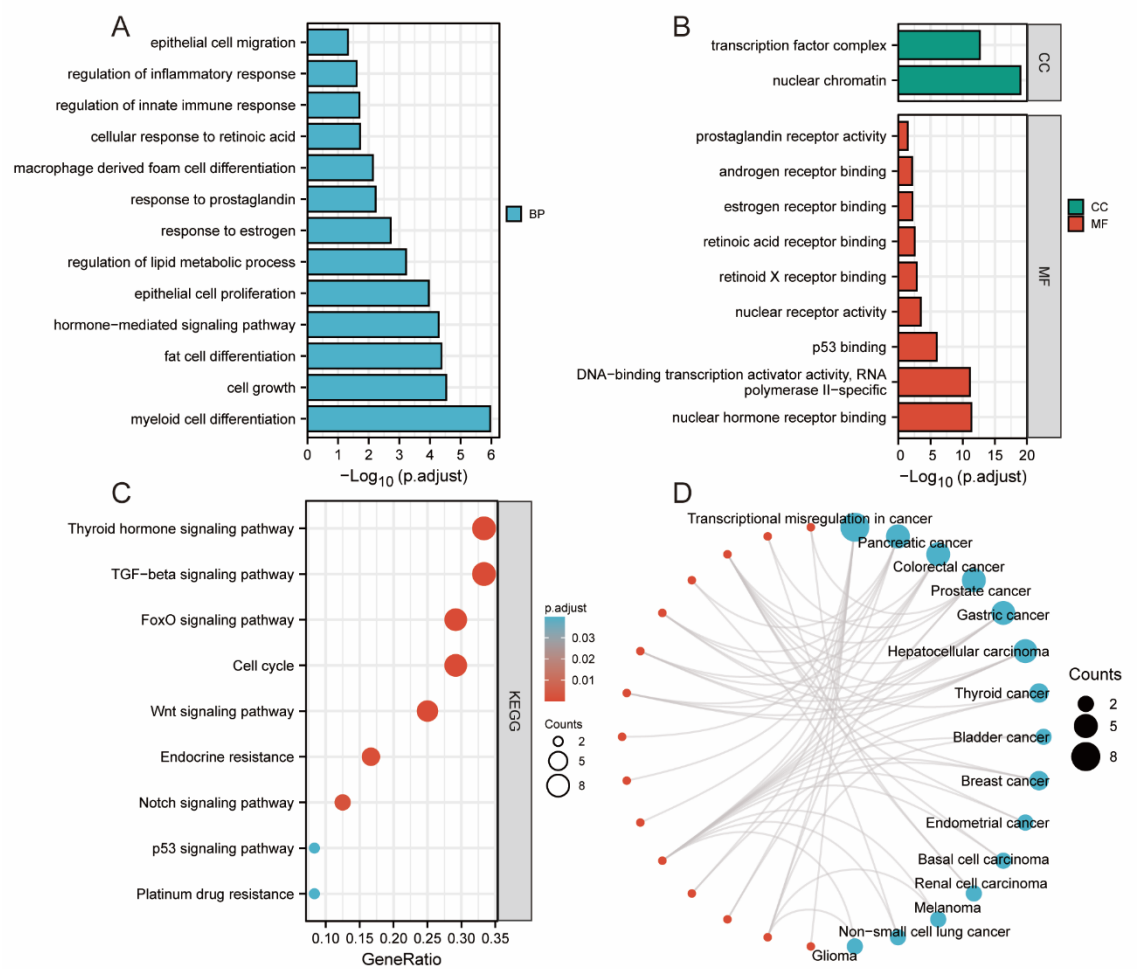


**Figure 3.4.2 Functional enrichment analysis of genes encode KLF11 and its interacted proteins.** **A-B.** Significant enriched GO-BP terms (**A**), GO-CC terms (**B**), and GO MF terms (**B**) of KLF11. **C.** Significant enriched KEGG pathways of KLF11. **D.** Significant enriched terms related to human cancers of KLF11.

These results indicate that, as a TF-KLF family member, KLF11 mostly might interact with NRs or be involved in cancer-related star signaling pathways. Then, it might regulate BC progression from two aspects. On the one hand, via regulating cells growth of tumor cells and, on the other hand, regulating components in the BC-TME such as macrophages differentiation or other related immune response.

## 3.5 The Relationship between Transcriptional Factor KLF11 and TAMs in BC

Regarding the regulation of KLF11 in TAM of BC, we firstly investigated the correlation between *KLF11* and TAMs infiltration in the TCGA-BC cohort. Secondly, we performed double IF staining of KLF11 and CD68 on BC tissue samples to confirm that KLF11 does express in TAMs. Thirdly, we correlated the protein levels of NRs and KLF11 and the infiltration number of BATMs and BTSMs in our BC cohort to explore whether there are some NRs associated with KLF11 as predicted by GO and KEGG enrichment analysis involved in transcriptional regulation of TAMs.

At last, we took advantage of scRNA-seq-explored specific Br-TAMs signatures. We performed correlation analyses between these TAM signatures and KLF11/NRs-related transactional enhancer, which developed at the third step based on our cohort to see whether KLF11 might regulate the gene program transcription of the specific phenotype of Br-TAMs.

### 3.5.1 *KLF11* Expression positively correlated to TAMs Infiltration in TCGA–BC Cohort

The correlation between *KLF11* and TAM infiltration in BC was analyzed using TIMER. We used the coefficient adjusted by tumor purity termed "partial. r" to assess the correlation between *KLF11* and TAM infiltration. The broadly categorized molecular subtype based on their clinical implication were included in this analysis: luminal type (ER+, PR+/−, HER2-), HER2 type (HER2+, ER+/−, PR+/−), and TNBC (ER−, PR−, HER2−).

A negative correlation between *KLF11* and "tumor purity" was observed (Cor = −0.188, p = 2.47e−09, **Figure 3.5.1 A**) in the overall BC cohort and specifically in luminal BC (Cor = −0.25, p = 3.40e−09, **Figure 3.5.1 D**) indicating that *KLF11* is expressed higher in the BC-TME, especially in the liminal type BC-TME than in the tumor cells of BC [305]. Moreover, *KLF11* positively related to TAM infiltration of TCGA-BC cohort (partial.r = 0.21, p = 2.87e−11, **Figure 3.5.1 A**). More nuancedly in subtypes, *KLF11* related positively to the infiltrating of TAM in TNBC (partial.r = 0.209, p = 1.82e−02, **Figure 3.5.1 B**) and in luminal BC (partial.r = 0.268, p = 2.36e−10, **Figure 3.5.1 D**). While of HER2 BC, we found the correlation of only borderline significance (partial.r = 0.256, p = 5.23e−02, **Figure 3.5.1 C**). These results indicate that KLF11 seems to have a more intimate relationship with TAM infiltration in the TME of luminal type BC.

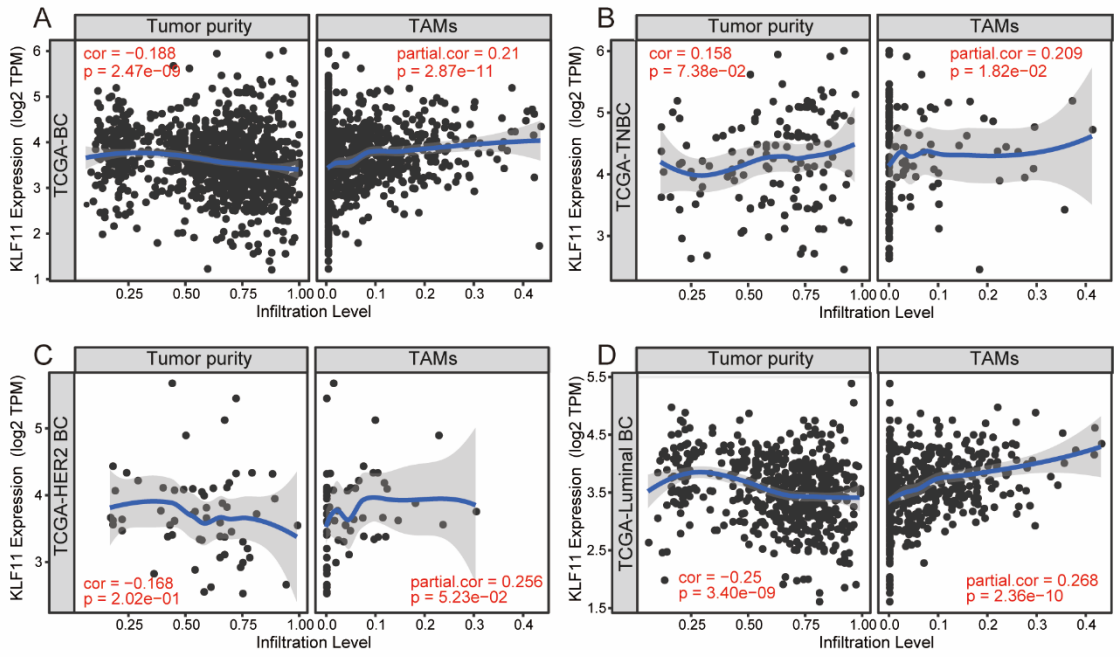


**Figure 3.5.1 Association of *KLF11* expression with TAMs infiltration in TCGA-BC**

**A.** *KLF11* was negatively correlated with tumor purity (cor = −0.188, p = 2.47e−09) and positively related to TAM infiltrating of the overall BC cohort (partial.cor = 0.21, p = 2.87e−11, n = 1212). **B.** *KLF11* did not relate to tumor purity but positively related to TAM infiltrating of TNBC (partial.cor = 0.209, p = 1.82e−02, n = 208). **C.** *KLF11* did not relate to tumor purity but related to TAMs infiltration of with a borderline significance of HER2 BC (partial.cor = 0.256, p = 5.23e−02, n = 91). **D.** *KLF11* was negatively correlated with tumor purity (r = −0.25, p = 3.40e−09) and positively related to TAM infiltrating of luminal BC (partial.cor = 0.268, p = 2.36e−10, n = 871). TAM, tumor-associated macrophage; TPM, Transcripts per million reads; cor, correlation coefficient of Spearmann analysis; partial.cor, correlation coefficient of Spearmann analysis adjusted by "tumor purity".

### 3.5.2 KLF11 did localize in the TAM Nucleus

To explore the mechanism underlying the positive association of KLF11 expression and TAMs infiltration in BC tissue, we first performed double IF staining of CD68 and KLF11 to confirm that KLF11 was expressed in the TAM. We observed that all TAMs showed positive staining of KLF11 on the IF-staining FFEP slides of BC tissues (**Figure 3.5.2**). KLF11 did express in the nuclei of BTSM (**Figure 3.5.2 A-C**) and BTAM (**Figure 3.5.2 D-F**), indicating that KLF11 regulated TAM infiltration might be through transcriptional regulation of specific gene programs of specific TAM phenotype.

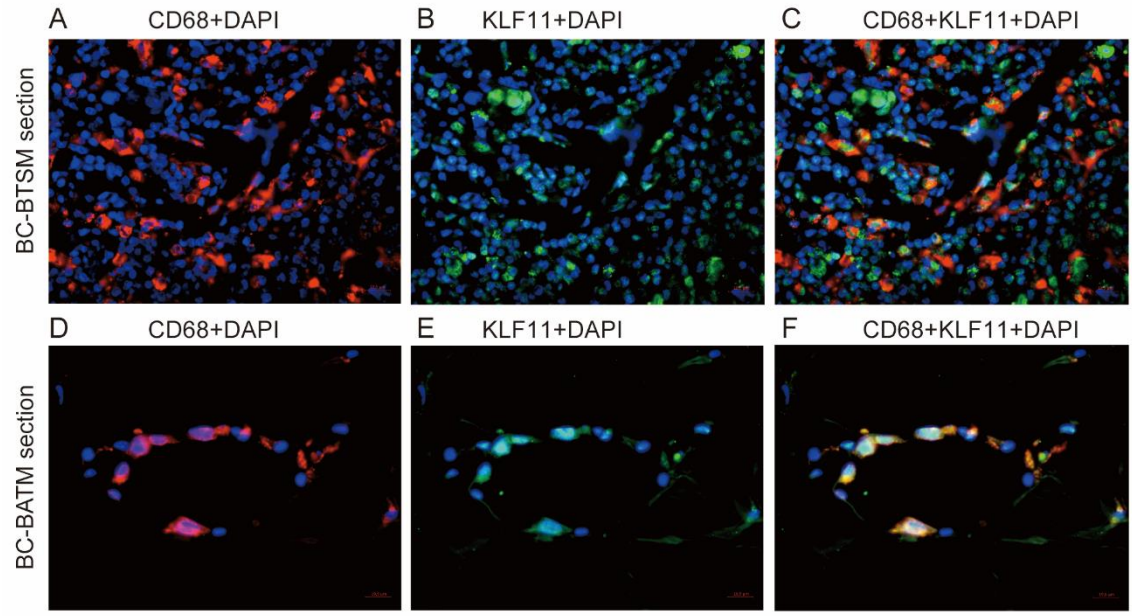


**Figure 3.5.2 Co-localization of CD68 and KLF11 was shown in the BC tissue samples.**
**A-C**. Representative IF images showed that KLF11 was localized in the nuclei of BTSMs. **D-E.** Representative IF images showed that KLF11 was localized in the nuclei of BATMs. DAPI stained for nucleus as blue; Cy2 stained KLF11 expression as green; Cy3 stained CD68/TAMs as red. CD68+DAPI to show TAMs (**A, D**), KLF11+DAPI to show KLF11 positive expression (**B, E**), CD68+KLF11+DAPI to show KLF11 localized in the Br-TAMs (**C, F**). Magnification x40, scale bar = 19, 5 μm (100 pixel).

### 3.5.3 The Association of KLF11 and NRs with BATM and BTSM in our BC Cohort

Our laboratory has long history been committed to studying the regulatory effects of the regulation factors in the nucleus. To find out whether there are some previously explored NRs involved in the transcriptional regulation role of KLF11 playing in TAM, we correlated KLF11, BATMs, and BTSMs with different nuclear elements previously analyzed in our lab, such as PPARγ [306, 307], retinoic X receptor alpha (RXRα) [306], vitamin D receptor (VDR) [306, 308], thyroid hormone receptor-alpha (THRα), and -beta (THRβ) [309], lysine (K)-specific demethylase 1 (LSD1) and “acetylation of lysine 27 on histone H3 protein subunit (H3K27ac)” [310], as well as EP3 aforementioned [282], which has been demonstrated to be also localized at the cell nucleus modulating gene expression through a series of biochemical events [311].

For BATM and BTSM, PPARγ and THRα were positively correlated to both BTSM infiltration (vs. PPARγ: Spearman's ρ = 0.29, p = 1.74e-05; and vs. THRα: Spearman's ρ = 0.22, p = 0.001, **Figure 3.5.3**) and BATM infiltration (vs. PPARγ: Spearman's ρ = 0.18, p = 0.01 and vs. THRα: Spearman's ρ = 0.18, p = 0.01, **Figure 3.5.3**). Additionally, the highly strong association between

PPARγ and THRα was also demonstrated (Spearman's ρ = 0.86, p = 0, **Figure 3.5.3**). VDR (Spearman's ρ = - 0.17, p = 0.001, **Figure 3.5.3**), THRβ (Spearman's ρ = 0.18, p = 0.008, **Figure 3.5.3**), LSD1 (Spearman's ρ = 0.22, p = 0.0006, **Figure 3.5.3**) and H3K27ac (Spearman's ρ = 0.14, p = 0.03, **Figure 3.5.3**) were only correlated to BTSM infiltration and EP3 (r = -0.19, p = 0.005, **Figure 3.5.3**) and RXRα (Spearman's ρ = - 0.15, p = 0.04, **Figure 3.5.3**) were only negatively correlated to BATM. For KLF11 protein level, it was shown that it positively related to VDR (Spearman's ρ = 0.15, p = 0.02, **Figure 3.5.3**), LSD1 (Spearman's ρ = 0.16, p = 0.006, **Figure 3.5.3**) and H3K27ac (Spearman's ρ = 0.19, p = 0.01, **Figure 3.5.3**) protein levels. However, there was no correlation between neither KLF11 and BATM infiltration nor KLF11 and BTSM infiltration, indicating that the up- or down-regulation of KLF11 protein expression does not influence the infiltration of TAMs in BC.

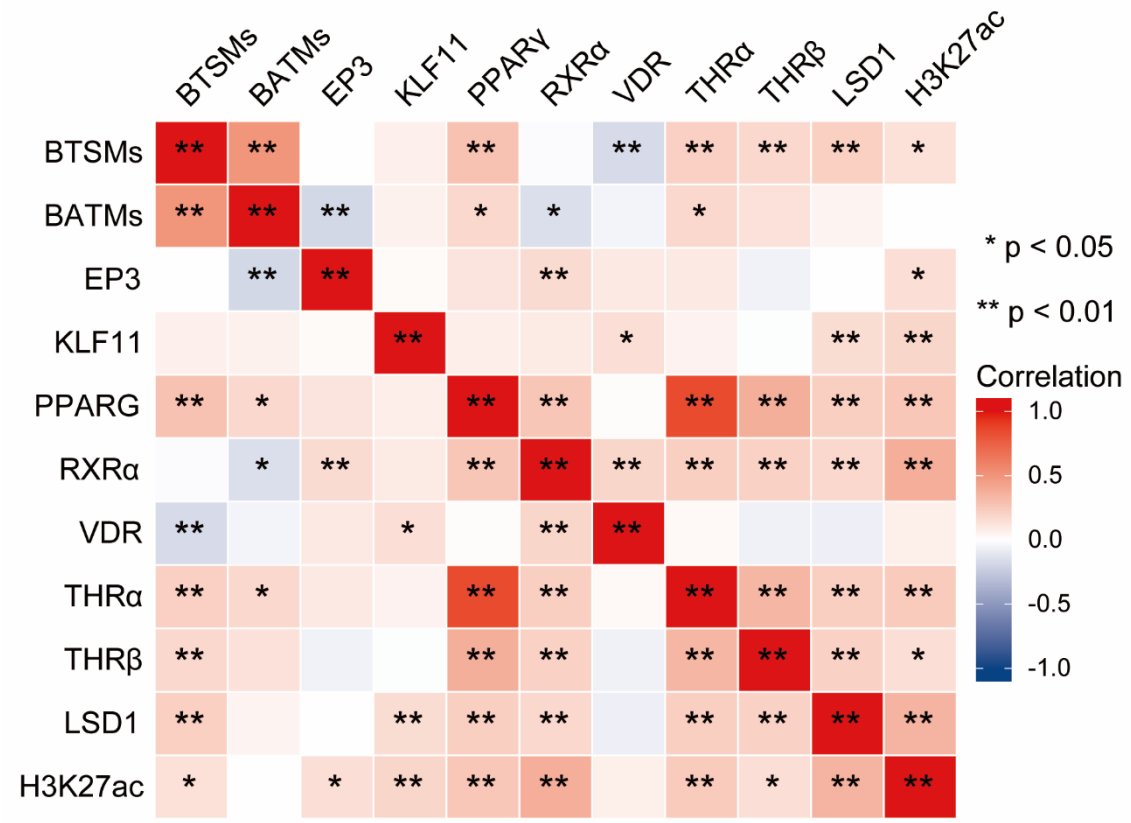


**Figure 3.5.3 The heat map showed the Pairwise Spearman correlation of KLF11, BTSMs, BATMs, and nuclear elements explored previously.**

PPARγ and THRα were positively correlated to both BTSM infiltration (vs. PPARγ: Spearman's ρ = 0.29, p = 1.74e-05; and vs. THRα: Spearman's ρ = 0.22, p = 0.001) and BATM (vs. PPARγ: Spearman's ρ = 0.18, p = 0.01 and vs. THRα: Spearman's ρ = 0.18, p = 0.01). The highly strong association between PPARγ and THRα was also demonstrated (Spearman's ρ = 0.86, p = 0). VDR (Spearman's ρ = - 0.17, p = 0.001), THRβ (Spearman's ρ = 0.18, p = 0.008), LSD1 (Spearman's ρ = 0.22, p = 0.0006) and H3K27ac (Spearman's ρ = 0.14, p = 0.03) were only correlated to BTSM infiltration and EP3 (Spearman's ρ = -0.19, p = 0.005) and RXRα (Spearman's ρ = - 0.15, p = 0.04) were only negatively associated with BATM. VDR (Spearman's ρ = 0.15, p = 0.02), LSD1 (Spearman's ρ = 0.16, p = 0.006) and H3K27ac (Spearman's ρ = 0.19, p = 0.01) were only positively associated with KLF11 expression. "*, p < 0.05; **, p < 0.01; ***, p < 0.001" [301].

### 3.5.4 The Association of KLF11 with TAMs Markers

Although the results from IHC-mediated analyses in our BC cohort did not show any direct association of the KLF11 protein level and TAM infiltration, *KLF11* mRNA expression significantly correlated to the most common marker genes of TAM that obtained from the CellMarker database: *MRC1* (encodes CD206) (partial.r = 0.419, p = 1.96e−43), *CD163* (partial.r = 0.332, p = 6.20e−27), *CD68* (partial.r = 0.189, p = 1.82e−09) in TCGA-BC cohort analyzed by TIMER server adjusted by "tumor purity"(**Figure 3.5.4**). These results indicated that the KLF11 did regulate the gene program transcription of TAM might not likely be dependent on protein levels alteration. However, KLF11 might act as a component of the transcriptional enhancer of TAM-specific gene program and be modulated by post-translational modification level or epigenetic changes.

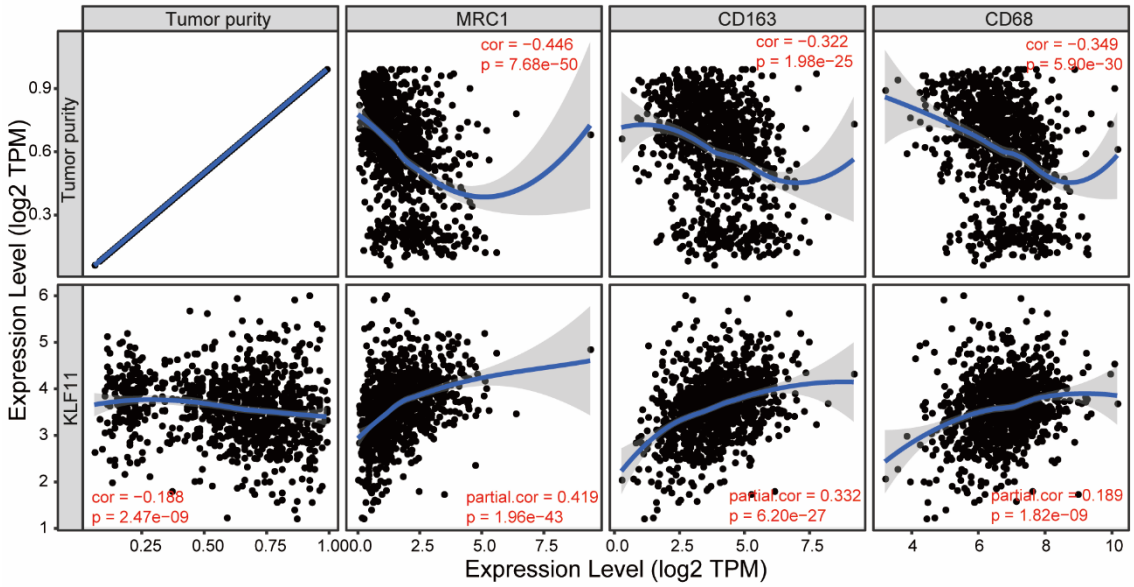


**Figure 3.5.4 *KLF11* expression positively correlated with TAMs common markers in BC.**
*KLF11* mRNA expression significantly correlated to the most common marker of TAM: MRC1 (encodes CD206) (partial.cor = 0.419, p = 1.96e−43), CD163 (partial.cor = 0.332, p = 6.20e−27, CD68 (partial.cor = 0.189, p = 1.82e−09). TAM, Tumor-associated macrophage; partial.cor, correlation coefficient of Spearmann analysis adjusted by "tumor purity".

### 3.5.5 The Association of *KLF11/PPARG* Gene Signature and *KLF11/PPARG/THRA* Gene Signature with Br-TAMs Signatures

Interestingly, the results of protein-protein network exploration showed that KLF11 does interact with PPARγ (**Figure 3.4.1**). The results of GO and KEGG enrichment suggested that KLF11 might consist of the complex transcriptional involved in prostaglandin receptor activity and DNA-binding transcription activity, nuclear hormone receptor binding, AR binding, ER binding, RaR binding, and RXR binding, thyroid hormone and TGFβ signaling pathways, consequently, contribute to the TME regulation (**Figure 3.4.2**). The results demonstrated the positive association of KLF11 with TAMs infiltration and the markers of specific TAMs in TCGA-BC (**Figure 3.5.1**, **Figure 3.5.4**). Predominantly, PPARγ transcriptionally regulates specific gene programmers by cooperating with other nuclear factors e.g. RXR [312-315], THRs, liver X receptor (LXR) [316, 317] CCAAT/enhancer-binding proteins (C/EBPs) [318], peroxisome proliferator-activated receptor coactivator (PGC)-1α [319] etc. Different ligands that bind to PPARγ recruit different coactivators or corepressors, thus regulating different gene transcriptional programs related to cell-specific differen-

tiation and different BPs [320-324]. More interestingly, a PPARγ-mediated cell-specific gene super-enhancer was found to have a cooperative relationship with transcriptional factor KLF11and H3K27ac that regulated target gene-program transcription [325]. Importantly, the results from our BC cohort revealed that PPARγ and THRα were positively correlated to both BTSM infiltration and BATM infiltration (**Figure 3.5.3**). A robust association was found between PPARγ and THRα (**Figure 3.5.3**). Additionally, KLF11 protein level was positively associated with H3K27ac protein levels in our BC cohort (**Figure 3.5.3**), and KLF11 did express in the nucleus of TAM. All these explored results lead to a hypothesis that KLF11 could cooperate with PPARγ or additional other NRs forming a transcriptional enhancer that activates specific selective gene programs of the specific phenotype of TAM in BC.

Previous studies have identified Br-TAMs specific signatures to decipher the distinct TAM phenotypes in BC-TME and its role in BC progression and prognosis [31, 72, 326]. Inspired by previously identified TAM signatures and the transcriptional regulation of TAM polarization, we attempted to develop transcriptional enhancers that regulate Br-TAM-specific genes. The *KLF11/PPARG* two-gene signature was developed as a fundamental transcriptional regulator component of a specific TAM phenotype-selective gene program. Further, *THRA* was added to the two-gene signature based on the observation that its encoded protein THRα was correlated both to BTSM and to BATM infiltration and also highly correlated to PPARγ protein level in the BC cohort. Thus, the KLF11/PPARG/THRA three-gene signature was also developed as a specific TAM phenotype-selective gene program component.

It is well known that macrophages polarized to different phenotypes in response to various stimuli in the TME [28]. M1- or M2-like polarization is generally accepted for the TAM phenotype. The M2-like TAM possesses a feature of immune suppressive and pro-tumoral has been suggested more likely as TAM [79]. We first performed correlation analyses of KLF11/PPARG and KLF11/PPARG/THRA gene signatures with the conventional M1/M2 signature [327].

Interestingly, we found that the correlation between *KLF11/PPARG* and *KLF11/PPARG/THRA* signature with M1-like gene signature was only apparent in BC but not in breast normal tissue.

And with the M2-like gene signature, the correlation in BC was higher than in breast normal tissues. Both *KLF11/PPARG* and *KLF11/PPARG/THRA* signatures were higher positively correlated to M2-like signature (vs. *KLF11/PPARG* signature: Cor = 0.6, p = 2.5e-108 and vs. *KLF11/PPARG/THRA* signature: Cor = 0.52, p = 0, **Table 3.5.1**) than M1-like signature (vs. *KLF11/PPARG* signature: Cor = 0.4, p = 2.1e-43 and vs. *KLF11/PPARG/THRA* signature: Cor = 0.27, p = 1.2e-19, **Table 3.5.1**) in breast tumor. These findings suggested that *KLF11/PPARG* and *KLF11/PPARG/THRA* signatures may have tumor-related transcriptional regulatory polarization gene sets only in Br-TAMs but not in macrophages in normal breast tissue, and this TAMs population might express more M2-like signature than M1-like signature.

However, increasing studies suggest using multiple markers to describe TAM phenotypes rather than simply using M1 or M2 to determine its phenotype even function [35]. Moreover, it was recently reported that TAMs show tissue-specific programming. Br-TAMs showed neither a preferential enrichment for M2-associated genes nor M1-associated genes [31], which means the Br-TAMs such as BTSM and BATM that were polarized in breast tissue is far more complicated than simply categorization of binary states. Therefore, for a more accurate description, we correlated *KLF11/PPARG* and *KLF11/PPARG/THRA* signatures with the TAMs signatures obtained from breast tumor-specific scRNA-seq analysis [31, 72]. Firstly, we correlated *KLF11/PPARG* and *KLF11/PPARG/THRA* signatures with the Br-TAM specific signature. We found impressively that both *KLF11/PPARG* (in tumor: Cor = 0.45, p = 4.1e-54 vs. in normal: Cor = - 0.45, p = 0) and

*KLF11/PPARG/THRA* (in tumor: Cor = 0.36, p = 0 vs. in normal: Cor = - 0.42, p = 1.8e-04) signatures were positively correlated with Br-TAM signature in breast tumor but negatively correlated this gene sets in breast normal tissue (**Table 3.5.1**).

Then, more specifically, we correlated *KLF11/PPARG* and *KLF11/PPARG/THRA* signatures with five sub-clusters of Br-TAMs defined by scRNA-seq data [72], including “Macrophage_2” with previously assigned functions as M1 phenotype and “ Macrophage_1” and “Macrophage_3” featured as M2 phenotype, all of which share some similarities with TAM [31] and two lipid-associated macrophages (LAMs) [71]: “LAM1” and “LAM2”, which are not in the traditional M1/M2 categorization.

Notably, we also found significant positive correlations of *KLF11/PPARG* and *KLF11/PPARG/THRA* signatures with these five sub-clusters of Br-TAMs only in breast tumors except “Macrophage_3” showed a low correlation in normal tissue instead of no correlation of other sub-clusters of Br-TAMs (**Table 3.5.1**). Interestingly, when we ranked the Br-TAMs sub-clusters based on the correlation coefficients, it demonstrated that *KLF11/PPARG* and *KLF11/PPARG/THRA* signatures correlated highest with “Macrophage_1” (vs. *KLF11/PPARG* signature: Cor = 0.46, p = 2.9e-57 and vs. *KLF11/PPARG/THRA* signature: Cor = 0.36, p = 0, **Table 3.5.1**) and “Macrophage_3” (vs. *KLF11/PPARG* signature: Cor = 0.46, p = 2.9e-59 and vs. *KLF11/PPARG/THRA* signature: Cor = 0.38, p = 0, **Table 3.5.1**) which resembling the M2 phenotype and lowest with “Macrophage_2” (vs. *KLF11/PPARG* signature: Cor = 0.35, p = 3.3e-33 and vs. *KLF11/PPARG/THRA* signature: Cor = 0.24, p = 2.4e-15, **Table 3.5.1**) with previously assigned functions as M1 phenotype which consistent to the correlation result of conventional M1/M2 signatures mentioned above. Furthermore, it must not be overlooked that the middle-ranked two clusters: “LAM1” (vs. *KLF11/PPARG* signature: Cor = 0.39, p = 1.1e-39 and vs. *KLF11/PPARG/THRA* signature: Cor = 0.27, p = 8.5e-20, **Table 3.5.1**) and “LAM2” (vs. *KLF11/PPARG* signature: Cor = 0.37, p = 6.3e-36 and vs. *KLF11/PPARG/THRA* signature: Cor = 0.27, p = 4.1e-19, **Table 3.5.1**), which are not in the traditional M1/M2 categorization. This two LAMs are also important for the TME and the progression of tumor [328], as well as the regulation of immune checkpoints-mediated immunotherapy [72].

These results suggest that *KLF11/PPARG*- or *KLF11/PPARG/THRA*-mediated transcriptional regulation of macrophages was context-dependent, which might also partly explain that *KLF11* is lower expressed in BC tumors than breast normal tissue but plays as an aggressive indicator in BC that we demonstrated above.

**Table 3.5.1 Correlation analysis of *KLF11/PPARG* and *KLF11/PPARG/THRA* gene signatures with the TAMs signatures**

| **Gene markers sets** | ***KLF11+PPARG*** | | | | ***KLF11+PPARG+THRA*** | | | |
|---|---|---|---|---|---|---|---|---|
| | **Tumor** | | Normal | | **Tumor** | | Normal | |
| **Conventional M1/M2 classification:** | **Cor** | **p** | **cor** | **p** | **Cor** | **p** | **cor** | **p** |
| M1-like genes | **0.4*** ** | **2.1e-43** | -0.063 | 0.28 | **0.27*** ** | **1.2e-19** | -0.08 | 0.17 |
| M2-like genes | **0.6*** ** | **2.5e-108** | **0.18** ** | **0.0021** | **0.52*** ** | **0** | **0.17** ** | **0.0035** |
| **BC_scRNA-seq:** | | | | | | | | |
| Br-TAM Signature | **0.45*** ** | **4.1e-54** | **-0.45*** ** | **0** | **0.36*** ** | **0** | **-0.42*** ** | **1.8e-14** |

| | | | | | | | | |
|---|---|---|---|---|---|---|---|---|
| Macrophage_2 | **0.35*** ** | **3.3e-33** | 0.028 | 0.63 | **0.24*** ** | **2.4e-15** | 0.0092 | 0.88 |
| Macrophage_1 | **0.46*** ** | **2.9e-57** | 0.094 | 0.11 | **0.36*** ** | **0** | 0.073 | 0.22 |
| Macrophage_3 | **0.46*** ** | **2.9e-59** | **0.21*** ** | **0.00036** | **0.38*** ** | **0** | **0.19** ** | **0.001** |
| LAM1 | **0.39*** ** | **1.1e-39** | **0.088** | **0.14** | **0.27*** ** | **8.5e-20** | **0.061** | **0.3** |
| LAM2 | **0.37*** ** | **6.3e-36** | **0.045** | **0.44** | **0.27*** ** | **4.1e-19** | **0.031** | **0.59** |

Cor, Spearmann Correlation coefficient; "*, p < 0.05; **, p < 0.01; ***, p < 0.001" [301].

## 3.6 Exploration of the Role of Transcriptional Factor KLF11 in Tumor Cells of BC

GO and KEGG functional enrichment analysis suggested that KLF11 might involve cell cycle pathways, and cancer-related pathways, such as thyroid hormone, TGFβ, FoxO, Wnt, Notch, and p53 signaling pathways. It might also regulate the cellular response to prostaglandin and estrogen. Additionally, KLF11 might be an essential element of the hormone-mediated signaling pathway. Consequently, KLF11 contributes to epithelial cell migration and proliferation and cell growth of multiple types of cancers, including BC (**Figure 3.4.2**). To investigate whether KLF11 is involved in regulating tumor cells of BC, we firstly took advantage of scRNA-seq identified epithelial cell signature of different molecular types of BC and did correlation analysis with KLF11 to confirm that KLF11 positively correlated with aggressive features of BC sample partly due to its transcriptional regulation of the marker signatures of tumor cells of different BC subtypes.

Secondly, we took advantage of scRNA-seq identified Gene Modules signatures developed based on epithelial cell signatures of BC to predict more precisely in which cellular functions KLF11 might be involved.

### 3.6.1 The Association of *KLF11* with signatures of distinct Signatures of different Molecular Subtypes of BC Identified by scRNA-seq Datasets

Therefore, to explore more precisely the role of KLF11 in tumor cells of BC, we correlated *KLF11* with the "intrinsic subtyping for scRNA-seq data (SCSubtype)" signatures obtained from a BC scRNA-seq study [72], including four marker gene sets of different molecular subtypes of BC: TNBC_SC, HER2_SC, LuA_SC, and LuB_SC. Interestingly, consistent with the result of the clinical studies, the highest correlation was observed between *KLF11* and the TNBC_SC signature (Cor = 0.49, p = 1.5e-65, **Table 3.6.1**), and then between *KLF11* and HER2_SC signature (Cor = 0.26, p = 1.1e-18, **Table 3.6.1**). There was no correlation between *KLF11* expression and LuA_SC or LuB_SC signatures in tumor tissues was demonstrated while a negative correlation was observed in normal breast tissue between KLF11 and LuA_SC signature(Cor = -0.2, p = 0.00076) (**Table 3.6.1**). We also found impressively that the positive correlation of *KLF11* and SCSubtype signatures in breast tumor turned to be negative in breast normal tissue for both TNBC_SC signatures (Cor = - 0.15, p = 0.0092, **Table 3.6.1**) and HER2_SC (Cor = - 0.21, p = 0.00036, **Table 3.6.1**). Taken together, it is suggested that KLF11-mediated transcriptional regulation of tumor cells of BC was also context (tumor or normal)-dependent, which might further

explain that *KLF11* is lower expressed in BC tumors than breast normal tissue but plays as an aggressive indicator in BC that we demonstrated above.

**Table 3.6.1 Correlation analysis of *KLF11* with the BC tumor cells-related signatures identified by scRNA-seq**

| | Tumor | | Normal | |
|---|---|---|---|---|
| **Gene markers sets** | **Cor (vs.*KLF11*)** | **p** | **Cor(vs.*KLF11*)** | **p** |
| **SCSubtype signatures** | | | | |
| TNBC_SC | 0.49*** | 1.5e-65 | - 0.15** | 0.0092 |
| HER2_SC | 0.26*** | 1.1e-18 | -0.21*** | 0.00036 |
| LuA_SC | -0.076 | 0.013 | -0.2*** | 0.00076 |
| LuB_SC | -0.014 | 0.65 | 0.011 | 0.85 |
| **Gene Modules** | | | | |
| Gene Modules_GM1 | 0.38*** | 2.4e-38 | 0.14* | 0.016 |
| Gene Modules_GM2 | -0.24*** | 3.0e-15 | -0.29*** | 4.4e-07 |
| Gene Modules_GM3 | 0.31e*** | 6.3e-25 | 0.25*** | 1.9e-05 |
| Gene Modules_GM4 | 0.33*** | 2.3e-29 | -0.13* | 0.024 |
| Gene Modules_GM5 | 0.077 | 0.011 | -0.078 | 0.18 |
| Gene Modules_GM6 | 0.072 | 0.018 | -0.24*** | 4.8e-05 |
| Gene Modules_GM7 | 0.59*** | 1.3e-100 | 0.009 | 0.88 |

Cor, Spearmann Correlation coefficient; SC, Single cell defined; TNBC, Triple negative BC; LuA, Luminal A; LuB, Luminal B; "*, p < 0.05; **, p < 0.01; ***, p < 0.001" [301]**.**

## 3.6.2 The Association of *KLF11* with signatures of distinct Gene Modules (GM) Identified by scRNA-seq Datasets

Gene modules (GMs) analysis of neoplastic signatures identified by scRNA-seq provide complementary new approaches to classify intratumor heterogeneity, and different GMs' signatures indicate distinct cellular functions [72]. To further explore the function of KLF11 involved in tumor cells, we correlated *KLF11* with the developed seven GMs [72]. We found that *KLF11* highly positively correlated to GM7 (Cor = 0.59, p = 1.3e-100), GM1 (Cor = 0.38, p = 2.4e-38), GM4 (Cor = 0.33, p = 2.3e-29), and GM3 (Cor = 0.31, p = 6.3e-25) and negatively correlated to GM2 (Cor = -0.24, p = 3.0e-15) in breast tumors (**Table 3.6.1**). Impressively, that the positive correlation of *KLF11* and GM7 (Cor = 0.009, p = 0.88) and GM4 (Cor = - 0.13, p = 0.024) signatures in breast tumor turned to be no correlation or even negative correlation in breast normal tissue (**Table 3.6.1**). GM1 and GM7 are enriched for hypoxia, tumor necrosis factor-α and p53 signaling and apoptosis, and estrogen response pathways [72]. GM4 signatures are especially enriched in cell cycle and proliferation-related BPs or signaling pathways [72]. GM3 is predominantly enriched for hallmarks of the interferon response, and antigen presentation [72]. Taken together, it is suggested that KLF11 might regulate the cell growth-related phenotypes such as proliferation, apoptosis in BC tumor cells, and the immune response of tumor cells. Interestingly, the KLF11-mediated proliferation and apoptosis function might be converse between tumor context and normal context.

## 3.7 Validation of the pro-tumor Role of KLF11 in BC Cell lines

To validate the predicted pro-tumor significance of KLF11 in tumor cells of BC, siRNA-mediated loss-of-function of KLF11 in ER-positive luminal type, HER2 amplified type, and triple-negative type BC cell lines were then respectively performed.

All of the cellular functional assays confirmed that KLF11 acts as a pro-tumor TF in BC cells via promoting cell proliferation and/or inducing cell apoptosis. However, due to neoplastic intratumor heterogeneity, different cancer molecular subtypes are likely to have different underlying mechanisms.

### 3.7.1 siRNA-mediated Knockdown of KLF11

MCF7 as luminal type, SKBR3 as HER2 type, and MDAMB231 as TNBC type were transfected with non-targeting control siRNA as negative control (NC), and two independent siRNAs target *KLF11* (*KLF11*-S1 and *KLF11*-S2). The knockdown effect was markedly at the mRNA level by RT-PCR (**Figure 3.7.1 A**) and at the protein level by colorimetric cell-based KLF11 ELISA (**Figure 3.7.1 B**).

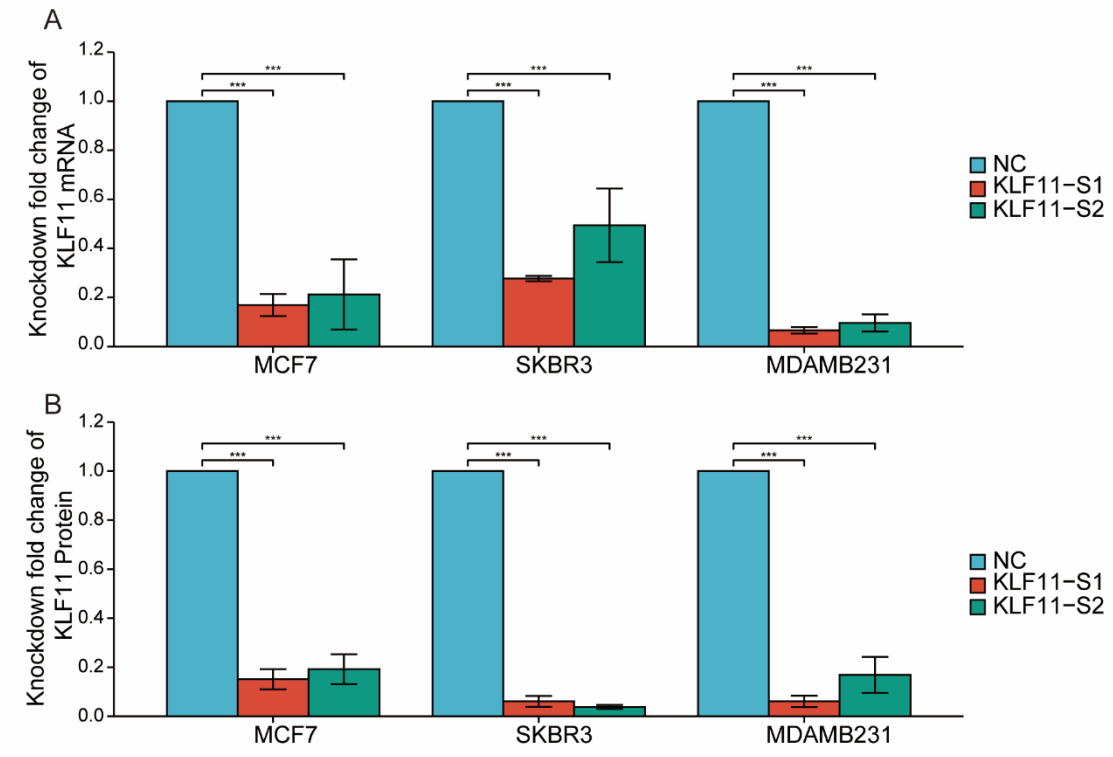


**Figure 3.7.1 siRNA-Mediated Knockdown of KLF11.**

**A.** *KLF11* mRNA in NC and si-KLF11 cells were analyzed by RT-PCR showed markedly knockdown in three BC cell lines. **B.** KLF11 protein levels in NC and si-KLF11 cells were analyzed by colorimetric cell-based KLF11 ELISA showed a substantial downregulation in the three cell lines. Error bars indicate the mean of RT-PCR and ELISA triplicates in each experiment. NC, negative control; ns, $p > 0.05$; "*, $p < 0.05$; **, $p < 0.01$; ***, $p < 0.001$" [301].

### 3.7.2 Knockdown of KLF11 inhibited the Proliferation of HER2 negative BC Cell Lines

To demonstrate the functional alteration of KLF11 knockdown on BC tumor cells, we performed relevant functional experiments in MCF7, SKBR3, and MDAMB231 cell lines. All cell lines showed a significant reduction of viable cells after transfection with KLF11-siRNAs compared to KLF11-NC (**Figure 3.7.2 A-C**). In addition, the highest inhibitory effect on cell viability was observed in the MDAMB231 cell line (**Figure 3.7.2 C**). These results indicated that KLF11-knockdown has an inhibitory effect on tumor cell survival.

Afterward, to assess whether the cell number increase was based on the influence of cell proliferation. After the knockdown of KLF11, a high inhibition of proliferation was obtained in MDAMB231 cells (**Figure 3.7.2 F**). Only modest inhibition of proliferation was observed in MCF7 cells (**Figure 3.7.2 D**). However, there was no proliferation inhibitory effect in the SKBR3 cells (**Figure 3.7.2 E**). We could demonstrate that KLF11-knockdown only inhibited cell proliferation of HER2 negative BC cell lines, the most effective impact was obtained on the TNBC cell line.

### 3.7.3 Knockdown of KLF11 Induced the Apoptosis of BC Cell Lines independent of Molecular Subtypes

Next, MCF7, SKBR3, and MDAMB231 cells lines were transfected KLF11-siRNAs and then performed cell apoptosis assays, which could be another reason that induces the inhibition of cell survival by downregulating KLF11 expression. We found that KLF11-knockdown induced MCF7, SKBR3, and MDAMB232 cells apoptosis. In addition, a higher induction of apoptosis was obtained in MCF7 (**Figure 3.8.2 G**) and SKBR3 cell lines (**Figure 3.8.2 H**). Only a modest induction of apoptosis was observed in the MDAMB231 cell line (**Figure 3.8.2 I**).

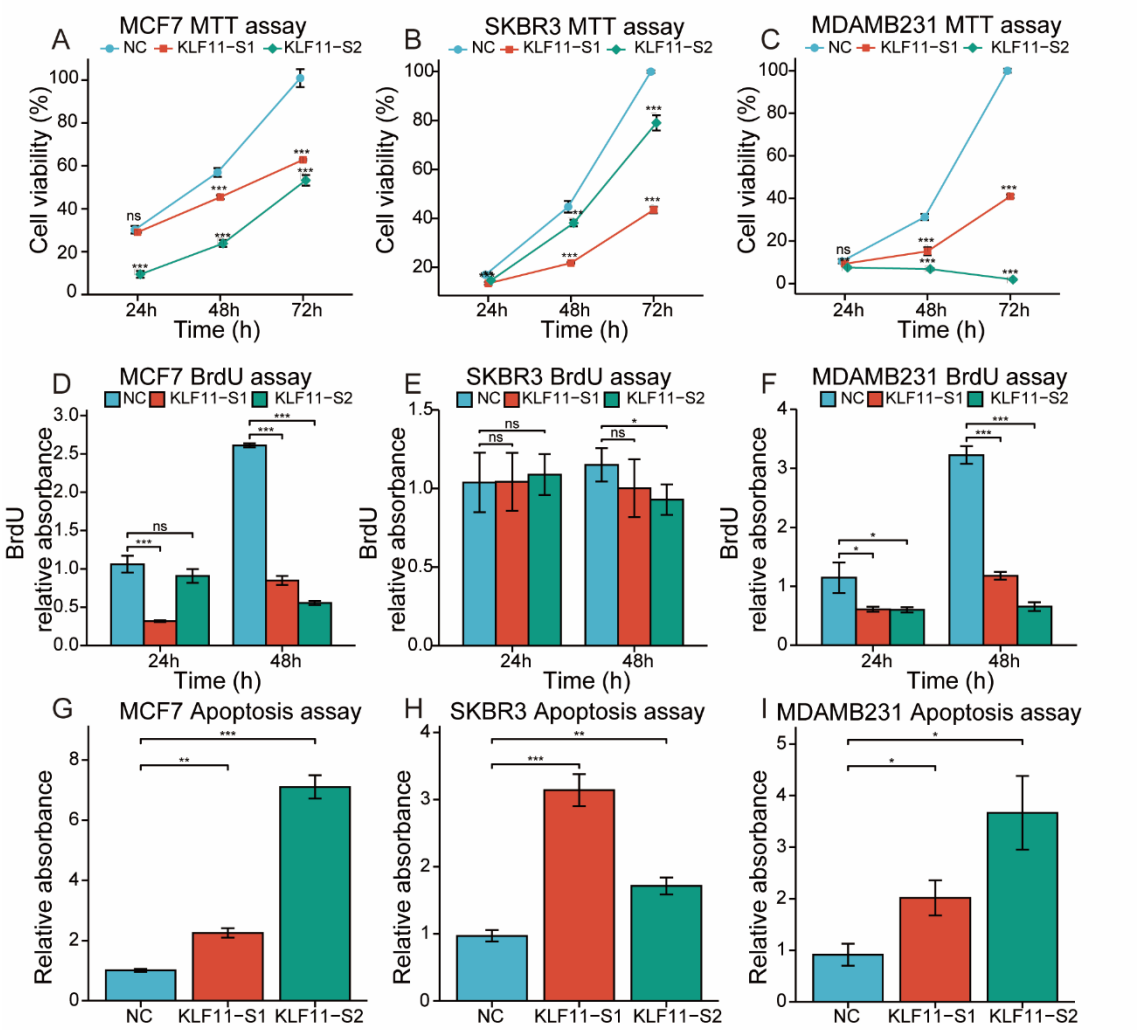


**Figure 3.7.2 Loss-of-function studies of KLF11 in different BC cell lines.**

**A-C.** MTT assay showed that the viable cells of MAF7 (**A**), SKBR3 (**B**), and MDAMB231 (**C**) were significantly reduced after transfection with KLF11-siRNAs compared to KLF11-NC. **D-E.** BrdU assay showed the effect of cell proliferation of MCF7 (**D**), SKBR3 (**E**), and MDAMB231 (**F**) after transfection with KLF11-siRNAs compared to KLF11-NC. **G-I.** Apoptosis assay showed the effect of cell apoptosis of MCF7 (**G**), SKBR3 (**H**), and MDAMB231 (**I**) after transfection with KLF11-siRNAs compared to KLF11-NC. ns, $p > 0.05$; "*, $p < 0.05$; **, $p < 0.01$; ***, $p < 0.001$" [301].

## 3.8 The Relationship between *KLF11* and Immune Checkpoints in BC

The last additional part is for the prospect of its therapeutic application based on observing its impressive regulation role both in the TAM and tumor cells of BC.

"Programmed cell death protein 1 (PD-1)" is expressed explicitly on the immuno-cell surface [329]. As the ligands of PD-1, PD-L1 and PD-L2 are expressed on "antigen-presenting cells (APC)" and tumor cells [330-332]. Tumors can also express PD-L1 inhibiting antitumor immune responses in the TME [333]. Blocking its ligands PDL1 and PDL2 or PD-1 limits immune effector responses and induces tumor immune escape [333]. PD-L1 and PD-L2 are broadly distributed across 5 Br-TAMs sub-clusters [71]. Moreover, tumors can express PD-L1 to inhibit antitumor immune responses in the TME [333]. Considering the potential transcriptional regulatory role of *KLF11* in TAMs and tumor cells of BC, the relationship of *KLF11* with the RNA encoding "PD-1 (*PDCD1*)",

"PD-L1 (*CD274*)", and "PD-L2 (*PDCD1LG2*)" [303] were assessed and the correlation adjusted by tumor purity using TIMER.

We found that *KLF11* related positively to PD-1, PD-L1, and PD-L2 in the overall BC cohort (**Figure 3.8.1 A**) and more nuancedly in TNBC_BC (**Figure 3.8.1 B**), HER2_BC (**Figure 3.8.1 C**), and luminal_BC (**Figure 3.8.1 D**). Interestingly, a stronger correlation existed between *KLF11* and PD-1 ligands: both with PD-L1 (partial.r = 0.406, p = 8.15e−41) and PD-L2 (partial.r = 0.426, p = 5.31e−45) than between *KLF11* and PD-1 (partial.r = 0.132, p = 2.98e−05) in the overall BC (**Figure 3.8.1 A**). This kind of stronger correlation was also observed across different molecular subtypes of BC (**Figure 3.8.1** B-D). These results indicate that tumor immune escape might contribute to the pro-tumor role of KLF11 in BC. Furthermore, PD-1/PD-L1 was well studied by numerous studies [330, 331]. Inhibitors of PD1/PD-L1 may not inhibit the PD1/PD-L2 interaction. Therefore, these results highlighted that paying attention to the interaction between PD1/PD-L2 might be a solution to treat PD1/PD-L1 resistance or improve low response rates. More importantly, particularly for tumors that show low response rates to immune checkpoints therapies, targeting transcription factors such as KLF11 might be a synergistic or an alternative option.

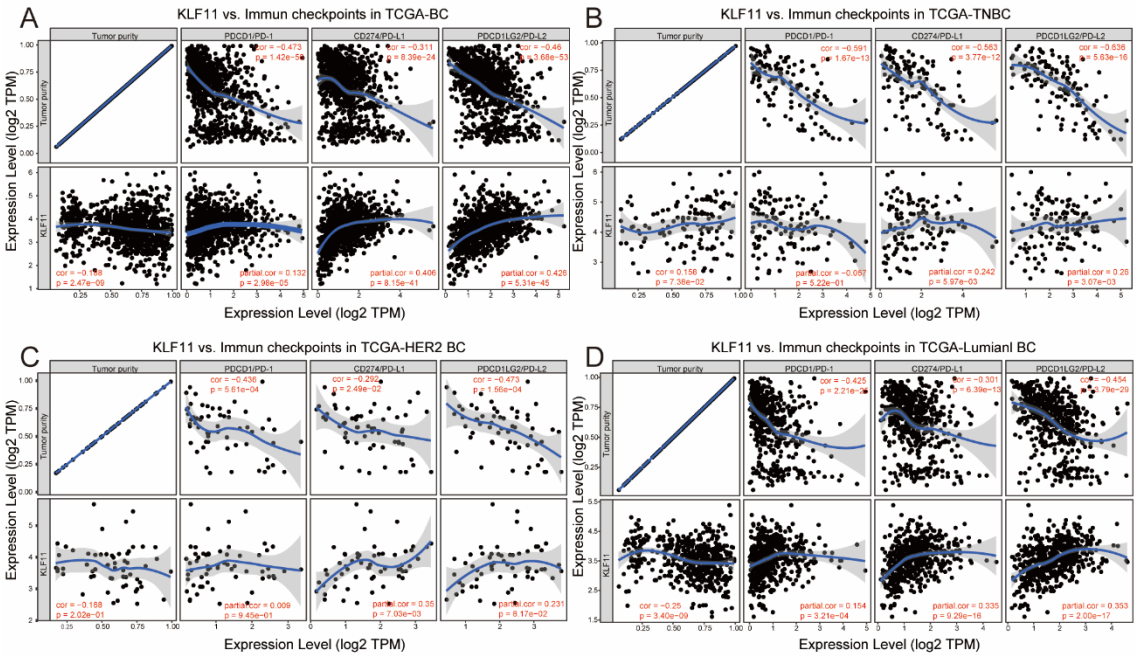


**Figure 3.8.1 Correlation of *KLF11* expression with PD-1, PD-L1, and PD-L2 in BC.**

**A-D.** Spearman correlation between *KLF11* and "PD-1 (*PDCD1*)", "PD-L1 (*CD274*)", and "PD-L2 (*PDCD1LG2*)" [303] of the overall BC cohort (A), of the TNBC BC (**B**), of the HER2 BC (**C**), and of the Luminal BC (**D**). partial.cor, the correlation coefficient of Spearman analysis adjusted by "tumor purity".

# 4. Discussion

## 4.1 The Different Roles of BATM and BTSM

Our work showed that the different phenotypes of TAMs based on their infiltrating location (in the tumor-stroma section or the adipose tissue section) were involved differently in BC. Of 298 cases of sporadically invasive BC, the infiltration of TAM both in breast tumor-stroma section termed BTSM and in breast adipose tissue termed BATM in BC patients was inversely correlated with OS. And patients with high-BATM characteristics had a low DFS probability. In addition, multivariate regression demonstrated that high infiltration of BATM independently indicated the poor OS and DFS of BC patients. However, BTSM infiltration was specifically correlated with BC molecular subtypes. Higher BTSM infiltration rates were accompanied by more aggressive clinical features in BC. For example, among the five BC molecular subtypes, the highest BTSM infiltrating level was observed in TNBC. Additionally, the infiltrating number of BTSM was more in ER-negative BC. And patients with Ki-67 expression > 14 % characteristic had a higher infiltration of BTSM than patients with Ki-67 expression ≤14 %

Regarding the role of TAM in adipose tissue, it has been reported to act as so-called CLS in obese BC patients [334, 335]. However, our study was not limited to adipose tissue in obese individuals. It is specifically designed to push the boundaries of "obesity" as breast fat tissue is an important part of the breast irrespective of obesity [95, 336]. From this perspective, it was the first time here to show that an increased incidence of BATMs independently indicated the impaired survival of BC patients. It indicates BATM might contribute to the formation and maintenance of the pro-tumor TME in BC. Of the obese individuals, BATMs might obtain the phenotype as CLS triggering the pro-tumor effect of the obese-adipose tissue during BC progression [337]. However, on the premise that “obesity” is abolished, it is still unknown whether there is a similar interaction between adipose tissue and macrophages, and further research is needed.

In recent years, research has focused on targeted therapy and immunotherapy strategies for TNBC to improve the prognosis of these patients [338]. TNBC accounts for approximately 15% to 20% of all BC patients [339]. It is the most aggressive subtype with malignant features, poorer clinical outcomes, and a higher likelihood of visceral metastases than other BC subtypes[340]. In addition, the current treatment of TNBC is still very limited due to the “negative” of conventional targeting molecules. Immunosuppressive-TME has been reported as a hallmark of TNBC that promotes tumor cell growth and metastasis via TAM-derived immunosuppressive cytokines [75, 78, 341]. Promising advances have recently been made in TNBC immunotherapy [342]. BTSMs might provide an option for future immunotherapies in TNBC. They might also act as a prognostic indicator to stratify patient risk and facilitate the implementation of more precise treatment strategies.

Furthermore, BATM and BTSM acted as prognostic impactors of BC patients in some subgroups grouped by clinicopathological characteristics. The progression of BC depends not only on the malignant features of tumor cells but also on the interaction between the BC cells and the BC-TME [343]. These suggest that the prognostic role of TAMs in BC patients may vary depending on the TME and TME-educated tumor characteristics. TAMs are vital components of TME involved in tumorigenesis and development [344]. Thus targeting TAM has gradually become a promising therapeutic strategy for cancer immunotherapy [344]. The two phenotypes of TAMs in the current study, BATM and BTSM, were highly and significantly correlated. This could lead to

speculation that BTSM and BATM might be partially involved in cellular phenotypic switching within the dynamically altered TME. Indeed, TAM within the flexible TME is highly plastic and can switch from one phenotype to another [136]. The plasticity of TAM and the inter- and intra-tumoral heterogeneity of TAMs complicate the definition of precise phenotypes and functions of TAM. Current knowledge of TAM phenotypes is limited, underscoring the need for an in-deep understanding of the specificity of TAM in the tissue-specific TME. In BC, further mechanistic analysis of the polarization of BATM and BTSM phenotypes is essential to gain insights into BTSM and BATM in BC progression and assess their value for application to immunotherapy.

## 4.2 The Relationship between EP3 and BATMs in BC

Interestingly, we also demonstrated that EP3 was negatively associated with BATM infiltration. Furthermore, the negative effect of BATM on BC survival was significantly attenuated by elevated EP3 expression. A combination of “BATM-high” and “EP3-low” led to an inferior outcome. PGE2 signaling pathway has been demonstrated that promotes the polarization of the M2 phenotype and also regulate cancer cells directly [345, 346]. The regulation of PGE2 and four prostaglandin E2 receptors (EP 1-4) in the development of BC are extensively elucidated [345, 346]. In our previous study [282], EP3 was positively associated with BC survival resembling EP1 [347]. However, in contrast to the pro-tumor role of EP2 and EP4 [345, 348]. However, tumor cell biology cannot explain the protective effect of EP3 on BC [302]. Based on this, we speculate that EP3 can be achieved its impact on BC progression through regulation of the TME.

Interestingly, the present study showed that EP3 attenuates the pro-tumor trend of BATM in the TME of BC. We speculate that the PGE2/EP3 signaling pathway may regulate the initiation and polarization of BATM in BC adipose tissue. More interestingly, EP3 has been demonstrated recently that involved in the phenotype switch of macrophages in response to the cellular environment [349]. A similar mechanism by which EP3 affects TAMs polarization might exist in BC. EP3 might reduce the polarization of pro-tumor BATM or switch it to an anti-tumor phenotype. Further studies should be performed to clarify how EP3 regulates BATM polarization in BC.

## 4.3 The Role of Transcriptional Factor KLF11 in BC Patients

*KLF11* was lower expressed in BC than in non-tumor/para-tumor tissue of BC. The lower expression of KLF11 in the tumor can be the effect of miR-30d upregulation in [238] and also may be due to the DNA hyper-methylation of KLF11 in BC [211]. In addition, KLF11 protein level was correlated with aggressive BC subtype features and negatively associated with BC patients’ prognosis. It seems reasonable to assume that the low level of KLF11 leads to an inhibition of its inhibitory effect, thereby contributing to promoting tumor progression. Consistently, a previous bioinformatics study also suggests that *KLF11* relates to the impaired prognosis of BC patients. Higher *KLF11* was expressed in more aggressive samples such as higher grade, lymphatic metastasis, and TNBC patients [350].

The study that explored the prognostic role of KLF11 in endometrial cancer, which is a hormone-independent female cancer similar to BC, demonstrated that KLF11 is positively associated with aggressive features, like PR negative status. Patients with higher KLF11 exhibit a poorer survival outcome [274]. In BC, our results demonstrated a consistent description of the prognostic role of KLF11, indicating that KLF11 might involve in the hormonal receptor-mediated tumor promotion pathway. Interestingly, it was shown that *KLF11* mRNA levels could be down-regulated by progesterone stimulation *in vitro* and *in vivo* [251], indicating that this may partly explain why KLF11 was higher expressed in TNBC patients than other molecular subtypes of BC. From the TME

perspective, KLF11 has been demonstrated as an inhibitor of proinflammatory chemokines when responding to the microenvironment [252, 270]. Pro-inflammatory effects indicate anti-tumor potential. This can also explain the low expression of KLF11 in BC, leading to a pro-tumor effect.

Furthermore, in prognostic analyses of KLF11 grouped by clinicopathological features, we found that KLF11 related to an impaired prognosis in BC patients of several subgroups, but not of their corresponding subgroups, indicating that the prognostic role of KLF11 might also be TME-dependent. In terms of treatment stratification, KLF11act is a better prognostic indicator in patients who underwent chemotherapy, which means that it can also be an indicator of treatment like some other members of this family. Observation of its expression during therapies may indicate the subsequent performance of more precise treatment. Interestingly, KLF11 does exert growth-inhibition functions in untransformed cultured cells [351]. However, mice models with KLF11-knockout do not perform any difference in erythropoiesis, growth, development, and lifespan compared to mice in the control group [351]. This indicates that targeting KLF11 as therapy can lead to fewer physical side effects.

Besides, different types of parameters mediated nomograms for predicting OS or DFS in BC patients have been developed [352-356]. We are glad to establish well-fitting DFS and DMFS prediction models from our BC cohort.

## 4.4 The Correlation of Transcriptional Factor KLF11 to Breast Tumor-Associated Macrophage

Our study demonstrated that KLF11 positively correlated to TAMs infiltration in the TCGA-BC cohort, and KLF11 was further experimentally confirmed expressed in TAMs nuclei. As a TF, KLF11 might cooperate with nuclear receptor PPARγ and/or other co-factors like thyroid hormone receptor alpha (THRα) to form a transcriptional enhancer of gene programs of different phenotypes of TAMs only in tumor tissue-associated macrophages but not in macrophages in normal breast tissue.

The correlation between *KLF11* and macrophage markers at the mRNA level indicates that *KLF11* does transcriptionally regulate macrophage polarization. However, we also found that the protein level of KLF11 with either PPARγ or TAMs infiltration is not relevant in our BC cohort. The explanation could be that the transcription factor KLF11 acts as a co-collaborator of nuclear receptor PPARγ in this case, not as its downstream or upstream regulator among the three interaction models of TFs-NRs. In addition, KLF11 protein levels did not correlate with the number of TAMs infiltrates in BC patients. Then, it seemed that KLF11 influences TAMs infiltration in BC by altering its function or by post-translational modifications rather than by reducing protein expression. It has been reported that the transcriptional complex that includes KLF11 is inactivated in target genes regulation because of the threonine phosphorylation of KLF11 in the co-factor interacting domain under tumor context [272]. This may also happen in TAMs, and it might be the frustration of the linkage that leads to phenotypic differential infiltration of macrophages. Given this, subsequent work on developing KLF11 phosphorylation antibodies and phosphorylated-KLF11 detection in TAMs or tumors appears to be promising.

PPARγ is a member of the NR superfamily and belongs to the group of ligand-activated TFs [322] that act as determinants of specific cell phenotype, involving adipocyte differentiation [357-359], macrophage polarization [150, 314, 360, 361], and driving the phenotype differentiation of regulatory T cells in adipose tissues [362]. Macrophage-specific PPARγ is involved in the immune response of adipose tissue [150, 363] and participates in lipid metabolism [316, 364-366]. Taken together, previous findings suggested that PPARγ in macrophages has transcriptional regulatory

functions. Cell-selective-specific PPARγ binding is featured by the presence of cooperating TFs and positive histone labeling at chromatin open sites [314]. However, the co-factors or co-localizing transcriptional factors have not been systematically reported. PPARγ binding is a key driver of the formation of selective transcriptional enhancers for the cell identify-defined gene programs [367, 368]. The transcriptional enhancer, also known as a super-enhancer, has been demonstrated to be bound by gene coding lineage-determining transcriptional regulators and essentially regulates the transcription of the gene program that defines a cell type. And the related DNA binding site is marked by specific gene epigenetic features [368, 369]. Additionally, since PPARγ is involved in transcriptional regulation in tumor cells, adipocytes, and macrophages, environmentally responsive nuclear receptor PPARγ might be the key component of the transcriptional enhancer of gene preprograms that drive the Br-TAMs in different sections of the breast (e.g., in breast adipose tissue or tumor-stroma tissue) differentiate into distinct phenotypes (e.g., BATMs or BTSMs).

As a member of the KLFs family, KLF11 associates mainly with the proximal promoter region of target genes [120, 181, 370]. KLF11 was also involved in the gene-programming regulator interacting with NRs [325]. It indicates that KLF11 might be involved in specifying and activating the TAM-specific phenotype selective gene programmer forms the transcriptional complex enhancer or repressor with nuclear receptors through its zinc-finger domains. Importantly, KLF11 is screened out to be a direct interacted transcriptional co-regulator of PPARγ [371]. More importantly, KLF11 was found to be a transcriptional regulator that cooperated with PPARγ related adipocyte selective super-enhancer and then regulated selective gene programs transcription [325]. And in this cell differentiation case [325], the KLF11/ PPARγ super-enhancer functioned based on the epigenetic feature of H3k27ac, and KLF11 interacted with PPARγ directly to regulate the gene program transcription. Interestingly, present data show that H3K27ac protein level positively correlated both to KLF11 and PPARγ and also possessed a positive relationship with TAMs infiltration, suggesting that H3k27ac might also be the epigenomic feature of KLF11/PPARγ transcriptional enhancer of the specific cell type of TAMs polarization. Additionally, a cofactor that may also contribute to this KLF11-PPARγ transcriptional enhancer could be THRα, which was correlated both to BTSMs and to BATMs infiltration and also highly correlated to PPARγ protein level PPARG in the BC cohort.

The transformation of TAMs phenotype is mainly dependent on the transcription of gene signatures. Transcriptome signatures of TAMs and TFs-driven transcriptional programs in TAMs have been explored in a mouse model of BC and predict poor prognosis in human BC using bioinformatics analysis [372]. In addition, TAMs-related CSF-1 response transcriptional signature has been demonstrated in BC patients and is correlated to high tumor grade and low expression of ER and PR [373, 374]. We speculate that *KLF11/PPARG* or *KLF11/PPARG/THRA* act as an “engine signature” that can drive distinct transcriptional programs in Br-TAMs to polarize the TAMs in BC towards a flexible context-dependent phenotype.

In addition, the correlation of *KLF11* mRNA expression with CD206 and CD163, which are the surface markers of M2-like phenotype [375], was higher than the correlation with pan-macrophage marker CD68. Consistently, the *KLF11/PPARG* and *KLF11/PPARG/THRA* signatures positively correlated to conventional M2 signatures higher than to M1 signatures. Moreover, the highest correlation between *KLF11/PPARG* and *KLF11/PPARG/THRA* signatures with signatures of five Br-TAMs sub-clusters was obtained in the clusters that featured M2-like phenotype defined by scRNA-seq analysis. And all these significant correlations only appeared in the breast tumor tissue, not normal tissue. Taken together, KLF11 might more possibly regulate pro-tumor TAMs

phenotype polarization in BC. Furthermore, the M2-like TAMs promote invasion and metastasis and hamper chemotherapy effects, leading to tumor progression and poor prognosis [51, 375, 376]. Especially, CD163+ TAM is highly presented in the aggressive BC subtype such as TNBC and HER2-amplified BC and indicates a poor prognosis [59]. This can also explain why KLF11 acted as a poor prognostic factor and is related to features of aggressive subtype in BC patients.

To our knowledge, this is the first time to mention KLF11 as the sequence-specific TF factor involved in TAMs polarization. Rerouting and remodeling of “bad” macrophage polarization is the holy grail of macrophage-targeted therapy [377]. Therapeutic targets transcriptional regulation elements such as target HDACs, IRF5, and NFκB have been increasingly explored to reprogram pro-tumor TAM phenotype to anti-tumor phenotype, thus suppressing tumor progression [378, 379]. Taken together, it is suggested that target transcriptional factor KLF11 to inhibit or re-program pro-tumor TAMs phenotypes polarization may enhance anti-tumor effects and reverse the immunosuppressive state in the TME.

## 4.5 The Role of Transcriptional Factor KLF11 in Tumor Cells of BC

Functional enrichment analysis demonstrated that *KLF11* was closely enriched to epithelial cell migration and proliferation. *KLF11 was* highly correlated to the signature of TNBC, which is the most aggressive BC subtype, and also was found to be highly associated with cell growth-related gene modules (GMs) signature in and only in the breast tumor context. Furthermore, siRNA-mediated loss-of-function confirmed that the down-regulation of KLF11 in the BC cell lines decreased cell viability, inhibited cell proliferation, and induced cell apoptosis.

Some microRNAs affect BC cell growth, depending on the low level of KLF11 [238] has been demonstrated previously, indicating that KLF11 might act as a tumor-suppressor in BC. Consistently, we observed that the expression of *KLF11* was lower in BC compared to its corresponding normal one. However, the present study experimentally confirmed that KLF11 acted as an oncogene in BC cell lines. In addition to the cell experiments confirmation, *KLF11* mRNA expression was highly and positively correlated to the TNBC epithelial signature, suggesting that KLF11 is a pro-tumor TF in BC tumor cells.

In conclusion, when restricted to a tumor context, the transcription-regulated genes by KLF11 in BC tumor cells were reversed compared to in the normal breast tissue. However, we do not know the mechanism by which KLF11 influences BC tumor cells. KLF11 suppresses growth in untransformed cells and even transforms normal fibroblasts [280]. However, it appears to be a pro-tumor regulator of several cancer types, e.g., pancreatic cancer, ovarian cancer, etc. [280]. More interestingly, in pancreatic cancer, different studies have found that the regulation of KLF11 on cells functions is the opposite [179, 260, 261]. However, the existence of this reversal is understandable from a mechanistic perspective [179, 260, 261], indicating that the role of KLF11 in tumors is also TME dependent. We cannot ignore the existence of this situation in BC, and in-depth studies are necessary to explain and explore the TME-dependent regulatory mechanism of KLF11 in BC. Compared to bulk RNA-seq, which focuses more on cellular heterogeneity, scRNA-seq can resolve TME complexity through unbiased cellular analysis based on transcriptome profiles and significantly transform transcriptome studies. Advanced scRNA-seq technics can detect the dynamical expression of RNAs at the single-cell level [380]. Recently developed spatial transcriptome (ST) can be complemented to provide detailed visualization of spatial information [381]. To further analyze the transcriptional network of KLF11 involved in the tumor cells, BATMs, BTSMs, respectively, and the special phenotype of KLF11-mediated TAMs that exist in a different section of BC tissues, a combination of scRNA-seq and ST can be optimized further applied in the future.

## 4.6 The Correlation of *KLF11* Expression and Immune Checkpoints in BC

“Programmed cell death protein 1 (PD-1)” and its ligands “PD-L1 and PD-L2” are key immune checkpoints [329-332]. We found that *KLF11* was strongly and positively related to PD-L1 and PD-L2 in BC. In particular, antibodies blocking this interaction by binding PD1/PDL1 have shown promising effects in TNBC patients [382]. However, response rates to immune checkpoint inhibitors in BC are the worst during these cancer types due to their lower immunogenicity [383]. To circumvent resistance, our results suggest that in addition to PD-L1, PD-L2 might also be a potential star for immunotherapy that needs to be paid more attention to in the future.

In addition, patients selected with ER-negative or PD-L1 positive responded better to immune checkpoint inhibitors than ER-positive or PD-L1 negative BC patients, respectively [383, 384]. Present work shows that KLF11 was negatively correlated to ER status and positively correlated to PD-L1 expression, suggesting that higher KLF11 expression might indicate a better response to immune checkpoint inhibitors; thus, KLF11 can be a selective marker for immune checkpoint therapy in BC patients.

Interestingly, a recent preclinical study has approached a therapy combination of blocking PD-L1, and TGFβ demonstrated promotion of durable rejection of tumors and immunity [385], indicating that targeting KLF11 might increase the efficacy of immunotherapy in BC both from the TME perspective and tumor cell perspective. Particularly for tumors showing low response rates to immune checkpoints therapy, targeting transcription factors such as KLF11 might be a synergistic or an alternative option.

## 4.7 Limitations of This Study

Various limitations have to be regarded when interpreting the results of this work. Our BC cohort is almost 20 years old (primary diagnosis 2000-2002). The advantage of an old patient cohort in terms of very long follow-up data is, in this case, also a disadvantage, as data on treatment cannot be obtained anymore. In addition, at that time, neoadjuvant chemotherapy therapies were not applied regularly in our clinic. However, the advantage of our data is that no patient in our cohort had undergone any prior treatment before surgery was performed. Regarding adjuvant therapy, even if we do not display it specifically, it is assumed to be the same in the two groups now subdivided by macrophage count (“BATM-high/-low”, “BTSM-high/-low”). Additionally, BATM was an independent prognostic factor in our cohort, which suggests that treatment (which depends on the other factors in this analysis, of which BATMs were independent) should not cause any bias in our data. Since neoadjuvant chemotherapy has become common recently, this factor must be regarded in any research using more recent patient samples.

Another limitation is that many analyses are bioinformatics analyses. Although the work described here involved rigorous bioinformatics analysis, it has some limitations that some important data might be overlooked caused of its reliance on known genes and known functions. We confirmed only some of the results through our validation but still left results that need to be further validated.

# 5. Conclusion

This is the first time that TAMs are shown to have different effects on BC based on different infiltration locations, i.e., BTSMs and BATMs. BTSM preferred to be associated with the clinicopathological characteristics of BC, while BATM appeared to be associated closely with the prognosis outcomes of BC. BTSM was shown to be mainly related to the BC molecular subtypes. Furthermore, we observed the highest abundance of BTSM in TNBC. This suggests that BTSM may provide a promising selection option for future targeted therapy in TNBC. In addition, it may also serve as a promising therapeutic pointing marker to participate in the risk stratification of patients and then select a more precise treatment strategy for patients.

However, a higher BATM infiltration independently indicated a lower survival probability of BC. Furthermore, we also found that BATM infiltration was negatively presented with EP3 expression in BC patients. In addition, the negative impact of BATM on survival prognosis was significantly attenuated by EP3 expression. A combination of “BATM-high” and “EP3-low” led to an inferior outcome. These results indicate that targeting BATM and targeting BATM accompanied with targeting the PGE2/EP3 pathway could be promising therapeutic concepts of BC immunotherapy.

In addition, we demonstrated *in silico* that *KLF11* mRNA was lower expressed in BC tumor tissue than in the non/para-cancerous breast tissues. Furthermore, *KLF11* mRNA expression was positively associated with aggressive BC features. Its elevated expression remained an independent indicator for poor OS of BC. We also showed a higher KLF11 protein level in the BC patients with a more aggressive molecular subtype. Moreover, a high KLF11 protein level was associated with an impaired prognosis. Furthermore, KLF11 remained an independent and unfavorable prognostic indicator for DFS and DMFS of BC identified by our patient’s cohort. To our knowledge, it is the first time to demonstrate directly and convincingly that although it was low expressed in BC tissues, KLF11 appeared to be a pro-tumor KLF member and a prognostic risk factor in BC.

Mechanistically GO and KEGG enrichment analysis indicate that KLF11 might regulate BC progression from two aspects. On the one hand, via regulating cells growth of tumor cells, and on the other hand, through regulating components in the BC-TME such as macrophages differentiation or other related immune response via interacting with NRs or involving in the cancer-related signaling pathways. From the KLF11-TAMs perspective, we demonstrated that KLF11 might act as a tumor-dependent transcriptional regulator of TAM polarization via formatting as a transcriptional enhancer with NRs such as *KLF11/PPARG*- or *KLF11/PPARG/THRA*- and involved in the regulation of the transcription of gene program of specific TAM phenotypes. From the KLF11-BC tumor cells perspective, we showed that KLF11 might act as a tumor-dependent transcriptional regulator of the transcription of gene programs of different molecular subtypes and of the gene programs that were related to cell proliferation and cell apoptosis. Importantly, it was experimentally validated that KLF11 did act as a pro-tumor factor of BC progression via promoting cell proliferation and inducing cell apoptosis of BC tumor cells.

Taken the explored effects of KLF11 on BC by this study together, it is the first time to explore the role of KLF11 directly in BC cell lines. More meaningfully, it is the first time introducing KLF11 into the regulation of TAMs polarization and the first time proposing the *KLF11/PPARG*- or *KLF11/PPARG/THRA*-mediated transcriptional enhancers of the gene program of Br-TAMs. However, the speculation of KLF11-TAMs regulation should be verified in future research. To further analyze the transcriptional network of KLF11 involved in the tumor cells, BATM, and BTSM, we prefer a combination of scRNA-seq and spatial transcriptome (ST) to be optimized further applied to the FFEP slides of BC tissue samples.

Finally, based on the observation of its impressive regulation role both in the TAM and tumor cells of BC, we also explored the correlation between the expression of *KLF11* and PD-1, PD-L1, and PD-L2 in BC. A stronger was observed between KLF11 and PD-1 ligands (PD-L1 and PD-L2) compared to that with PD-1. Therefore, we propose that paying attention to the interaction between PD1/PD-L2 might be a solution to treat PD1/PD-L1 resistance or improve low response rates. More importantly, particularly for tumors that show low response rates to immune checkpoints therapies, targeting transcription factors such as KLF11 might be a synergistic or an alternative option for immune checkpoints therapy.

# References


1. Woolston, C., *Breast cancer.* Nature, 2015. **527**(7578): p. S101.
2. Harbeck, N. and M. Gnant, *Breast cancer.* Lancet, 2017. **389**(10074): p. 1134-1150.
3. Waks, A.G. and E.P. Winer, *Breast Cancer Treatment: A Review.* JAMA, 2019. **321**(3): p. 288-300.
4. Torre, L.A., et al., *Global Cancer in Women: Burden and Trends.* Cancer Epidemiol Biomarkers Prev, 2017. **26**(4): p. 444-457.
5. Perou, C.M., et al., *Molecular portraits of human breast tumours.* Nature, 2000. **406**(6797): p. 747-52.
6. Sorlie, T., et al., *Gene expression patterns of breast carcinomas distinguish tumor subclasses with clinical implications.* Proc Natl Acad Sci U S A, 2001. **98**(19): p. 10869-74.
7. Hu, Z., et al., *The molecular portraits of breast tumors are conserved across microarray platforms.* BMC Genomics, 2006. **7**: p. 96.
8. Coates, A.S., et al., *Tailoring therapies--improving the management of early breast cancer: St Gallen International Expert Consensus on the Primary Therapy of Early Breast Cancer 2015.* Ann Oncol, 2015. **26**(8): p. 1533-46.
9. Goldhirsch, A., et al., *Strategies for subtypes--dealing with the diversity of breast cancer: highlights of the St. Gallen International Expert Consensus on the Primary Therapy of Early Breast Cancer 2011.* Ann Oncol, 2011. **22**(8): p. 1736-47.
10. Muftah, A.A., et al., *Ki67 expression in invasive breast cancer: the use of tissue microarrays compared with whole tissue sections.* Breast Cancer Res Treat, 2017. **164**(2): p. 341-348.
11. Turner, N.C., et al., *Advances in the treatment of advanced oestrogen-receptor-positive breast cancer.* Lancet, 2017. **389**(10087): p. 2403-2414.
12. The, L., *Breast cancer targeted therapy: successes and challenges.* Lancet, 2017. **389**(10087): p. 2350.
13. Harvey, J.M., et al., *Estrogen receptor status by immunohistochemistry is superior to the ligand-binding assay for predicting response to adjuvant endocrine therapy in breast cancer.* J Clin Oncol, 1999. **17**(5): p. 1474-81.
14. Higgins, M.J. and J. Baselga, *Targeted therapies for breast cancer.* J Clin Invest, 2011. **121**(10): p. 3797-803.
15. Osborne, C.K. and R. Schiff, *Mechanisms of endocrine resistance in breast cancer.* Annu Rev Med, 2011. **62**: p. 233-47.
16. Cardoso, F., et al., *Clinical application of the 70-gene profile: the MINDACT trial.* J Clin Oncol, 2008. **26**(5): p. 729-35.
17. Sparano, J.A. and S. Paik, *Development of the 21-gene assay and its application in clinical practice and clinical trials.* J Clin Oncol, 2008. **26**(5): p. 721-8.
18. June, C.H. and M. Sadelain, *Chimeric Antigen Receptor Therapy.* N Engl J Med, 2018. **379**(1): p. 64-73.
19. Bagley, S.J. and D.M. O'Rourke, *Clinical investigation of CAR T cells for solid tumors: Lessons learned and future directions.* Pharmacol Ther, 2020. **205**: p. 107419.
20. Moon, E.K., et al., *Multifactorial T-cell hypofunction that is reversible can limit the efficacy of chimeric antigen receptor-transduced human T cells in solid tumors.* Clin Cancer Res, 2014. **20**(16): p. 4262-73.
21. Wang, H., et al., *Immune checkpoint blockade and CAR-T cell therapy in hematologic malignancies.* J Hematol Oncol, 2019. **12**(1): p. 59.

22. Lorenzo-Sanz, L. and P. Munoz, *Tumor-Infiltrating Immunosuppressive Cells in Cancer-Cell Plasticity, Tumor Progression and Therapy Response.* Cancer Microenviron, 2019. **12**(2-3): p. 119-132.

23. Constantinidou, A., C. Alifieris, and D.T. Trafalis, *Targeting Programmed Cell Death -1 (PD-1) and Ligand (PD-L1): A new era in cancer active immunotherapy.* Pharmacol Ther, 2019. **194**: p. 84-106.

24. Gide, T.N., et al., *Primary and Acquired Resistance to Immune Checkpoint Inhibitors in Metastatic Melanoma.* Clin Cancer Res, 2018. **24**(6): p. 1260-1270.

25. Kim, J.M. and D.S. Chen, *Immune escape to PD-L1/PD-1 blockade: seven steps to success (or failure).* Ann Oncol, 2016. **27**(8): p. 1492-504.

26. Pitt, J.M., et al., *Resistance Mechanisms to Immune-Checkpoint Blockade in Cancer: Tumor-Intrinsic and -Extrinsic Factors.* Immunity, 2016. **44**(6): p. 1255-69.

27. McAllister, S.S. and R.A. Weinberg, *Tumor-host interactions: a far-reaching relationship.* J Clin Oncol, 2010. **28**(26): p. 4022-8.

28. Mills, C.D., et al., *M-1/M-2 macrophages and the Th1/Th2 paradigm.* J Immunol, 2000. **164**(12): p. 6166-73.

29. Biswas, S.K. and A. Mantovani, *Macrophage plasticity and interaction with lymphocyte subsets: cancer as a paradigm.* Nat Immunol, 2010. **11**(10): p. 889-96.

30. Weigert, A., et al., *mPGES-1 and ALOX5/-15 in tumor-associated macrophages.* Cancer Metastasis Rev, 2018. **37**(2-3): p. 317-334.

31. Cassetta, L., et al., *Human Tumor-Associated Macrophage and Monocyte Transcriptional Landscapes Reveal Cancer-Specific Reprogramming, Biomarkers, and Therapeutic Targets.* Cancer Cell, 2019. **35**(4): p. 588-602 e10.

32. Ostuni, R., et al., *Macrophages and cancer: from mechanisms to therapeutic implications.* Trends Immunol, 2015. **36**(4): p. 229-39.

33. Elliott, L.A., et al., *Human Tumor-Infiltrating Myeloid Cells: Phenotypic and Functional Diversity.* Front Immunol, 2017. **8**: p. 86.

34. Yang, M., et al., *Diverse Functions of Macrophages in Different Tumor Microenvironments.* Cancer Res, 2018. **78**(19): p. 5492-5503.

35. Ginhoux, F., et al., *New insights into the multidimensional concept of macrophage ontogeny, activation and function.* Nat Immunol, 2016. **17**(1): p. 34-40.

36. Huang, X., et al., *Induced CD10 expression during monocyte-to-macrophage differentiation identifies a unique subset of macrophages in pancreatic ductal adenocarcinoma.* Biochem Biophys Res Commun, 2020. **524**(4): p. 1064-1071.

37. Wu, H., et al., *Tumour-associated macrophages mediate the invasion and metastasis of bladder cancer cells through CXCL8.* PeerJ, 2020. **8**: p. e8721.

38. El-Arabey, A.A., et al., *GATA3 as a master regulator for interactions of tumor-associated macrophages with high-grade serous ovarian carcinoma.* Cell Signal, 2020. **68**: p. 109539.

39. Edin, S., et al., *Macrophages: Good guys in colorectal cancer.* Oncoimmunology, 2013. **2**(2): p. e23038.

40. Feng, P.H., et al., *Tumor-associated macrophages in stage IIIA pN2 non-small cell lung cancer after neoadjuvant chemotherapy and surgery.* Am J Transl Res, 2014. **6**(5): p. 593-603.

41. Dai, F., et al., *The number and microlocalization of tumor-associated immune cells are associated with patient's survival time in non-small cell lung cancer.* BMC Cancer, 2010. **10**: p. 220.

42. Park, J.Y., et al., *Polarized CD163+ tumor-associated macrophages are associated with increased angiogenesis and CXCL12 expression in gastric cancer.* Clin Res Hepatol Gastroenterol, 2016. **40**(3): p. 357-365.

43. Hu, J.M., et al., *The increased number of tumor-associated macrophage is associated with overexpression of VEGF-C, plays an important role in Kazakh ESCC invasion and metastasis.* Exp Mol Pathol, 2017. **102**(1): p. 15-21.

44. Jensen, T.O., et al., *Macrophage markers in serum and tumor have prognostic impact in American Joint Committee on Cancer stage I/II melanoma.* J Clin Oncol, 2009. **27**(20): p. 3330-7.

45. Leek, R.D. and A.L. Harris, *Tumor-associated macrophages in breast cancer.* J Mammary Gland Biol Neoplasia, 2002. **7**(2): p. 177-89.

46. Clynes, R.A., et al., *Inhibitory Fc receptors modulate in vivo cytotoxicity against tumor targets.* Nat Med, 2000. **6**(4): p. 443-6.

47. Lin, L., et al., *Breast adipose tissue macrophages (BATMs) have a stronger correlation with breast cancer survival than breast tumor stroma macrophages (BTSMs).* Breast Cancer Res, 2021. **23**(1): p. 45.

48. Qian, B.Z. and J.W. Pollard, *Macrophage diversity enhances tumor progression and metastasis.* Cell, 2010. **141**(1): p. 39-51.

49. Noy, R. and J.W. Pollard, *Tumor-associated macrophages: from mechanisms to therapy.* Immunity, 2014. **41**(1): p. 49-61.

50. Tao, S., et al., *The role of macrophages during breast cancer development and response to chemotherapy.* Clin Transl Oncol, 2020.

51. Cassetta, L. and J.W. Pollard, *Targeting macrophages: therapeutic approaches in cancer.* Nat Rev Drug Discov, 2018. **17**(12): p. 887-904.

52. Lin, E.Y., et al., *Progression to malignancy in the polyoma middle T oncoprotein mouse breast cancer model provides a reliable model for human diseases.* Am J Pathol, 2003. **163**(5): p. 2113-26.

53. Lin, E.Y., et al., *Macrophages regulate the angiogenic switch in a mouse model of breast cancer.* Cancer Res, 2006. **66**(23): p. 11238-46.

54. Mor, G., et al., *Macrophages, estrogen and the microenvironment of breast cancer.* J Steroid Biochem Mol Biol, 1998. **67**(5-6): p. 403-11.

55. Ch'ng, E.S., S.E. Tuan Sharif, and H. Jaafar, *In human invasive breast ductal carcinoma, tumor stromal macrophages and tumor nest macrophages have distinct relationships with clinicopathological parameters and tumor angiogenesis.* Virchows Arch, 2013. **462**(3): p. 257-67.

56. Leek, R.D., et al., *Necrosis correlates with high vascular density and focal macrophage infiltration in invasive carcinoma of the breast.* Br J Cancer, 1999. **79**(5-6): p. 991-5.

57. Lewis, J.S., et al., *Expression of vascular endothelial growth factor by macrophages is up-regulated in poorly vascularized areas of breast carcinomas.* J Pathol, 2000. **192**(2): p. 150-8.

58. Sousa, S., et al., *Human breast cancer cells educate macrophages toward the M2 activation status.* Breast Cancer Res, 2015. **17**: p. 101.

59. Klingen, T.A., et al., *Tumor-associated macrophages are strongly related to vascular invasion, non-luminal subtypes, and interval breast cancer.* Hum Pathol, 2017. **69**: p. 72-80.

60. Lee, A.H., et al., *Angiogenesis and inflammation in invasive carcinoma of the breast.* J Clin Pathol, 1997. **50**(8): p. 669-73.

61. Steele, R.J., et al., *Oestrogen receptor concentration and macrophage infiltration in human breast cancer.* Eur J Surg Oncol, 1986. **12**(3): p. 273-6.

62. Medrek, C., et al., *The presence of tumor associated macrophages in tumor stroma as a prognostic marker for breast cancer patients.* BMC Cancer, 2012. **12**: p. 306.

63. Yu, T. and G. Di, *Role of tumor microenvironment in triple-negative breast cancer and its prognostic significance.* Chin J Cancer Res, 2017. **29**(3): p. 237-252.

64. Leek, R.D., et al., *Association of macrophage infiltration with angiogenesis and prognosis in invasive breast carcinoma.* Cancer Res, 1996. **56**(20): p. 4625-9.

65. Shabo, I., et al., *Breast cancer expression of CD163, a macrophage scavenger receptor, is related to early distant recurrence and reduced patient survival.* Int J Cancer, 2008. **123**(4): p. 780-6.

66. Ding, J., et al., *Tumor associated macrophage x cancer cell hybrids may acquire cancer stem cell properties in breast cancer.* PLoS One, 2012. **7**(7): p. e41942.

67. Zhu, Z., et al., *Yin-yang effect of tumour cells in breast cancer: from mechanism of crosstalk between tumour-associated macrophages and cancer-associated adipocytes.* Am J Cancer Res, 2020. **10**(2): p. 383-392.

68. Robinson, B.D., et al., *Tumor microenvironment of metastasis in human breast carcinoma: a potential prognostic marker linked to hematogenous dissemination.* Clin Cancer Res, 2009. **15**(7): p. 2433-41.

69. Rohan, T.E., et al., *Tumor microenvironment of metastasis and risk of distant metastasis of breast cancer.* J Natl Cancer Inst, 2014. **106**(8).

70. Yang, J., et al., *The role of tumor-associated macrophages in breast carcinoma invasion and metastasis.* Int J Clin Exp Pathol, 2015. **8**(6): p. 6656-64.

71. Jaitin, D.A., et al., *Lipid-Associated Macrophages Control Metabolic Homeostasis in a Trem2-Dependent Manner.* Cell, 2019. **178**(3): p. 686-698 e14.

72. Wu, S.Z., et al., *A single-cell and spatially resolved atlas of human breast cancers.* Nat Genet, 2021. **53**(9): p. 1334-1347.

73. Bandura, D.R., et al., *Mass cytometry: technique for real time single cell multitarget immunoassay based on inductively coupled plasma time-of-flight mass spectrometry.* Anal Chem, 2009. **81**(16): p. 6813-22.

74. Bendall, S.C., et al., *Single-cell mass cytometry of differential immune and drug responses across a human hematopoietic continuum.* Science, 2011. **332**(6030): p. 687-96.

75. Wagner, J., et al., *A Single-Cell Atlas of the Tumor and Immune Ecosystem of Human Breast Cancer.* Cell, 2019. **177**(5): p. 1330-1345 e18.

76. Quail, D.F. and J.A. Joyce, *Microenvironmental regulation of tumor progression and metastasis.* Nat Med, 2013. **19**(11): p. 1423-37.

77. Jahchan, N.S., et al., *Tuning the Tumor Myeloid Microenvironment to Fight Cancer.* Front Immunol, 2019. **10**: p. 1611.

78. DeNardo, D.G. and B. Ruffell, *Macrophages as regulators of tumour immunity and immunotherapy.* Nat Rev Immunol, 2019. **19**(6): p. 369-382.

79. Martinez, F.O., et al., *Transcriptional profiling of the human monocyte-to-macrophage differentiation and polarization: new molecules and patterns of gene expression.* J Immunol, 2006. **177**(10): p. 7303-11.

80. Aharinejad, S., et al., *Colony-stimulating factor-1 blockade by antisense oligonucleotides and small interfering RNAs suppresses growth of human mammary tumor xenografts in mice.* Cancer Res, 2004. **64**(15): p. 5378-84.

81. Paulus, P., et al., *Colony-stimulating factor-1 antibody reverses chemoresistance in human MCF-7 breast cancer xenografts.* Cancer Res, 2006. **66**(8): p. 4349-56.

82. Anderson, N.R., et al., *Macrophage-Based Approaches for Cancer Immunotherapy.* Cancer Res, 2021. **81**(5): p. 1201-1208.

83. Qian, B.Z., et al., *CCL2 recruits inflammatory monocytes to facilitate breast-tumour metastasis.* Nature, 2011. **475**(7355): p. 222-5.

84. Pienta, K.J., et al., *Phase 2 study of carlumab (CNTO 888), a human monoclonal antibody against CC-chemokine ligand 2 (CCL2), in metastatic castration-resistant prostate cancer.* Invest New Drugs, 2013. **31**(3): p. 760-8.

85. Fetterly, G.J., et al., *Utilizing pharmacokinetics/pharmacodynamics modeling to simultaneously examine free CCL2, total CCL2 and carlumab (CNTO 888) concentration time data.* J Clin Pharmacol, 2013. **53**(10): p. 1020-7.

86. Bonapace, L., et al., *Cessation of CCL2 inhibition accelerates breast cancer metastasis by promoting angiogenesis.* Nature, 2014. **515**(7525): p. 130-3.

87. Brubaker, S.W., et al., *Innate immune pattern recognition: a cell biological perspective.* Annu Rev Immunol, 2015. **33**: p. 257-90.

88. Mercalli, A., et al., *Rapamycin unbalances the polarization of human macrophages to M1.* Immunology, 2013. **140**(2): p. 179-90.

89. Feng, Y., et al., *A toll-like receptor agonist mimicking microbial signal to generate tumor-suppressive macrophages.* Nat Commun, 2019. **10**(1): p. 2272.

90. Rodell, C.B., et al., *Development of Adamantane-Conjugated TLR7/8 Agonists for Supramolecular Delivery and Cancer Immunotherapy.* Theranostics, 2019. **9**(26): p. 8426-8436.

91. Adams, S., et al., *Topical TLR7 agonist imiquimod can induce immune-mediated rejection of skin metastases in patients with breast cancer.* Clin Cancer Res, 2012. **18**(24): p. 6748-57.

92. Guerin, M.V., et al., *TGFbeta blocks IFNalpha/beta release and tumor rejection in spontaneous mammary tumors.* Nat Commun, 2019. **10**(1): p. 4131.

93. Zhang, W., et al., *Chimeric antigen receptor macrophage therapy for breast tumours mediated by targeting the tumour extracellular matrix.* Br J Cancer, 2019. **121**(10): p. 837-845.

94. Klichinsky, M., et al., *Human chimeric antigen receptor macrophages for cancer immunotherapy.* Nat Biotechnol, 2020. **38**(8): p. 947-953.

95. Massa, M., et al., *Interaction Between Breast Cancer Cells and Adipose Tissue Cells Derived from Fat Grafting.* Aesthet Surg J, 2016. **36**(3): p. 358-63.

96. Choi, J., Y.J. Cha, and J.S. Koo, *Adipocyte biology in breast cancer: From silent bystander to active facilitator.* Prog Lipid Res, 2018. **69**: p. 11-20.

97. Dirat, B., et al., *Cancer-associated adipocytes exhibit an activated phenotype and contribute to breast cancer invasion.* Cancer Res, 2011. **71**(7): p. 2455-65.

98. Lee, J., J.Y. Imm, and S.H. Lee, *beta-Catenin Mediates Anti-adipogenic and Anticancer Effects of Arctigenin in Preadipocytes and Breast Cancer Cells.* J Agric Food Chem, 2017. **65**(12): p. 2513-2520.

99. Cinti, S., et al., *Adipocyte death defines macrophage localization and function in adipose tissue of obese mice and humans.* J Lipid Res, 2005. **46**(11): p. 2347-55.

100. Iyengar, N.M., et al., *Menopause is a determinant of breast adipose inflammation.* Cancer Prev Res (Phila), 2015. **8**(5): p. 349-58.

101. Subbaramaiah, K., et al., *Obesity is associated with inflammation and elevated aromatase expression in the mouse mammary gland.* Cancer Prev Res (Phila), 2011. **4**(3): p. 329-46.

102. Morris, P.G., et al., *Inflammation and increased aromatase expression occur in the breast tissue of obese women with breast cancer.* Cancer Prev Res (Phila), 2011. **4**(7): p. 1021-9.

103. Sun, X., et al., *Normal breast tissue of obese women is enriched for macrophage markers and macrophage-associated gene expression.* Breast Cancer Res Treat, 2012. **131**(3): p. 1003-12.

104. Berger, N.A., *Crown-like Structures in Breast Adipose Tissue from Normal Weight Women: Important Impact.* Cancer Prev Res (Phila), 2017. **10**(4): p. 223-225.

105. Iyengar, N.M., et al., *Systemic Correlates of White Adipose Tissue Inflammation in Early-Stage Breast Cancer.* Clin Cancer Res, 2016. **22**(9): p. 2283-9.

106. Picon-Ruiz, M., et al., *Obesity and adverse breast cancer risk and outcome: Mechanistic insights and strategies for intervention.* CA Cancer J Clin, 2017. **67**(5): p. 378-397.

107. Cildir, G., S.C. Akincilar, and V. Tergaonkar, *Chronic adipose tissue inflammation: all immune cells on the stage.* Trends Mol Med, 2013. **19**(8): p. 487-500.

108. Weisberg, S.P., et al., *Obesity is associated with macrophage accumulation in adipose tissue.* J Clin Invest, 2003. **112**(12): p. 1796-808.

109. Lumeng, C.N., J.L. Bodzin, and A.R. Saltiel, *Obesity induces a phenotypic switch in adipose tissue macrophage polarization.* J Clin Invest, 2007. **117**(1): p. 175-84.

110. Lumeng, C.N., et al., *Phenotypic switching of adipose tissue macrophages with obesity is generated by spatiotemporal differences in macrophage subtypes.* Diabetes, 2008. **57**(12): p. 3239-46.

111. Castoldi, A., et al., *The Macrophage Switch in Obesity Development.* Front Immunol, 2015. **6**: p. 637.

112. Fujisaka, S., et al., *Regulatory mechanisms for adipose tissue M1 and M2 macrophages in diet-induced obese mice.* Diabetes, 2009. **58**(11): p. 2574-82.

113. Shaul, M.E., et al., *Dynamic, M2-like remodeling phenotypes of CD11c+ adipose tissue macrophages during high-fat diet--induced obesity in mice.* Diabetes, 2010. **59**(5): p. 1171-81.

114. Tiainen, S., et al., *Tumor microenvironment and breast cancer survival: combined effects of breast fat, M2 macrophages and hyaluronan create a dismal prognosis.* Breast Cancer Res Treat, 2020. **179**(3): p. 565-575.

115. Carroll, S.B., *Evo-devo and an expanding evolutionary synthesis: a genetic theory of morphological evolution.* Cell, 2008. **134**(1): p. 25-36.

116. Mattick, J.S., *RNA regulation: a new genetics?* Nat Rev Genet, 2004. **5**(4): p. 316-23.

117. Mann, R.S. and S.B. Carroll, *Molecular mechanisms of selector gene function and evolution.* Curr Opin Genet Dev, 2002. **12**(5): p. 592-600.

118. Lee, T.I. and R.A. Young, *Transcriptional regulation and its misregulation in disease.* Cell, 2013. **152**(6): p. 1237-51.

119. Mangelsdorf, D.J., et al., *The nuclear receptor superfamily: the second decade.* Cell, 1995. **83**(6): p. 835-9.

120. Mackeh, R., et al., *C2H2-Type Zinc Finger Proteins: Evolutionarily Old and New Partners of the Nuclear Hormone Receptors.* Nucl Recept Signal, 2018. **15**: p. 1550762918801071.

121. Sallam, T., et al., *Transcriptional regulation of macrophage cholesterol efflux and atherogenesis by a long noncoding RNA.* Nat Med, 2018. **24**(3): p. 304-312.

122. Calkin, A.C. and P. Tontonoz, *Transcriptional integration of metabolism by the nuclear sterol-activated receptors LXR and FXR.* Nat Rev Mol Cell Biol, 2012. **13**(4): p. 213-24.

123. Potthoff, M.J., S.A. Kliewer, and D.J. Mangelsdorf, *Endocrine fibroblast growth factors 15/19 and 21: from feast to famine.* Genes Dev, 2012. **26**(4): p. 312-24.

124. Claessens, F. and D.T. Gewirth, *DNA recognition by nuclear receptors.* Essays Biochem, 2004. **40**: p. 59-72.

125. Cotnoir-White, D., D. Laperriere, and S. Mader, *Evolution of the repertoire of nuclear receptor binding sites in genomes.* Mol Cell Endocrinol, 2011. **334**(1-2): p. 76-82.

126. Mader, S., et al., *The patterns of binding of RAR, RXR and TR homo- and heterodimers to direct repeats are dictated by the binding specificites of the DNA binding domains.* EMBO J, 1993. **12**(13): p. 5029-41.

127. Bookout, A.L., et al., *Anatomical profiling of nuclear receptor expression reveals a hierarchical transcriptional network.* Cell, 2006. **126**(4): p. 789-99.

128. Wynn, T.A., A. Chawla, and J.W. Pollard, *Macrophage biology in development, homeostasis and disease.* Nature, 2013. **496**(7446): p. 445-55.

129. Murray, P.J. and T.A. Wynn, *Protective and pathogenic functions of macrophage subsets.* Nat Rev Immunol, 2011. **11**(11): p. 723-37.

130. Gordon, S., A. Pluddemann, and F. Martinez Estrada, *Macrophage heterogeneity in tissues: phenotypic diversity and functions.* Immunol Rev, 2014. **262**(1): p. 36-55.

131. Davies, L.C., et al., *Tissue-resident macrophages.* Nat Immunol, 2013. **14**(10): p. 986-95.

132. Murray, P.J., et al., *Macrophage activation and polarization: nomenclature and experimental guidelines.* Immunity, 2014. **41**(1): p. 14-20.

133. Van den Bossche, J., et al., *Macrophage polarization: the epigenetic point of view.* Curr Opin Lipidol, 2014. **25**(5): p. 367-73.

134. Chen, X., et al., *Requirement for the histone deacetylase Hdac3 for the inflammatory gene expression program in macrophages.* Proc Natl Acad Sci U S A, 2012. **109**(42): p. E2865-74.

135. Mullican, S.E., et al., *Histone deacetylase 3 is an epigenomic brake in macrophage alternative activation.* Genes Dev, 2011. **25**(23): p. 2480-8.

136. Sica, A. and A. Mantovani, *Macrophage plasticity and polarization: in vivo veritas.* J Clin Invest, 2012. **122**(3): p. 787-95.

137. O'Shea, J.J., et al., *A new modality for immunosuppression: targeting the JAK/STAT pathway.* Nat Rev Drug Discov, 2004. **3**(7): p. 555-64.

138. Pauleau, A.L., et al., *Enhancer-mediated control of macrophage-specific arginase I expression.* J Immunol, 2004. **172**(12): p. 7565-73.

139. Mantovani, A., et al., *Macrophage polarization: tumor-associated macrophages as a paradigm for polarized M2 mononuclear phagocytes.* Trends Immunol, 2002. **23**(11): p. 549-55.

140. Lang, R., et al., *Shaping gene expression in activated and resting primary macrophages by IL-10.* J Immunol, 2002. **169**(5): p. 2253-63.

141. Gordon, S., *Alternative activation of macrophages.* Nat Rev Immunol, 2003. **3**(1): p. 23-35.

142. Takeda, N., et al., *Differential activation and antagonistic function of HIF-{alpha} isoforms in macrophages are essential for NO homeostasis.* Genes Dev, 2010. **24**(5): p. 491-501.

143. El Kasmi, K.C., et al., *Adventitial fibroblasts induce a distinct proinflammatory/profibrotic macrophage phenotype in pulmonary hypertension.* J Immunol, 2014. **193**(2): p. 597-609.

144. Fleetwood, A.J., et al., *GM-CSF- and M-CSF-dependent macrophage phenotypes display differential dependence on type I interferon signaling.* J Leukoc Biol, 2009. **86**(2): p. 411-21.

145. Krausgruber, T., et al., *IRF5 promotes inflammatory macrophage polarization and TH1-TH17 responses.* Nat Immunol, 2011. **12**(3): p. 231-8.

146. Satoh, T., et al., *The Jmjd3-Irf4 axis regulates M2 macrophage polarization and host responses against helminth infection.* Nat Immunol, 2010. **11**(10): p. 936-44.

147. Bonizzi, G. and M. Karin, *The two NF-kappaB activation pathways and their role in innate and adaptive immunity.* Trends Immunol, 2004. **25**(6): p. 280-8.

148. Porta, C., et al., *Tolerance and M2 (alternative) macrophage polarization are related processes orchestrated by p50 nuclear factor kappaB.* Proc Natl Acad Sci U S A, 2009. **106**(35): p. 14978-83.

149. Lawrence, T. and C. Fong, *The resolution of inflammation: anti-inflammatory roles for NF-kappaB.* Int J Biochem Cell Biol, 2010. **42**(4): p. 519-23.

150. Odegaard, J.I., et al., *Macrophage-specific PPARgamma controls alternative activation and improves insulin resistance.* Nature, 2007. **447**(7148): p. 1116-20.

151. Odegaard, J.I., et al., *Alternative M2 activation of Kupffer cells by PPARdelta ameliorates obesity-induced insulin resistance.* Cell Metab, 2008. **7**(6): p. 496-507.

152. Kang, K., et al., *Adipocyte-derived Th2 cytokines and myeloid PPARdelta regulate macrophage polarization and insulin sensitivity.* Cell Metab, 2008. **7**(6): p. 485-95.

153. Stienstra, R., et al., *Peroxisome proliferator-activated receptor gamma activation promotes infiltration of alternatively activated macrophages into adipose tissue.* J Biol Chem, 2008. **283**(33): p. 22620-7.

154. Szanto, A., et al., *STAT6 transcription factor is a facilitator of the nuclear receptor PPARgamma-regulated gene expression in macrophages and dendritic cells.* Immunity, 2010. **33**(5): p. 699-712.

155. Vats, D., et al., *Oxidative metabolism and PGC-1beta attenuate macrophage-mediated inflammation.* Cell Metab, 2006. **4**(1): p. 13-24.

156. Poh, A.R. and M. Ernst, *Targeting Macrophages in Cancer: From Bench to Bedside.* Front Oncol, 2018. **8**: p. 49.

157. Colegio, O.R., et al., *Functional polarization of tumour-associated macrophages by tumour-derived lactic acid.* Nature, 2014. **513**(7519): p. 559-63.

158. Tripathi, C., et al., *Macrophages are recruited to hypoxic tumor areas and acquire a pro-angiogenic M2-polarized phenotype via hypoxic cancer cell derived cytokines Oncostatin M and Eotaxin.* Oncotarget, 2014. **5**(14): p. 5350-68.

159. Biswas, S.K., et al., *A distinct and unique transcriptional program expressed by tumor-associated macrophages (defective NF-kappaB and enhanced IRF-3/STAT1 activation).* Blood, 2006. **107**(5): p. 2112-22.

160. Saccani, A., et al., *p50 nuclear factor-kappaB overexpression in tumor-associated macrophages inhibits M1 inflammatory responses and antitumor resistance.* Cancer Res, 2006. **66**(23): p. 11432-40.

161. Hagemann, T., et al., *"Re-educating" tumor-associated macrophages by targeting NF-kappaB.* J Exp Med, 2008. **205**(6): p. 1261-8.

162. Aune, G.J., et al., *Von Hippel-Lindau-coupled and transcription-coupled nucleotide excision repair-dependent degradation of RNA polymerase II in response to trabectedin.* Clin Cancer Res, 2008. **14**(20): p. 6449-55.

163. Forni, C., et al., *Trabectedin (ET-743) promotes differentiation in myxoid liposarcoma tumors.* Mol Cancer Ther, 2009. **8**(2): p. 449-57.

164. Soares, D.G., et al., *Replication and homologous recombination repair regulate DNA double-strand break formation by the antitumor alkylator ecteinascidin 743.* Proc Natl Acad Sci U S A, 2007. **104**(32): p. 13062-7.

165. McConnell, B.B. and V.W. Yang, *Mammalian Kruppel-like factors in health and diseases.* Physiol Rev, 2010. **90**(4): p. 1337-81.

166. Kaczynski, J., T. Cook, and R. Urrutia, *Sp1- and Kruppel-like transcription factors.* Genome Biol, 2003. **4**(2): p. 206.

167. Swamynathan, S.K., *Kruppel-like factors: three fingers in control.* Hum Genomics, 2010. **4**(4): p. 263-70.

168. Tetreault, M.P., Y. Yang, and J.P. Katz, *Kruppel-like factors in cancer.* Nat Rev Cancer, 2013. **13**(10): p. 701-13.

169. Cao, Z., et al., *Role of Kruppel-like factors in leukocyte development, function, and disease.* Blood, 2010. **116**(22): p. 4404-14.

170. Wells, J.M. and F.M. Watt, *Diverse mechanisms for endogenous regeneration and repair in mammalian organs.* Nature, 2018. **557**(7705): p. 322-328.

171. Pollak, N.M., et al., *Kruppel-like factors: Crippling and un-crippling metabolic pathways.* JACC Basic Transl Sci, 2018. **3**(1): p. 132-156.

172. Kim, G.D., et al., *Kruppel-like factor 6 and miR-223 signaling axis regulates macrophage-mediated inflammation.* FASEB J, 2019. **33**(10): p. 10902-10915.

173. Coppo, M., et al., *The transcriptional coregulator GRIP1 controls macrophage polarization and metabolic homeostasis.* Nat Commun, 2016. **7**: p. 12254.

174. Oishi, Y. and I. Manabe, *Kruppel-Like Factors in Metabolic Homeostasis and Cardiometabolic Disease.* Front Cardiovasc Med, 2018. **5**: p. 69.

175. Chinenov, Y., et al., *Glucocorticoid receptor coordinates transcription factor-dominated regulatory network in macrophages.* BMC Genomics, 2014. **15**: p. 656.

176. Yang, Y., et al., *p53 mutation alters the effect of the esophageal tumor suppressor KLF5 on keratinocyte proliferation.* Cell Cycle, 2012. **11**(21): p. 4033-9.

177. Rowland, B.D., R. Bernards, and D.S. Peeper, *The KLF4 tumour suppressor is a transcriptional repressor of p53 that acts as a context-dependent oncogene.* Nat Cell Biol, 2005. **7**(11): p. 1074-82.

178. Fernandez-Zapico, M.E., et al., *An mSin3A interaction domain links the transcriptional activity of KLF11 with its role in growth regulation.* EMBO J, 2003. **22**(18): p. 4748-58.

179. Ellenrieder, V., et al., *KLF11 mediates a critical mechanism in TGF-beta signaling that is inactivated by Erk-MAPK in pancreatic cancer cells.* Gastroenterology, 2004. **127**(2): p. 607-20.

180. Yang, Y., et al., *Loss of transcription factor KLF5 in the context of p53 ablation drives invasive progression of human squamous cell cancer.* Cancer Res, 2011. **71**(20): p. 6475-84.

181. Knoedler, J.R. and R.J. Denver, *Kruppel-like factors are effectors of nuclear receptor signaling.* Gen Comp Endocrinol, 2014. **203**: p. 49-59.

182. Iuchi, S., *Three classes of C2H2 zinc finger proteins.* Cell Mol Life Sci, 2001. **58**(4): p. 625-35.

183. Feinberg, M.W., et al., *Kruppel-like factor 4 is a mediator of proinflammatory signaling in macrophages.* J Biol Chem, 2005. **280**(46): p. 38247-58.

184. Liao, X., et al., *Kruppel-like factor 4 regulates macrophage polarization.* J Clin Invest, 2011. **121**(7): p. 2736-49.

185. Li, Z., et al., *Kruppel-Like Factor 4 Regulation of Cholesterol-25-Hydroxylase and Liver X Receptor Mitigates Atherosclerosis Susceptibility.* Circulation, 2017. **136**(14): p. 1315-1330.

186. Mahabeleshwar, G.H., et al., *The myeloid transcription factor KLF2 regulates the host response to polymicrobial infection and endotoxic shock.* Immunity, 2011. **34**(5): p. 715-28.

187. Date, D., et al., *Kruppel-like transcription factor 6 regulates inflammatory macrophage polarization.* J Biol Chem, 2014. **289**(15): p. 10318-10329.

188. Zhang, Y., et al., *Kruppel-like factor 6 is a co-activator of NF-kappaB that mediates p65-dependent transcription of selected downstream genes.* J Biol Chem, 2014. **289**(18): p. 12876-85.

189. Kim, G.D., et al., *Kruppel-like Factor 6 Promotes Macrophage-mediated Inflammation by Suppressing B Cell Leukemia/Lymphoma 6 Expression.* J Biol Chem, 2016. **291**(40): p. 21271-21282.

190. Bureau, C., et al., *Expression and Function of Kruppel Like-Factors (KLF) in Carcinogenesis.* Curr Genomics, 2009. **10**(5): p. 353-60.

191. Zhang, J., et al., *Kruppel-like factors in breast cancer: Function, regulation and clinical relevance.* Biomed Pharmacother, 2019. **123**: p. 109778.

192. Foster, K.W., et al., *Increase of GKLF messenger RNA and protein expression during progression of breast cancer.* Cancer Res, 2000. **60**(22): p. 6488-95.

193. Hu, D., et al., *Novel insight into KLF4 proteolytic regulation in estrogen receptor signaling and breast carcinogenesis.* J Biol Chem, 2012. **287**(17): p. 13584-97.

194. Farrugia, M.K., et al., *Regulation of anti-apoptotic signaling by Kruppel-like factors 4 and 5 mediates lapatinib resistance in breast cancer.* Cell Death Dis, 2015. **6**: p. e1699.

195. Pandya, A.Y., et al., *Nuclear localization of KLF4 is associated with an aggressive phenotype in early-stage breast cancer.* Clin Cancer Res, 2004. **10**(8): p. 2709-19.

196. Song, X., et al., *Expression of Kruppel-like factor 4 in breast cancer tissues and its effects on the proliferation of breast cancer MDA-MB-231 cells.* Exp Ther Med, 2017. **13**(5): p. 2463-2467.

197. Wang, B., et al., *Kruppel-like factor 4 induces apoptosis and inhibits tumorigenic progression in SK-BR-3 breast cancer cells.* FEBS Open Bio, 2015. **5**: p. 147-54.

198. Akaogi, K., et al., *KLF4 suppresses estrogen-dependent breast cancer growth by inhibiting the transcriptional activity of ERalpha.* Oncogene, 2009. **28**(32): p. 2894-902.

199. Jia, Y., et al., *KLF4 overcomes tamoxifen resistance by suppressing MAPK signaling pathway and predicts good prognosis in breast cancer.* Cell Signal, 2018. **42**: p. 165-175.

200. Nagata, T., et al., *KLF4 and NANOG are prognostic biomarkers for triple-negative breast cancer.* Breast Cancer, 2017. **24**(2): p. 326-335.

201. Tong, D., et al., *Expression of KLF5 is a prognostic factor for disease-free survival and overall survival in patients with breast cancer.* Clin Cancer Res, 2006. **12**(8): p. 2442-8.

202. Takagi, K., et al., *Kruppel-like factor 5 in human breast carcinoma: a potent prognostic factor induced by androgens.* Endocr Relat Cancer, 2012. **19**(6): p. 741-50.

203. Hatami, R., et al., *KLF6-SV1 drives breast cancer metastasis and is associated with poor survival.* Sci Transl Med, 2013. **5**(169): p. 169ra12.

204. Wang, X., et al., *KLF8 promotes human breast cancer cell invasion and metastasis by transcriptional activation of MMP9.* Oncogene, 2011. **30**(16): p. 1901-11.

205. Wang, X., et al., *Kruppel-like factor 8 induces epithelial to mesenchymal transition and epithelial cell invasion.* Cancer Res, 2007. **67**(15): p. 7184-93.

206. Ali, A., et al., *KLF17 attenuates estrogen receptor alpha-mediated signaling by impeding ERalpha function on chromatin and determines response to endocrine therapy.* Biochim Biophys Acta, 2016. **1859**(7): p. 883-95.

207. Zhang, W., et al., *Kruppel-like factor 2 suppresses mammary carcinoma growth by regulating retinoic acid signaling.* Oncotarget, 2015. **6**(34): p. 35830-42.

208. Limame, R., et al., *Expression profiling of migrated and invaded breast cancer cells predicts early metastatic relapse and reveals Kruppel-like factor 9 as a potential suppressor of invasive growth in breast cancer.* Oncoscience, 2014. **1**(1): p. 69-81.

209. Jin, W., et al., *TIEG1 inhibits breast cancer invasion and metastasis by inhibition of epidermal growth factor receptor (EGFR) transcription and the EGFR signaling pathway.* Mol Cell Biol, 2012. **32**(1): p. 50-63.

210. Reinholz, M.M., et al., *Differential gene expression of TGF beta inducible early gene (TIEG), Smad7, Smad2 and Bard1 in normal and malignant breast tissue.* Breast Cancer Res Treat, 2004. **86**(1): p. 75-88.

211. Faryna, M., et al., *Genome-wide methylation screen in low-grade breast cancer identifies novel epigenetically altered genes as potential biomarkers for tumor diagnosis.* FASEB J, 2012. **26**(12): p. 4937-50.

212. Kim, S.H. and S.V. Singh, *Role of Kruppel-like Factor 4-p21(CIP1) Axis in Breast Cancer Stem-like Cell Inhibition by Benzyl Isothiocyanate.* Cancer Prev Res (Phila), 2019. **12**(3): p. 125-134.

213. Yu, F., et al., *Kruppel-like factor 4 (KLF4) is required for maintenance of breast cancer stem cells and for cell migration and invasion.* Oncogene, 2011. **30**(18): p. 2161-72.

214. Yori, J.L., et al., *Kruppel-like factor 4 inhibits epithelial-to-mesenchymal transition through regulation of E-cadherin gene expression.* J Biol Chem, 2010. **285**(22): p. 16854-63.

215. Yori, J.L., et al., *Kruppel-like factor 4 inhibits tumorigenic progression and metastasis in a mouse model of breast cancer.* Neoplasia, 2011. **13**(7): p. 601-10.

216. Ray, A., M. Alalem, and B.K. Ray, *Loss of epigenetic Kruppel-like factor 4 histone deacetylase (KLF-4-HDAC)-mediated transcriptional suppression is crucial in increasing vascular endothelial growth factor (VEGF) expression in breast cancer.* J Biol Chem, 2013. **288**(38): p. 27232-42.

217. Ben-Porath, I., et al., *An embryonic stem cell-like gene expression signature in poorly differentiated aggressive human tumors.* Nat Genet, 2008. **40**(5): p. 499-507.

218. Liu, R., et al., *The induction of KLF5 transcription factor by progesterone contributes to progesterone-induced breast cancer cell proliferation and dedifferentiation.* Mol Endocrinol, 2011. **25**(7): p. 1137-44.

219. Jia, L., et al., *KLF5 promotes breast cancer proliferation, migration and invasion in part by upregulating the transcription of TNFAIP2.* Oncogene, 2016. **35**(16): p. 2040-51.

220. Zhou, W., et al., *miR-217 inhibits triple-negative breast cancer cell growth, migration, and invasion through targeting KLF5.* PLoS One, 2017. **12**(4): p. e0176395.

221. Zhao, D., et al., *TAZ antagonizes the WWP1-mediated KLF5 degradation and promotes breast cell proliferation and tumorigenesis.* Carcinogenesis, 2012. **33**(1): p. 59-67.

222. Jia, X., et al., *KLF5 regulated lncRNA RP1 promotes the growth and metastasis of breast cancer via repressing p27kip1 translation.* Cell Death Dis, 2019. **10**(5): p. 373.

223. Zheng, H.Q., et al., *Kruppel-like factor 5 promotes breast cell proliferation partially through upregulating the transcription of fibroblast growth factor binding protein 1.* Oncogene, 2009. **28**(42): p. 3702-13.

224. Shi, J., et al., *[Roles of KLF5 in inhibition TNFalpha-induced SK-BR-3 breast cancer cell apoptosis].* Zhonghua Yi Xue Za Zhi, 2014. **94**(26): p. 2004-7.

225. Liu, R., et al., *Krupple-like factor 5 is essential for mammary gland development and tumorigenesis.* J Pathol, 2018. **246**(4): p. 497-507.

226. Guo, P., et al., *Estrogen-induced interaction between KLF5 and estrogen receptor (ER) suppresses the function of ER in ER-positive breast cancer cells.* Int J Cancer, 2010. **126**(1): p. 81-9.

227. Ferralli, J., R. Chiquet-Ehrismann, and M. Degen, *KLF4alpha stimulates breast cancer cell proliferation by acting as a KLF4 antagonist.* Oncotarget, 2016. **7**(29): p. 45608-45621.

228. *An oncogenic splice variant drives EMT and metastasis in breast cancer.* Cancer Discov, 2013. **3**(3): p. OF16.

229. Olson, O.C. and J.A. Joyce, *A splicing twist on metastasis.* Sci Transl Med, 2013. **5**(169): p. 169fs2.

230. Wang, X. and J. Zhao, *KLF8 transcription factor participates in oncogenic transformation.* Oncogene, 2007. **26**(3): p. 456-61.

231. Mukherjee, D., et al., *Kruppel-like factor 8 activates the transcription of C-X-C cytokine receptor type 4 to promote breast cancer cell invasion, transendothelial migration and metastasis.* Oncotarget, 2016. **7**(17): p. 23552-68.

232. Li, T., et al., *Identification of epidermal growth factor receptor and its inhibitory microRNA141 as novel targets of Kruppel-like factor 8 in breast cancer.* Oncotarget, 2015. **6**(25): p. 21428-42.

233. Wang, X., et al., *Kruppel-like factor 8 promotes tumorigenic mammary stem cell induction by targeting miR-146a.* Am J Cancer Res, 2013. **3**(4): p. 356-73.

234. Liu, J., et al., *KLF6 inhibits estrogen receptor-mediated cell growth in breast cancer via a c-Src-mediated pathway.* Mol Cell Biochem, 2010. **335**(1-2): p. 29-35.

235. Bai, X.Y., et al., *Kruppel-like factor 9 down-regulates matrix metalloproteinase 9 transcription and suppresses human breast cancer invasion.* Cancer Lett, 2018. **412**: p. 224-235.

236. Hsu, C.F., et al., *Klf10 induces cell apoptosis through modulation of BI-1 expression and Ca2+ homeostasis in estrogen-responding adenocarcinoma cells.* Int J Biochem Cell Biol, 2011. **43**(4): p. 666-73.

237. Gumireddy, K., et al., *KLF17 is a negative regulator of epithelial-mesenchymal transition and metastasis in breast cancer.* Nat Cell Biol, 2009. **11**(11): p. 1297-304.

238. Han, M., et al., *microRNA-30d mediated breast cancer invasion, migration, and EMT by targeting KLF11 and activating STAT3 pathway.* J Cell Biochem, 2018. **119**(10): p. 8138-8145.

239. Guan, B., et al., *MicroRNA-205 directly targets Kruppel-like factor 12 and is involved in invasion and apoptosis in basal-like breast carcinoma.* Int J Oncol, 2016. **49**(2): p. 720-34.

240. Dong, M.J., et al., *The transcription factor KLF4 as an independent predictive marker for pathologic complete remission in breast cancer neoadjuvant chemotherapy: a case-control study.* Onco Targets Ther, 2014. **7**: p. 1963-9.

241. Li, Z., et al., *Dexamethasone induces docetaxel and cisplatin resistance partially through up-regulating Kruppel-like factor 5 in triple-negative breast cancer.* Oncotarget, 2017. **8**(7): p. 11555-11565.

242. Liu, R., et al., *Mifepristone Suppresses Basal Triple-Negative Breast Cancer Stem Cells by Down-regulating KLF5 Expression.* Theranostics, 2016. **6**(4): p. 533-44.

243. Lin, Y., et al., *Discovery of novel mifepristone derivatives via suppressing KLF5 expression for the treatment of triple-negative breast cancer.* Eur J Med Chem, 2018. **146**: p. 354-367.

244. Liu, R., et al., *Mithramycin A suppresses basal triple-negative breast cancer cell survival partially via down-regulating Kruppel-like factor 5 transcription by Sp1.* Sci Rep, 2018. **8**(1): p. 1138.

245. Ebert, R., et al., *Kruppel-like factors KLF2 and 6 and Ki-67 are direct targets of zoledronic acid in MCF-7 cells.* Bone, 2012. **50**(3): p. 723-32.

246. Ebert, R., et al., *Probenecid as a sensitizer of bisphosphonate-mediated effects in breast cancer cells.* Mol Cancer, 2014. **13**: p. 265.

247. Ismail, I.A., G.H. El-Sokkary, and S.H. Saber, *Low doses of Paclitaxel repress breast cancer invasion through DJ-1/KLF17 signalling pathway.* Clin Exp Pharmacol Physiol, 2018.

248. El-Sokkary, G.H., I.A. Ismail, and S.H. Saber, *Melatonin inhibits breast cancer cell invasion through modulating DJ-1/KLF17/ID-1 signaling pathway.* J Cell Biochem, 2019. **120**(3): p. 3945-3957.

249. Cook, T., et al., *Molecular cloning and characterization of TIEG2 reveals a new subfamily of transforming growth factor-beta-inducible Sp1-like zinc finger-encoding genes involved in the regulation of cell growth.* J Biol Chem, 1998. **273**(40): p. 25929-36.

250. Rakhshandehroo, M., et al., *Comparative analysis of gene regulation by the transcription factor PPARalpha between mouse and human.* PLoS One, 2009. **4**(8): p. e6796.

251. Yin, P., et al., *Transcription factor KLF11 integrates progesterone receptor signaling and proliferation in uterine leiomyoma cells.* Cancer Res, 2010. **70**(4): p. 1722-30.

252. Fan, Y., et al., *Kruppel-like factor-11, a transcription factor involved in diabetes mellitus, suppresses endothelial cell activation via the nuclear factor-kappaB signaling pathway.* Arterioscler Thromb Vasc Biol, 2012. **32**(12): p. 2981-8.

253. Zhang, J.S., et al., *A conserved alpha-helical motif mediates the interaction of Sp1-like transcriptional repressors with the corepressor mSin3A.* Mol Cell Biol, 2001. **21**(15): p. 5041-9.

254. Lomberk, G., et al., *Sequence-specific recruitment of heterochromatin protein 1 via interaction with Kruppel-like factor 11, a human transcription factor involved in tumor suppression and metabolic diseases.* J Biol Chem, 2012. **287**(16): p. 13026-39.

255. Fernandez-Zapico, M.E., et al., *MODY7 gene, KLF11, is a novel p300-dependent regulator of Pdx-1 (MODY4) transcription in pancreatic islet beta cells.* J Biol Chem, 2009. **284**(52): p. 36482-90.

256. Seo, S., et al., *Kruppel-like factor 11 differentially couples to histone acetyltransferase and histone methyltransferase chromatin remodeling pathways to transcriptionally*

*regulate dopamine D2 receptor in neuronal cells.* J Biol Chem, 2012. **287**(16): p. 12723-35.

257. Lomberk, G., et al., *Kruppel-like factor 11 regulates the expression of metabolic genes via an evolutionarily conserved protein interaction domain functionally disrupted in maturity onset diabetes of the young.* J Biol Chem, 2013. **288**(24): p. 17745-58.

258. Wang, Z., et al., *Human TIEG2/KLF11 induces oligodendroglial cell death by downregulation of Bcl-XL expression.* J Neural Transm (Vienna), 2007. **114**(7): p. 867-75.

259. Gohla, G., K. Krieglstein, and B. Spittau, *Tieg3/Klf11 induces apoptosis in OLI-neu cells and enhances the TGF-beta signaling pathway by transcriptional repression of Smad7.* J Cell Biochem, 2008. **104**(3): p. 850-61.

260. Buck, A., et al., *The tumor suppressor KLF11 mediates a novel mechanism in transforming growth factor beta-induced growth inhibition that is inactivated in pancreatic cancer.* Mol Cancer Res, 2006. **4**(11): p. 861-72.

261. Fernandez-Zapico, M.E., et al., *A functional family-wide screening of SP/KLF proteins identifies a subset of suppressors of KRAS-mediated cell growth.* Biochem J, 2011. **435**(2): p. 529-37.

262. Massague, J., S.W. Blain, and R.S. Lo, *TGFbeta signaling in growth control, cancer, and heritable disorders.* Cell, 2000. **103**(2): p. 295-309.

263. Derynck, R. and Y.E. Zhang, *Smad-dependent and Smad-independent pathways in TGF-beta family signalling.* Nature, 2003. **425**(6958): p. 577-84.

264. Spittau, B. and K. Krieglstein, *Klf10 and Klf11 as mediators of TGF-beta superfamily signaling.* Cell Tissue Res, 2012. **347**(1): p. 65-72.

265. Cook, T., et al., *Three conserved transcriptional repressor domains are a defining feature of the TIEG subfamily of Sp1-like zinc finger proteins.* J Biol Chem, 1999. **274**(41): p. 29500-4.

266. Hayashi, H., et al., *The MAD-related protein Smad7 associates with the TGFbeta receptor and functions as an antagonist of TGFbeta signaling.* Cell, 1997. **89**(7): p. 1165-73.

267. Nakao, A., et al., *Identification of Smad7, a TGFbeta-inducible antagonist of TGF-beta signalling.* Nature, 1997. **389**(6651): p. 631-5.

268. de Caestecker, M.P., E. Piek, and A.B. Roberts, *Role of transforming growth factor-beta signaling in cancer.* J Natl Cancer Inst, 2000. **92**(17): p. 1388-402.

269. Dumont, N. and C.L. Arteaga, *Targeting the TGF beta signaling network in human neoplasia.* Cancer Cell, 2003. **3**(6): p. 531-6.

270. Zhao, G., et al., *KLF11 protects against abdominal aortic aneurysm through inhibition of endothelial cell dysfunction.* JCI Insight, 2021. **6**(5).

271. Karin, M. and F.R. Greten, *NF-kappaB: linking inflammation and immunity to cancer development and progression.* Nat Rev Immunol, 2005. **5**(10): p. 749-59.

272. Buttar, N.S., et al., *Distinct role of Kruppel-like factor 11 in the regulation of prostaglandin E2 biosynthesis.* J Biol Chem, 2010. **285**(15): p. 11433-44.

273. Wang, G., et al., *Promoter DNA methylation is associated with KLF11 expression in epithelial ovarian cancer.* Genes Chromosomes Cancer, 2015. **54**(7): p. 453-62.

274. Viola, L., et al., *Prognostic Role of Kruppel-Like Factors 5, 9, and 11 in Endometrial Endometrioid Cancer.* Pathol Oncol Res, 2020. **26**(4): p. 2265-2272.

275. Ji, Q., et al., *KLF11 promotes gastric cancer invasion and migration by increasing Twist1 expression.* Neoplasma, 2019. **66**(1): p. 92-100.

276. Fu, J., et al., *The TWIST/Mi2/NuRD protein complex and its essential role in cancer metastasis.* Cell Res, 2011. **21**(2): p. 275-89.

277. Hujie, G., et al., *MicroRNA-10b regulates epithelial-mesenchymal transition by modulating KLF4/KLF11/Smads in hepatocellular carcinoma.* Cancer Cell Int, 2018. **18**: p. 10.

278. Wang, Y., et al., *Genome-wide CRISPR-Cas9 screen identified KLF11 as a druggable suppressor for sarcoma cancer stem cells.* Sci Adv, 2021. **7**(5).

279. Son, B., et al., *Radiotherapy in combination with hyperthermia suppresses lung cancer progression via increased NR4A3 and KLF11 expression.* Int J Radiat Biol, 2019. **95**(12): p. 1696-1707.

280. Lin, L., et al., *The Distinct Roles of Transcriptional Factor KLF11 in Normal Cell Growth Regulation and Cancer as a Mediator of TGF-beta Signaling Pathway.* Int J Mol Sci, 2020. **21**(8).

281. Potapova, A., et al., *Epigenetic inactivation of tumour suppressor gene KLF11 in myelodysplastic syndromes*.* Eur J Haematol, 2010. **84**(4): p. 298-303.

282. Semmlinger, A., et al., *EP3 (prostaglandin E2 receptor 3) expression is a prognostic factor for progression-free and overall survival in sporadic breast cancer.* BMC Cancer, 2018. **18**(1): p. 431.

283. Cao, X., et al., *Macrophage polarization in the maculae of age-related macular degeneration: a pilot study.* Pathol Int, 2011. **61**(9): p. 528-35.

284. Kawamura, K., et al., *Detection of M2 macrophages and colony-stimulating factor 1 expression in serous and mucinous ovarian epithelial tumors.* Pathol Int, 2009. **59**(5): p. 300-5.

285. Cho, K.Y., et al., *The phenotype of infiltrating macrophages influences arteriosclerotic plaque vulnerability in the carotid artery.* J Stroke Cerebrovasc Dis, 2013. **22**(7): p. 910-8.

286. Unal, I., *Defining an Optimal Cut-Point Value in ROC Analysis: An Alternative Approach.* Comput Math Methods Med, 2017. **2017**: p. 3762651.

287. Remmele, W. and H.E. Stegner, *[Recommendation for uniform definition of an immunoreactive score (IRS) for immunohistochemical estrogen receptor detection (ER-ICA) in breast cancer tissue].* Pathologe, 1987. **8**(3): p. 138-40.

288. Li, T., et al., *TIMER: A Web Server for Comprehensive Analysis of Tumor-Infiltrating Immune Cells.* Cancer Res, 2017. **77**(21): p. e108-e110.

289. Yoshihara, K., et al., *Inferring tumour purity and stromal and immune cell admixture from expression data.* Nat Commun, 2013. **4**: p. 2612.

290. Ru, B., et al., *TISIDB: an integrated repository portal for tumor-immune system interactions.* Bioinformatics, 2019.

291. Lanczky, A. and B. Gyorffy, *Web-Based Survival Analysis Tool Tailored for Medical Research (KMplot): Development and Implementation.* J Med Internet Res, 2021. **23**(7): p. e27633.

292. Gyorffy, B., *Survival analysis across the entire transcriptome identifies biomarkers with the highest prognostic power in breast cancer.* Comput Struct Biotechnol J, 2021. **19**: p. 4101-4109.

293. Szklarczyk, D., et al., *STRING v11: protein-protein association networks with increased coverage, supporting functional discovery in genome-wide experimental datasets.* Nucleic Acids Res, 2019. **47**(D1): p. D607-D613.

294. Zhang, X., et al., *CellMarker: a manually curated resource of cell markers in human and mouse.* Nucleic Acids Res, 2019. **47**(D1): p. D721-D728.

295. Tang, Z., et al., *GEPIA2: an enhanced web server for large-scale expression profiling and interactive analysis.* Nucleic Acids Res, 2019. **47**(W1): p. W556-W560.

296. Smyth, G.K., J. Michaud, and H.S. Scott, *Use of within-array replicate spots for assessing differential expression in microarray experiments.* Bioinformatics, 2005. **21**(9): p. 2067-75.

297. Liu, J., et al., *An Integrated TCGA Pan-Cancer Clinical Data Resource to Drive High-Quality Survival Outcome Analytics.* Cell, 2018. **173**(2): p. 400-416 e11.

298. Yu, G., et al., *clusterProfiler: an R package for comparing biological themes among gene clusters*, in *OMICS*. 2012. p. 284-7.

299. Wolbers, M., et al., *Prognostic models with competing risks: methods and application to coronary risk prediction.* Epidemiology, 2009. **20**(4): p. 555-61.

300. Muller, K., et al., *Prognostic relevance of RIP140 and ERbeta expression in unifocal versus multifocal breast cancers: a preliminary report.* Int J Mol Sci, 2019. **20**(2).

301. Yamagata, S., et al., *Progression of Hypopituitarism and Hypothyroidism after Treatment with Pembrolizumab in a Patient with Adrenal Metastasis from Non-small-cell Lung Cancer.* Intern Med, 2019. **58**(24): p. 3557-3562.

302. Hester, A., et al., *EP3 receptor antagonist L798,106 reduces proliferation and migration of SK-BR-3 breast cancer cells.* Onco Targets Ther, 2019. **12**: p. 6053-6068.

303. Liu, X.S. *TIMER: Tumor IMmune Estimation Resource*. 2017 [cited 2021; Available from: https://cistrome.shinyapps.io/timer/.

304. Zhao, Y., et al., *Paranasal Sinus Invasion Should Be Classified as T4 Disease in Advanced Nasopharyngeal Carcinoma Patients Receiving Radiotherapy.* Front Oncol, 2020. **10**: p. 01465.

305. Li, T., et al., *TIMER2.0 for analysis of tumor-infiltrating immune cells.* Nucleic Acids Res, 2020. **48**(W1): p. W509-W514.

306. Heublein, S., et al., *Vitamin D receptor, Retinoid X receptor and peroxisome proliferator-activated receptor gamma are overexpressed in BRCA1 mutated breast cancer and predict prognosis.* J Exp Clin Cancer Res, 2017. **36**(1): p. 57.

307. Shao, W., et al., *Cytoplasmic PPARgamma is a marker of poor prognosis in patients with Cox-1 negative primary breast cancers.* J Transl Med, 2020. **18**(1): p. 94.

308. Zati Zehni, A., et al., *Hormone Receptor Expression in Multicentric/Multifocal versus Unifocal Breast Cancer: Especially the VDR Determines the Outcome Related to Focality.* Int J Mol Sci, 2019. **20**(22).

309. Shao, W., et al., *Cytoplasmic and Nuclear Forms of Thyroid Hormone Receptor beta1 Are Inversely Associated with Survival in Primary Breast Cancer.* Int J Mol Sci, 2020. **21**(1).

310. Berger, L., et al., *Expression of H3K4me3 and H3K9ac in breast cancer.* J Cancer Res Clin Oncol, 2020. **146**(8): p. 2017-2027.

311. Gobeil, F., Jr., et al., *Nuclear prostaglandin signaling system: biogenesis and actions via heptahelical receptors.* Can J Physiol Pharmacol, 2003. **81**(2): p. 196-204.

312. Schoonjans, K., B. Staels, and J. Auwerx, *Role of the peroxisome proliferator-activated receptor (PPAR) in mediating the effects of fibrates and fatty acids on gene expression.* J Lipid Res, 1996. **37**(5): p. 907-25.

313. A, I.J., et al., *Polarity and specific sequence requirements of peroxisome proliferator-activated receptor (PPAR)/retinoid X receptor heterodimer binding to DNA. A functional analysis of the malic enzyme gene PPAR response element.* J Biol Chem, 1997. **272**(32): p. 20108-17.

314. Lefterova, M.I., et al., *Cell-specific determinants of peroxisome proliferator-activated receptor gamma function in adipocytes and macrophages.* Mol Cell Biol, 2010. **30**(9): p. 2078-89.

315. Nielsen, R., et al., *Genome-wide profiling of PPARgamma:RXR and RNA polymerase II occupancy reveals temporal activation of distinct metabolic pathways and changes in RXR dimer composition during adipogenesis.* Genes Dev, 2008. **22**(21): p. 2953-67.

316. Chawla, A., et al., *A PPAR gamma-LXR-ABCA1 pathway in macrophages is involved in cholesterol efflux and atherogenesis.* Mol Cell, 2001. **7**(1): p. 161-71.

317. Savic, D., et al., *Distinct gene regulatory programs define the inhibitory effects of liver X receptors and PPARG on cancer cell proliferation.* Genome Med, 2016. **8**(1): p. 74.

318. Lefterova, M.I., et al., *PPARgamma and C/EBP factors orchestrate adipocyte biology via adjacent binding on a genome-wide scale.* Genes Dev, 2008. **22**(21): p. 2941-52.

319. Hondares, E., et al., *Thiazolidinediones and rexinoids induce peroxisome proliferator-activated receptor-coactivator (PGC)-1alpha gene transcription: an autoregulatory loop controls PGC-1alpha expression in adipocytes via peroxisome proliferator-activated receptor-gamma coactivation.* Endocrinology, 2006. **147**(6): p. 2829-38.

320. Kajimura, S., et al., *Initiation of myoblast to brown fat switch by a PRDM16-C/EBP-beta transcriptional complex.* Nature, 2009. **460**(7259): p. 1154-8.

321. Seale, P., et al., *PRDM16 controls a brown fat/skeletal muscle switch.* Nature, 2008. **454**(7207): p. 961-7.

322. Koeffler, H.P., *Peroxisome proliferator-activated receptor gamma and cancers.* Clin Cancer Res, 2003. **9**(1): p. 1-9.

323. Ricote, M. and C.K. Glass, *PPARs and molecular mechanisms of transrepression.* Biochim Biophys Acta, 2007. **1771**(8): p. 926-35.

324. Pascual, G., et al., *A SUMOylation-dependent pathway mediates transrepression of inflammatory response genes by PPAR-gamma.* Nature, 2005. **437**(7059): p. 759-63.

325. Loft, A., et al., *Browning of human adipocytes requires KLF11 and reprogramming of PPARgamma superenhancers.* Genes Dev, 2015. **29**(1): p. 7-22.

326. Chung, W., et al., *Single-cell RNA-seq enables comprehensive tumour and immune cell profiling in primary breast cancer.* Nat Commun, 2017. **8**: p. 15081.

327. Martinez, F.O. and S. Gordon, *The M1 and M2 paradigm of macrophage activation: time for reassessment.* F1000Prime Rep, 2014. **6**: p. 13.

328. Chen, J., et al., *CCL18 from tumor-associated macrophages promotes breast cancer metastasis via PITPNM3.* Cancer Cell, 2011. **19**(4): p. 541-55.

329. Topalian, S.L., et al., *Safety, activity, and immune correlates of anti-PD-1 antibody in cancer.* N Engl J Med, 2012. **366**(26): p. 2443-54.

330. Latchman, Y., et al., *PD-L2 is a second ligand for PD-1 and inhibits T cell activation.* Nat Immunol, 2001. **2**(3): p. 261-8.

331. Freeman, G.J., et al., *Engagement of the PD-1 immunoinhibitory receptor by a novel B7 family member leads to negative regulation of lymphocyte activation.* J Exp Med, 2000. **192**(7): p. 1027-34.

332. Topalian, S.L., C.G. Drake, and D.M. Pardoll, *Targeting the PD-1/B7-H1(PD-L1) pathway to activate anti-tumor immunity.* Curr Opin Immunol, 2012. **24**(2): p. 207-12.

333. Pardoll, D.M., *The blockade of immune checkpoints in cancer immunotherapy.* Nat Rev Cancer, 2012. **12**(4): p. 252-64.

334. Faria, S.S., et al., *Obesity and Breast Cancer: The Role of Crown-Like Structures in Breast Adipose Tissue in Tumor Progression, Prognosis, and Therapy.* J Breast Cancer, 2020. **23**(3): p. 233-245.

335. Engin, A.B., A. Engin, and Gonul, II, *The effect of adipocyte-macrophage crosstalk in obesity-related breast cancer.* J Mol Endocrinol, 2019. **62**(3): p. R201-R222.

336. Vandeweyer, E. and D. Hertens, *Quantification of glands and fat in breast tissue: an experimental determination.* Ann Anat, 2002. **184**(2): p. 181-4.

337. Bai, Y. and Q. Sun, *Macrophage recruitment in obese adipose tissue.* Obes Rev, 2015. **16**(2): p. 127-36.

338. Oner, G., et al., *Triple-negative breast cancer-Role of immunology: A systemic review.* Breast J, 2020. **26**(5): p. 995-999.

339. Denkert, C., et al., *Molecular alterations in triple-negative breast cancer-the road to new treatment strategies.* Lancet, 2017. **389**(10087): p. 2430-2442.

340. Geyer, F.C., et al., *The Spectrum of Triple-Negative Breast Disease: High- and Low-Grade Lesions.* Am J Pathol, 2017. **187**(10): p. 2139-2151.

341. Lim, B., et al., *Inflammatory breast cancer biology: the tumour microenvironment is key.* Nat Rev Cancer, 2018. **18**(8): p. 485-499.

342. Schmid, P., et al., *Atezolizumab plus nab-paclitaxel as first-line treatment for unresectable, locally advanced or metastatic triple-negative breast cancer (IMpassion130): updated efficacy results from a randomised, double-blind, placebo-controlled, phase 3 trial.* Lancet Oncol, 2020. **21**(1): p. 44-59.

343. Burgos-Panadero, R., et al., *The tumour microenvironment as an integrated framework to understand cancer biology.* Cancer Lett, 2019. **461**: p. 112-122.

344. Chen, Y., et al., *Tumor-associated macrophages: an accomplice in solid tumor progression.* J Biomed Sci, 2019. **26**(1): p. 78.

345. Reader, J., D. Holt, and A. Fulton, *Prostaglandin E2 EP receptors as therapeutic targets in breast cancer.* Cancer Metastasis Rev, 2011. **30**(3-4): p. 449-63.

346. Sugimoto, Y. and S. Narumiya, *Prostaglandin E receptors.* J Biol Chem, 2007. **282**(16): p. 11613-7.

347. Ma, X., et al., *Prostaglandin E receptor EP1 suppresses breast cancer metastasis and is linked to survival differences and cancer disparities.* Mol Cancer Res, 2010. **8**(10): p. 1310-8.

348. Majumder, M., et al., *EP4 as a Therapeutic Target for Aggressive Human Breast Cancer.* Int J Mol Sci, 2018. **19**(4).

349. Nakamoto, S., et al., *EP3 signaling in dendritic cells promotes liver repair by inducing IL-13-mediated macrophage differentiation in mice.* FASEB J, 2020. **34**(4): p. 5610-5627.

350. Cheng, L., L. Shi, and H. Dai, *Bioinformatics analysis of potential prognostic biomarkers among Kruppel-like transcription Factors (KLFs) in breast cancer.* Cancer Biomark, 2019. **26**(4): p. 411-420.

351. Song, C.Z., et al., *Functional study of transcription factor KLF11 by targeted gene inactivation.* Blood Cells Mol Dis, 2005. **34**(1): p. 53-9.

352. Su, J., et al., *Development of prognostic signature and nomogram for patients with breast cancer.* Medicine (Baltimore), 2019. **98**(11): p. e14617.

353. Li, S., et al., *Development and validation of a nomogram predicting the overall survival of stage IV breast cancer patients.* Cancer Med, 2017. **6**(11): p. 2586-2594.

354. Gong, Y., et al., *Development and Validation of Nomograms for Predicting Overall and Breast Cancer-Specific Survival in Young Women with Breast Cancer: A Population-Based Study.* Transl Oncol, 2018. **11**(6): p. 1334-1342.

355. Rudloff, U., et al., *Nomogram for predicting the risk of local recurrence after breast-conserving surgery for ductal carcinoma in situ.* J Clin Oncol, 2010. **28**(23): p. 3762-9.

356. Lischka, A., et al., *Genome Instability Profiles Predict Disease Outcome in a Cohort of 4,003 Patients with Breast Cancer.* Clin Cancer Res, 2020. **26**(17): p. 4606-4615.

357. Tontonoz, P. and B.M. Spiegelman, *Fat and beyond: the diverse biology of PPARgamma.* Annu Rev Biochem, 2008. **77**: p. 289-312.

358. Lefterova, M.I. and M.A. Lazar, *New developments in adipogenesis.* Trends Endocrinol Metab, 2009. **20**(3): p. 107-14.

359. Schupp, M., et al., *Re-expression of GATA2 cooperates with peroxisome proliferator-activated receptor-gamma depletion to revert the adipocyte phenotype.* J Biol Chem, 2009. **284**(14): p. 9458-64.

360. Moore, K.J., et al., *The role of PPAR-gamma in macrophage differentiation and cholesterol uptake.* Nat Med, 2001. **7**(1): p. 41-7.

361. Bouhlel, M.A., et al., *PPARgamma activation primes human monocytes into alternative M2 macrophages with anti-inflammatory properties.* Cell Metab, 2007. **6**(2): p. 137-43.

362. Cipolletta, D., et al., *Appearance and disappearance of the mRNA signature characteristic of Treg cells in visceral adipose tissue: age, diet, and PPARgamma effects.* Proc Natl Acad Sci U S A, 2015. **112**(2): p. 482-7.

363. Hevener, A.L., et al., *Macrophage PPAR gamma is required for normal skeletal muscle and hepatic insulin sensitivity and full antidiabetic effects of thiazolidinediones.* J Clin Invest, 2007. **117**(6): p. 1658-69.

364. Ricote, M., et al., *Expression of the peroxisome proliferator-activated receptor gamma (PPARgamma) in human atherosclerosis and regulation in macrophages by colony stimulating factors and oxidized low density lipoprotein.* Proc Natl Acad Sci U S A, 1998. **95**(13): p. 7614-9.

365. Tontonoz, P., et al., *PPARgamma promotes monocyte/macrophage differentiation and uptake of oxidized LDL.* Cell, 1998. **93**(2): p. 241-52.

366. Gallardo-Soler, A., et al., *Arginase I induction by modified lipoproteins in macrophages: a peroxisome proliferator-activated receptor-gamma/delta-mediated effect that links lipid metabolism and immunity.* Mol Endocrinol, 2008. **22**(6): p. 1394-402.

367. Loven, J., et al., *Selective inhibition of tumor oncogenes by disruption of super-enhancers.* Cell, 2013. **153**(2): p. 320-34.

368. Whyte, W.A., et al., *Master transcription factors and mediator establish super-enhancers at key cell identity genes.* Cell, 2013. **153**(2): p. 307-19.

369. Heinz, S., et al., *The selection and function of cell type-specific enhancers.* Nat Rev Mol Cell Biol, 2015. **16**(3): p. 144-54.

370. Pilon, A.M., et al., *Genome-wide ChIP-Seq reveals a dramatic shift in the binding of the transcription factor erythroid Kruppel-like factor during erythrocyte differentiation.* Blood, 2011. **118**(17): p. e139-48.

371. Yin, K.J., et al., *KLF11 mediates PPARgamma cerebrovascular protection in ischaemic stroke.* Brain, 2013. **136**(Pt 4): p. 1274-87.

372. Ojalvo, L.S., et al., *High-density gene expression analysis of tumor-associated macrophages from mouse mammary tumors.* Am J Pathol, 2009. **174**(3): p. 1048-64.

373. Beck, A.H., et al., *The macrophage colony-stimulating factor 1 response signature in breast carcinoma.* Clin Cancer Res, 2009. **15**(3): p. 778-87.

374. Sharma, M., et al., *Analysis of stromal signatures in the tumor microenvironment of ductal carcinoma in situ.* Breast Cancer Res Treat, 2010. **123**(2): p. 397-404.

375. Jayasingam, S.D., et al., *Evaluating the Polarization of Tumor-Associated Macrophages Into M1 and M2 Phenotypes in Human Cancer Tissue: Technicalities and Challenges in Routine Clinical Practice.* Front Oncol, 2019. **9**: p. 1512.

376. Pathria, P., T.L. Louis, and J.A. Varner, *Targeting Tumor-Associated Macrophages in Cancer.* Trends Immunol, 2019. **40**(4): p. 310-327.

377. Mantovani, A. and A. Sica, *Macrophages, innate immunity and cancer: balance, tolerance, and diversity.* Curr Opin Immunol, 2010. **22**(2): p. 231-7.

378. Kowal, J., M. Kornete, and J.A. Joyce, *Re-education of macrophages as a therapeutic strategy in cancer.* Immunotherapy, 2019. **11**(8): p. 677-689.

379. Zhang, F., et al., *Genetic programming of macrophages to perform anti-tumor functions using targeted mRNA nanocarriers.* Nat Commun, 2019. **10**(1): p. 3974.

380. Hung, J.H. and Z. Weng, *Analysis of Microarray and RNA-seq Expression Profiling Data.* Cold Spring Harb Protoc, 2017. **2017**(3).

381. Stahl, P.L., et al., *Visualization and analysis of gene expression in tissue sections by spatial transcriptomics.* Science, 2016. **353**(6294): p. 78-82.

382. Ribas, A. and J.D. Wolchok, *Cancer immunotherapy using checkpoint blockade.* Science, 2018. **359**(6382): p. 1350-1355.

383. Dieci, M.V., et al., *The immune system and hormone-receptor positive breast cancer: Is it really a dead end?* Cancer Treat Rev, 2016. **46**: p. 9-19.

384. Wein, L., et al., *Checkpoint blockade in the treatment of breast cancer: current status and future directions.* Br J Cancer, 2018. **119**(1): p. 4-11.

385. Dodagatta-Marri, E., et al., *alpha-PD-1 therapy elevates Treg/Th balance and increases tumor cell pSmad3 that are both targeted by alpha-TGFbeta antibody to promote durable rejection and immunity in squamous cell carcinomas.* J Immunother Cancer, 2019. **7**(1): p. 62.

# Acknowledgements

I would like to acknowledge my gratitude to the following who have made the completion of this thesis possible:

Thank God for the creation of all existence.

Thank my mother and sister for their vital encouragement and support.

Thank my supervisors Prof. Dr. Udo Jeschke and Anna Hester for the support and trust in my research work.

Thank the department director Prof. Dr.Sven Mahner for the support of the lab work.

Thank the lab members, Mirjana Kessler, Christina Kuhn, Martina Rahmeh, Laurent Soussana, Sabine Fink, Gabriele Weimer, and Cornelia Herbst for the experimental and technical support.

Thank myself for my persistence and perseverance.

At last, I would like to share my life philosophy:

*“I am still a doctor*

*And a scientist*

*In view of this*

*I still have two unshirkable responsibilities*

*Seeking the truth and saving lives.”*

# Affidavit

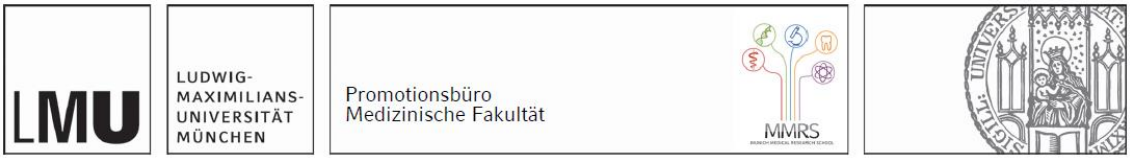


**Affidavit**

Lin, Lili

Surname, first name

Street

Zip code, town, country

I hereby declare, that the submitted thesis entitled:

**The role of Tumor-associated Macrophages (TAMs) and Transcription Factor KLF11 in breast cancer (BC) and KLF11-mediated Transcriptional Regulation of BC-associated TAMs**

is my own work. I have only used the sources indicated and have not made unauthorized use of services of a third party. Where the work of others has been quoted or reproduced, the source is always given.

I further declare that the submitted thesis or parts thereof have not been presented as part of an examination degree to any other university.

Munich, 30.09.2022 Lili Lin

place, date Signature doctoral candidate